White Rose Research Online

eprints@whiterose.ac.uk
https://eprints.whiterose.ac.uk
Universities of Leeds, Sheffield and York

Deposited via The University of Sheffield.

White Rose Research Online URL for this paper:
https://eprints.whiterose.ac.uk/id/eprint/208395/

Version: Published Version

Article:
Dev, P.S.B., Koerner, L.W., Saad, S. et al. (2024) Searches for baryon number violation in neutrino experiments: a white paper. Journal of Physics G: Nuclear and Particle Physics, 51 (3). 033001. ISSN: 0954-3899

https://doi.org/10.1088/1361-6471/ad1658

Reuse
This article is distributed under the terms of the Creative Commons Attribution (CC BY) licence. This licence allows you to distribute, remix, tweak, and build upon the work, even commercially, as long as you credit the authors for the original work. More information and the full terms of the licence here:
https://creativecommons.org/licenses/

Takedown
If you consider content in White Rose Research Online to be in breach of UK law, please notify us by emailing eprints@whiterose.ac.uk including the URL of the record and the reason for the withdrawal request.

UNIVERSITY OF LEEDS
University of Sheffield
UNIVERSITY of York

Journal of Physics G: Nuclear and Particle Physics

TOPICAL REVIEW • **OPEN ACCESS**

Searches for baryon number violation in neutrino experiments: a white paper

To cite this article: P S B Dev *et al* 2024 *J. Phys. G: Nucl. Part. Phys.* **51** 033001

View the article online for updates and enhancements.

You may also like

- The minimal seesaw and leptogenesis models
Zhi-zhong Xing and Zhen-hua Zhao
- Neutrinoless double beta decay
Heinrich Päs and Werner Rodejohann
- Influence of hyperon–hyperon interaction on the properties of neutron stars
R M Aguirre

This content was downloaded from IP address 89.240.190.132 on 29/01/2024 at 12:32

OPEN ACCESS
IOP Publishing
Journal of Physics G: Nuclear and Particle Physics
J. Phys. G: Nucl. Part. Phys. **51** (2024) 033001 (69pp)
https://doi.org/10.1088/1361-6471/ad1658

Topical Review

Searches for baryon number violation in neutrino experiments: a white paper

P S B Dev[1,*], L W Koerner[2], S Saad[3], S Antusch[3], M Askins[4,5], K S Babu[6], J L Barrow[7,8], J Chakrabortty[9], A de Gouvêa[10], Z Djurcic[11], S Girmohanta[12], I Gogoladze[13], M C Goodman[11], A Higuera[14], D Kalra[15], G Karagiorgi[15], E Kearns[16], V A Kudryavtsev[17], T Kutter[18], M Malinský[19], D A Martinez Caicedo[20], R N Mohapatra[21], P Nath[22], S Nussinov[8], J P Ochoa-Ricoux[23], V Pec[24], A Rafique[11], J Rodriguez Rondon[20], R Shrock[12], H W Sobel[23], T Stokes[18], M Strait[25], R Svoboda[26], S Syritsyn[12,27], V Takhistov[28], Y-T Tsai[29], R A Wendell[28,30] and Y-L Zhou[31,32]

[1] Department of Physics and McDonnell Center for the Space Sciences, Washington University, St. Louis, MO 63130, United States of America
[2] Department of Physics, University of Houston, Houston, TX 77204, United States of America
[3] Department of Physics, University of Basel, Klingelbergstrasse 82, CH-4056 Basel, Switzerland
[4] Department of Physics, University of California, Berkeley, CA 94720, United States of America
[5] Lawrence Berkeley National Laboratory, 1 Cyclotron Road, Berkeley, CA 94720-8153, United States of America
[6] Department of Physics, Oklahoma State University, Stillwater, OK 74078, United States of America
[7] The Massachusetts Institute of Technology, Department of Physics, 77 Massachusetts Avenue, Building 4, Room 304, Cambridge, MA 02139, United States of America
[8] Tel Aviv University, Tel Aviv 6997801, Israel
[9] Department of Physics, Indian Institute of Technology Kanpur, Kanpur 208016, India
[10] Northwestern University, Department of Physics & Astronomy, 2145 Sheridan Road, Evanston, IL 60208, United States of America
[11] Argonne National Laboratory, Argonne, IL 60439, United States of America
[12] C. N. Yang Institute for Theoretical Physics and Department of Physics and Astronomy, Stony Brook University, Stony Brook, NY 11794, United States of America
[13] Department of Physics & Astronomy, 224 Sharp Laboratory, University of Delaware, Newark, DE 19716, United States of America
[14] Department of Physics and Astronomy, Rice University, Houston, TX 77005, United States of America

© 2024 The Author(s). Published by IOP Publishing Ltd

[15] Department of Physics, Columbia University, New York, NY 10025, United States of America
[16] Department of Physics, Boston University, Boston, MA 02215, United States of America
[17] University of Sheffield, Sheffield S3 7RH, United Kingdom
[18] Department of Physics and Astronomy, Louisiana State University, Baton Rouge, LA 70803, United States of America
[19] Institute of Particle and Nuclear Physics, Charles University, V Holešovičkách 2, 180 00 Praha 8, Czech Republic
[20] Department of Physics, South Dakota School of Mines and Technology, Rapid City, SD 57701, United States of America
[21] Maryland Center for Fundamental Physics, Department of Physics, University of Maryland, College Park, MD 20742, United States of America
[22] Department of Physics, Northeastern University, Boston, MA 02115-5000, United States of America
[23] Department of Physics and Astronomy, University of California, Irvine, CA 92697, United States of America
[24] Institute of Physics, The Czech Academy of Sciences, Prague, Czech Republic
[25] School of Physics and Astronomy, University of Minnesota Twin Cities, Minneapolis, MN 55455, United States of America
[26] Department of Physics and Astronomy, University of California Davis, Davis, CA 95616, United States of America
[27] RIKEN-BNL Research Center, Brookhaven National Lab, Upton, NY 11973, United States of America
[28] Kavli Institute for the Physics and Mathematics of the Universe (WPI), UTIAS, The University of Tokyo, Kashiwa, Chiba 277-8583, Japan
[29] SLAC National Accelerator Laboratory, Menlo Park, CA 94025, United States of America
[30] Department of Physics, Kyoto University, Kyoto, Kyoto 606-8502, Japan
[31] School of Fundamental Physics and Mathematical Sciences, Hangzhou Institute for Advanced Study, UCAS, Hangzhou, People's Republic of China
[32] International Centre for Theoretical Physics Asia-Pacific, Beijing/Hangzhou, People's Republic of China

E-mail: bdev@wustl.edu, lkoerner@central.uh.edu and shaikh.saad@unibas.ch

Received 1 May 2023, revised 4 December 2023
Accepted for publication 15 December 2023
Published 23 January 2024

Abstract

Baryon number conservation is not guaranteed by any fundamental symmetry within the standard model, and therefore has been a subject of experimental and theoretical scrutiny for decades. So far, no evidence for baryon number violation has been observed. Large underground detectors have long been used for both neutrino detection and searches for baryon number violating processes. The next generation of large neutrino detectors will seek to improve

* Author to whom any correspondence should be addressed

Original content from this work may be used under the terms of the Creative Commons Attribution 4.0 licence. Any further distribution of this work must maintain attribution to the author(s) and the title of the work, journal citation and DOI.

upon the limits set by past and current experiments and will cover a range of lifetimes predicted by several Grand Unified Theories. In this White Paper, we summarize theoretical motivations and experimental aspects of searches for baryon number violation in neutrino experiments.

Keywords: Proton decay, neutrino experiments, baryon number violation

1. Introduction and executive summary

1.1. Theory summary

The stability of ordinary matter has long been a subject of both theoretical and experimental interests. The electron is stable because of electric charge conservation. On the other hand, in the standard model (SM), the stability of the proton is guaranteed by the accidental global symmetry of baryon number at the renormalizable level. In models of quark-lepton unification, such as the grand unified theories (GUTs), baryon number is necessarily violated. As a result, the proton is not stable, and decays dominantly into $e^+\pi^0$ (in non-supersymmetric theories) or $K^+\bar{\nu}$ (in supersymmetric theories). Another compelling reason for baryon non-conservation is that understanding the origin of matter in the Universe requires it as one of the three fundamental Sakharov conditions in addition to CP violation and thermal non-equilibrium.

This striking prediction of GUTs on proton decay, which are otherwise inaccessible to laboratory experiments, motivated the construction of large-scale water Cherenkov detectors like Irvine–Michigan–Brookhaven (IMB), Kamiokande, and its subsequent upgrade, Super-Kamiokande. Although there is no direct evidence of proton decay so far, but only stringent lower limits on the proton lifetime, it is important to continue the searches for proton (and bound neutron) decay and other baryon number violating (BNV) processes in general. A large class of GUTs predict proton lifetime to be within an order of magnitude above the current experimental limit. It is also important to keep in mind that the same experiments originally constructed to search for proton decay have now become truly multi-purpose experiments. In particular, they have played a major role in neutrino physics, starting with the serendipitous detection of SN1987A neutrinos, as well as the discovery of neutrino oscillations in atmospheric and solar neutrinos.

Therefore, the significance of current and next-generation neutrino experiments *simultaneously* searching for baryon number violation and studying neutrino properties cannot be overemphasized. While the main focus of the BNV experiments is on proton decay searches, there also exist other equally important baryon and/or lepton number violating processes, such as dinucleon decays and neutron-antineutron oscillations which must be studied as well along with their experimental detection prospects. Possible connections of BNV observables to other beyond the SM (BSM) physics, such as neutrino mass, baryogenesis, dark matter (DM), flavor physics, and gravitational waves are also being explored. The recent lattice developments for the relevant nucleon and nuclear matrix elements of effective BNV operators are also crucial for reducing the theoretical uncertainties in the BNV predictions.

1.2. Experimental summary

Experiments have long sought evidence of the decay of the proton as proof of physics BSM. The lower limit on the proton's lifetime is currently of order 10^{34} years. Experimental

searches that seek to probe beyond this limit therefore need a huge source of protons and years of exposure. The large mass and long operation times of detectors used for observation of neutrino oscillations make them well-suited for searches for baryon number violation, including nucleon decay and neutron-antineutron oscillations. The Super-Kamiokande neutrino experiment, which uses a water Cherenkov detector with a fiducial mass of 22.5 ktons and began operation in 1996, has published leading limits on 30 BNV processes. Next-generation neutrino detectors, such as DUNE (40 kton fiducial mass liquid argon TPC), Hyper-Kamiokande (HK) (190 kton fiducial mass water Cherenkov), and JUNO (20 kton fiducial mass liquid scintillator), all include searches for baryon number violation as a major component of their physics programs and hope to improve upon the limits set by Super-Kamiokande, if not observe baryon number violation for the first time.

Detector mass is a crucial characteristic in next-generation baryon number violation searches. For small detectors, the exposure required to improve upon limits already set by Super-Kamiokande can exceed the likely lifetime of the experiment. Clearly HK has the advantage in this respect. That being said, detector technology is also extremely important; DUNE's excellent imaging capabilities and JUNO's superb timing resolution offer advantages in some channels over HK's larger mass. NOvA, a currently-running neutrino experiment with a 14 kton segmented liquid scintillator detector, is developing a search for neutron-antineutron oscillations that could potentially have sensitivity comparable to current limits. THEIA is a proposed water-based liquid scintillator detector that would combine the advantages of the large mass of a water Cherenkov detector with the good resolution of a liquid scintillator detector. With this worldwide program, should a BNV signal be observed by any of the detectors in the next generation, confirmation from other detectors using different technologies would provide powerful evidence of physics BSM.

In addition to detector mass and technology, simulation and analysis techniques can also affect the potential of these searches. As with neutrino interactions, the experimental community has come to understand how important nuclear effects are in predicting the characteristics of final-state particles. Final-state interactions (FSIs) in the nucleus alter the multiplicity and momenta of final-state particles. Uncertainties in modeling FSIs therefore introduce uncertainties into the signal efficiency estimates and lifetime limits. Furthermore, analysis techniques are continually improving. For example, Super-Kamiokande made improvements to the search for proton decay via $p \to e^+\pi^0$ by reducing backgrounds via neutron tagging. Potential improvements to searches in a liquid argon TPC could come from tagging of nuclear de-excitations.

The experimental neutrino physics community has long been conducting searches for baryon number violation using neutrino detectors. The next generation of neutrino detectors, situated in underground laboratories with good shielding to reduce cosmic ray backgrounds, will allow the continued pursuit of this goal, with massive detectors and continually improving analysis techniques.

2. Theoretical motivations

2.1. Historical context

'Is ordinary matter stable?' This question has been a subject of experimental and theoretical interest over many decades. Ordinary matter made up of electrons and nucleons (protons and neutrons) is stable first because electrons are stable because of electric charge conservation; but what about nucleons? So far, experimental searches for the decay of protons and bound neutrons have not found evidence for nucleon decay and have only led to decay mode

dependent upper limits on the nucleon lifetime. From a theoretical point of view, the stability of matter can be guaranteed by assigning a baryon number $B = +1$ to the proton (the lightest baryon), which is known as the principle of conservation of baryon number formulated by Weyl in 1929 [1] (see also [2–4]). Baryon number conservation, however, is not guaranteed by any fundamental symmetry within the SM. Instead, baryon number is an accidental classical (global) symmetry of the SM Lagrangian, which is violated by small amounts via non-perturbative effects (namely, $SU(2)_L$ sphalerons) [5–8]. These are however negligibly small at temperatures low compared with the electroweak scale, but are important in the early universe.

After the recent discovery [9, 10] of the Higgs boson, the SM seems to be remarkably complete; furthermore, as modified to include nonzero neutrino masses and lepton mixing (which were absent in the original SM), it is generally consistent with the current experimental data. (Here, we note that there are indications of possible violation of lepton flavor universality in the B-meson decays reported by the LHCb experiment [11]. Furthermore, the $(g-2)_\mu$ measured value shows a significant deviation compared to the SM prediction recently confirmed by the Fermilab experiment [12]. There is an intensive experimental program to check these indications.) However, it is clear that the SM has several deficiencies [13]. For example, even apart from its prediction of (i) zero neutrino masses, the original SM accommodated, but did not explain, the quark and charged lepton masses or the observed Cabibbo–Kobayashi–Maskawa (CKM) quark mixing. Other deficiencies include the fact that (ii) there is no cold DM candidate in the SM (aside from primordial black holes, whose possible contributions to DM have long been studied), (iii) the observed matter-antimatter asymmetry of the Universe cannot be explained, (iv) the fundamental reason for electric charge quantization is not understood, and (v) the Higgs hierarchy (fine-tuning) problem is not solved. These are clear indications that the SM must be extended. A natural pathway towards building an ultraviolet (UV) complete model follows directly from the unification of the electromagnetic and weak forces already realized within the SM. These two interactions are of quite different strengths at low energy scales, owing to the electroweak symmetry breaking (EWSB), which produces masses of $O(10^2)$ GeV for the W and Z vector bosons, while keeping the photon massless. However, at energy scales above the EWSB scale, the $SU(2)_L$ and $U(1)_Y$ gauge interactions have coupling that are of comparable strength.

Therefore, a natural expectation is that all forces might unify at some higher scale. Historically, the first such attempts at unification were the Pati-Salam (PS) model [14, 15] that unifies quarks and leptons and the Georgi–Glashow (GG) [16] model that unifies all three forces (electromagnetic, weak, and strong) within a fundamental symmetry group $SU(5)$, which also unifies particles and antiparticles. Spontaneous breaking of these symmetries at some ultrahigh-energy scale leads to the SM with three distinct unbroken symmetries that result in separate electroweak and strong forces. This idea of embedding the entire SM into a single unified group is called Grand Unification [15–20].

An immediate consequence of GUTs is that baryon number is necessarily violated and the proton decays. These processes are mediated by the new superheavy gauge bosons associated with the GUT group. Assuming the unified gauge coupling to take a value similar to the fine-structure constant, and using the best experimental lower limit of the proton lifetime known around the time unified theories were proposed (1974) [21]: $\tau_p \gtrsim 10^{30}$ years (using 20 tons of liquid scintillator), one obtains a limit on the superheavy gauge boson mass $M_X \gtrsim 10^{14}$ GeV. This corresponds to a scale at which SM gauge couplings are expected to be unified. Being twelve orders of magnitude larger than the electroweak scale, there is no hope to directly test GUT scale physics at colliders (see however [22] for indirect tests). On the other hand, proton decay (and the decay of neutrons that would otherwise be stably bound in nuclei) provides a

clear signature of GUTs, and therefore, it was the prime target of early experiments using water Cherenkov and other detectors. Since 1 kiloton of water contains about 6×10^{32} nucleons, it was thought that proton decay predicted by GUTs should be within reach of experimental searches.

The search for nucleon decay has a long history. The first useful limits on nucleon decay rates were obtained using radiochemical methods. Alternatively, nucleon decays were also searched for using geochemical techniques. Both of these methods are discussed in [23], and a strong bound on the nucleon lifetime of $\tau_p > 2 \times 10^{27}$ years was obtained using the second method [24]. The advantage of these indirect methods was that limits on nucleon lifetime were obtained independent of the decay modes. On the other hand, the direct detection method is based on detecting particles emitted by the decay of a nucleon. The primary advantage of detectors of this type is that much larger quantities of matter can be used as nucleon sources. Furthermore, large backgrounds encountered in the nuclear experiments can be significantly reduced in the direct detection experiments. The CERN group [25] carried out the first deep underground experiment hunting for proton decay in a railway tunnel (in Switzerland) that provided an upper bound on the nucleon lifetime of 3×10^{26} years (1960). By analyzing results from earlier deep underground experiments, the proton lifetime reached about $\tau_p > 3 \times 10^{30}$ years by 1981 [26, 27]. For an overview of early proton decay experiments, see [28].

During the 1980s, five underground detectors started searching for proton decay. Three of them were based on calorimeter-type detectors: (i) NUSEX (in Europe) [29], (ii) Frejus (in Europe) [30], (iii) Soudan-2 (in Minnesota) [31], and two of them were water Cerenkov detectors: (iv) IMB (in Ohio) [32], (v) Kamiokande (in Japan) [33]. After several years of operation, these experiments observed no clear indication of nucleon decay; however, some of these experiments led to unexpected groundbreaking discoveries in neutrino physics. Kamiokande (Kamioka Nucleon Decay Experiment), funded in 1982, listed in its proposal the possibility of detecting neutrino bursts from supernovae as well as studying neutrino oscillations through the measurements of atmospheric neutrinos. Shortly after Kamiokande started taking data in 1983, it was realized that this experiment could be upgraded to measure solar neutrinos. The upgraded experiment Kamiokande-II started taking data in 1987 and, immediately after, it detected a neutrino burst from supernova SN1987A [34]. Neutrinos from this supernova explosion were also detected by the IMB experiment [35]. This historical observation demonstrates the excellent capability of water Cherenkov detectors to measure low-energy neutrinos. Two years later, Kamiokande-II also successfully detected solar neutrinos and confirmed the deficit of neutrinos from the Sun [33].

Subsequently, the construction of Super-K (Super-Kamiokande) was approved in 1991, which had proton decay and neutrino astronomy (solar neutrinos and supernova neutrinos) in its top-listed search agenda. The making of the Super-K detector was completed in 1996, and within two years of data taking, the discovery of neutrino oscillation (of the atmospheric neutrinos) was announced in 1998 [36]. Remarkably, the data analysis exhibited that a muon neutrino produced in the atmosphere was converting to another neutrino flavor. The Super-K experiment also played a significant role in discovering neutrino oscillation in solar neutrinos. Measurements of the solar neutrino flux at Super-K showed that solar electron neutrinos were transforming to different neutrino flavors [37, 38]. These two major milestones clearly depict the importance of experiments that are simultaneously searching for BNV processes and studying neutrino properties. At the time of writing this White Paper, no convincing evidence of proton decay has been reported, and the current lower limit on the proton lifetime exceeds 10^{34} years for some channels.

2.2. Proton decay in GUTs

The basic idea of GUTs is the embedding of the entire SM gauge group $SU(3)_c \times SU(2)_L \times U(1)_Y \equiv G_{\rm SM}$ in a larger (non-Abelian) group $G_{\rm GUT}$, which thus involves a single gauge coupling. Importantly, electric charge quantization is guaranteed in this framework, since the electric charge operator is a generator of $G_{\rm GUT}$. Even though the values of three gauge couplings associated with $G_{\rm SM}$ are different at the low energy scales, they are expected to get unified at the GUT scale. However, within the SM, these gauge couplings do not quite combine into a single coupling. Interestingly, if TeV scale supersymmetry (SUSY) [39–43] is assumed, the Minimal Supersymmetric SM (MSSM) leads to unification at about $M_{\rm GUT} = 2 \times 10^{16}$ GeV. Since SUSY can also provide a solution to the hierarchy problem [40, 44–46] and since a DM candidate naturally arises in an R-parity-conserving SUSY theory if the lightest SUSY particle (LSP) does not carry electric and/or color charge, SUSY GUTs [47] can be considered an appealing extensions of the SM. In order for SUSY to provide a solution to the fine-tuning problem with the Higgs mass, it was necessary that the SUSY breaking scale should not be much higher than the EWSB scale of 250 GeV. Thus, it was widely expected that supersymmetric partners of SM particles would be observed at the LHC. However, no evidence of these superpartners (in particular, the squarks and gluinos, which interact strongly) has been seen at the LHC running at 14 TeV [13]. This subsection summarizes the state of theoretical knowledge of both non-SUSY and SUSY GUTs. In our discussion, we mostly focus on minimal models; however, nucleon decay predictions of a wide range of models are summarized in table 2. For reviews on this subject, see [20, 48–50].

- $SU(\mathbf{5})$ **GUTs:** The simplest GUT model is the GG model [16] with the gauge group $G_{\rm GUT} = SU(5)$. In this model, the GUT group is spontaneously broken to the $G_{\rm SM}$ in a single step by a Higgs field in the adjoint (**24**) representation. Finally, SM symmetry is broken down to $SU(3)_c \times U(1)_{\rm em}$ when a scalar field in the fundamental (**5**) representation acquires VEU. The latter field contains the SM Higgs doublet that remains light, whereas its color-triplet partner needs to reside roughly above 10^{11} GeV since it leads to proton decay predominantly through $p \to \bar{\nu} K^+$ channel [51]. The SM fermions of each generation are contained in a $\bar{\mathbf{5}}$- and a **10**-dimensional representations. Notably, the $\bar{\mathbf{5}}$ contains the lepton doublet and the d^c quark field, while the 10 contains the quark doublet, and the u^c as well as the e^c fields. The gauge multiplet belonging to the adjoint representation contains twelve SM and twelve BSM vector bosons (labeled by X and Y with electric charges $4/3$ and $1/3$, respectively). These new gauge boson interactions involve both quarks and leptons; consequently, the new interactions violate baryon number B, and lead to proton decay via dimension-6 operators of the form such as $\overline{u^c}\gamma^\mu Q \overline{e^c}\gamma_\mu Q$ etc [48, 52–54]. An example diagram is presented in figure 1 (diagram on the left).

Non-observation of proton decay requires these gauge bosons to be superheavy, and this bound can be computed easily by approximating the left diagram in figure 1 by a four-fermion interaction; by doing so, one obtains,

$$\tau_p \sim \frac{16\pi^2 M_X^4}{g_{\rm GUT}^4 m_p^5}, \tag{1}$$

where $g_{\rm GUT}$ is the unified gauge coupling and m_p and M_X are the proton and superheavy gauge boson masses, respectively. Then the current experimental bound of $\tau_p(p \to e^+\pi^0) > 2.4 \times 10^{34}$ years from the Super-Kamiokande Collaboration [55] typically implies $M_X \sim M_{\rm GUT} \gtrsim 5 \times 10^{15}$ GeV. In addition to $p \to e^+\pi^0$, current (as well as future) experimental bounds (sensitivities) on other important proton decay modes are summarized in

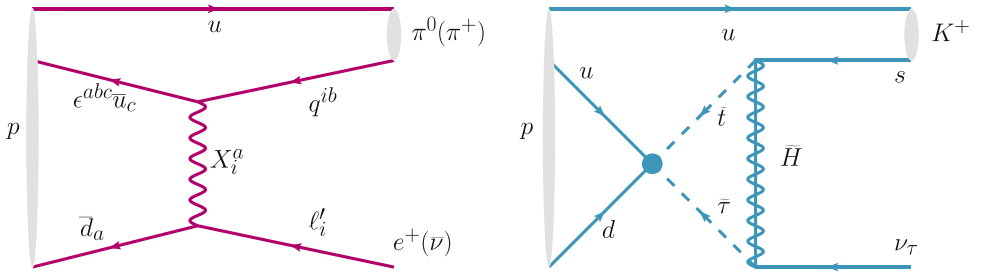

Figure 1. Left-diagram: Dominant proton decay mode $p \to e^+\pi^0$ in non-SUSY GUTs (here $(X_\mu)_i^a = (X_\mu^a, Y_\mu^a)^T$ is the iso-doublet gauge field). Right-diagram: Dominant proton decay mode $p \to \overline{\nu}K^+$ in SUSY GUTs (example diagram with Higgsino dressing, see text for details). The blob here represents the dimension-5 operator induced by colored Higgs exchange.

Table 1. Current lower limits from Super-Kamiokande on partial lifetime for different proton decay modes are presented in the second column. The third column shows future sensitivities at 90% CL of the Hyper-K, DUNE, JUNO, and THEIA detectors.

Modes (partial lifetime)	Current limit [90% CL] (10^{34} years)	Future Sensitivity [90% CL] (10^{34} years)
$\tau_p(p \to e^+\pi^0)$	Super-K: 2.4 [55]	Hyper-K (1900kton-yrs): 7.8 [56]
DUNE (400 kton-yrs): ∼1.0 [57]		
THEIA (800 kton-yrs): 4.1		
$\tau_p(p \to \mu^+\pi^0)$	Super-K: 1.6 [55]	Hyper-K (1900 kton-yrs): 7.7 [56]
$\tau_p(p \to \overline{\nu}K^+)$	Super-K: 0.66 [58]	Hyper-K (1900 kton-yrs): 3.2 [56]
DUNE (400 kton-yrs): 1.3 [59]		
JUNO (200 kton-yrs): 1.9 [60]		
THEIA (800 kton-yrs) 3.8		

table 1. Further information about nucleon decays and relevant experiments are also provided in table 4 and table 7. For the convenience of the readers, in the following, we list the table numbers and the information (regarding nucleon decays) contained within:

Table no.	Information contained
Table 1	• Current proton decay limits of the most important decay modes (namely, $p \to e^+\pi^0$, $p \to \mu^+\pi^0$, and $p \to \overline{\nu}K^+$) along with the name of the relevant experiments. • Future proton decay sensitivities of the most important decay modes (namely, $p \to e^+\pi^0$, $p \to \mu^+\pi^0$, and $p \to \overline{\nu}K^+$)after 10 years of operation along with the names of the relevant experiments.
Table 4	• Current limits from Super-Kamiokande of various BNV processes such as $p \to \overline{\ell}M$ ($\overline{\ell}$= anti-lepton and M = meson), $n \to \nu\gamma$, $p \to \overline{\ell}\ell\ell$, as well as some selected dinucleon (for example, pp, np) decays.
Table 7	• Future sensitivities of numerous single nucleon decay modes (such as $p \to \overline{\ell}M$ and $p \to \overline{\ell}\ell\ell$) after 10 years of Hyper-Kamiokande operation.

(Continued.)

Table no.	Information contained
	• Future sensitivities of several dinucleon decay modes after 20 years of Hyper-Kamiokande operation.

In fact, the minimal $SU(5)$ GUT (GG model) in combination with imprecise unification of gauge couplings predicts the proton lifetime of order $\tau_p \approx 10^{28}-10^{32}$ years and was already ruled out by early proton decay experiments. Moreover, there are additional flaws of the GG model: (i) gauge couplings do not unify, (ii) it predicts an incorrect fermion mass relation, $m_e/m_\mu = m_d/m_s$, (iii) there is a doublet-triplet splitting problem [61, 62] (a generic problem in most of the GUT models), i.e. the fine tuning needed to render the electroweak-doublet Higgs in the **5**-dimensional $SU(5)$ Higgs light while keeping the color-triplet components at the GUT scale, and (iii) neutrinos remain massless, as in the SM. Nevertheless, many proposals were made in the literature towards building a viable GUT by extending the GG model; for an incomplete list of realistic models that also incorporate non-zero neutrino masses, see, e.g., [20, 63–86]. One of the most minimal renormalizable extensions of the GG model was advanced recently in [81] and employs fields residing in the first five lowest dimensional representations of the $SU(5)$ group. In this model, a vectorlike fermion in the **15**-dimensional representation is assisted with a **35**-dimensional scalar multiplet to serve three purposes: (a) the wrong fermion mass relations are corrected, (b) unification is achieved at a high enough scale to be consistent with the current experimental bounds, and (c) neutrinos receive non-zero masses via 1-loop quantum corrections. In addition to having the least number of parameters in the Yukawa sector, this model inextricably connects the origin of neutrino masses with the experimentally observed difference between the charged lepton and down-type quark masses. Due to its minimality, this model turns out to be very predictive. The outcomes are as follows: (a) neutrinos are Majorana particles and predicted to have normal mass ordering, (b) the lightest neutrino is massless, (c) there are four light scalar relics at or below a 100 TeV mass scale, and (d) the proton lifetime is expected to be within $\tau_p(p \to e^+\pi^0) \approx 10^{34} - 10^{36}$ yrs with an upper bound of $\tau_p \lesssim 2.3 \times 10^{36}$ years.

One can also attempt to correct the wrong fermion mass relations by adding a **45**-dimensional Higgs field [87] or by considering non-renormalizable operators [88]. However, these modifications reduce the predictivity of the model. Higher-dimensional operators, however, are not enough to provide sufficient contributions to neutrino masses. In building realistic extensions along this line, the options include the following (i) a **15**-dimensional scalar [63] or (ii) a **24**-dimensional fermionic [64] representation. The former (latter) option generates correct neutrino mass via a type-II [89–92] (type-III [93] + type-I [94–98]) seesaw mechanism. The analyses of both these theories typically suggest that proton lifetime has an upper bound of $\tau_p(p \to e^+\pi^0) \lesssim 10^{36}$ years [67].

On the other hand, predictivity can be achieved by employing the *single operator dominance* [99, 100], where a single higher-dimensional operator dominates each Yukawa entry. Group-theoretical factors from GUT symmetry breaking can lead to predictions for the ratios of quark and lepton masses at the unification scale [99, 100] that can be utilized to correct the bad mass relations between the down-type quarks and the charged-leptons. For a recent analysis utilizing this concept in the context of non-SUSY $SU(5)$ GUT that predicts nucleon decay rates from specific quark-lepton Yukawa ratios at the GUT scale, see, e.g. [101].

• **SUSY $SU(5)$ GUTs:** If supersymmetry is realized in nature and the SUSY breaking scale is not too far above the electroweak scale, then gauge coupling unification takes place close to

$M_{\rm GUT} = 2 \times 10^{16}$ GeV, and therefore the gauge-boson-induced proton lifetime is predicted to be $\tau_p \approx 10^{35}$ years [102], which is above the current experimental lower limit. However, SUSY GUTs predict new proton decay contributions arising from dangerous dimension-5 [52, 103] operators of the type $QQQL$, among which the dominant decay mode is $p \to \overline{\nu} K^+$ [104, 105] generated by the exchange of the colored Higgs multiplet (of mass M_{H_c}); these operators are proportional to $1/M_{H_c}$. Therefore the colored Higgs fields must be superheavy. By dressing these dimension-5 operators by gauginos or Higgsinos, dimension-6 operators are generated [106–108] that cause the proton to decay as shown in figure 1 (diagram on the right). Typically the Wino exchange dominates; however, for larger $\tan\beta$, the Higgsino exchange (the one shown in figure 1) also becomes important. Also, the Higgsino exchange dominates the Wino exchange if the Higgsino mass is much larger than the Wino masssuch a situation is realized in, e.g. mini-split SUSY. This is because the loop diagram like the right figure in figure 1 is accompanied with a chirality flip and thus is proportional to the mass of the exchanged particle. Interestingly, assuming SUSY particles of masses of order of the electroweak scale, the lifetime of the proton is typically found to be $\tau_p(p \to \overline{\nu} K^+) \lesssim 10^{30}$ years [108, 109]. On the other hand, the Super-Kamiokande experiment gives a stringent limit on this channel: $\tau_p(p \to \overline{\nu} K^+) \gtrsim 6.6 \times 10^{33}$ years [58]. This apparent contradiction rules out minimal SUSY $SU(5)$ GUT [42, 43] with low-scale SUSY (typically for sfermion masses $\lesssim$ TeV).

The solution to this problem resides in the Higgs boson mass which is currently accurately measured at 125.35 ± 0.15 GeV. This is close to the upper limit of $\sim$131 GeV predicted in supergravity unified models [111, 112] and implies that the weak SUSY scale is high lying in the several TeV region which in turn implies that the sfermion masses could be high, even as large as 10 TeV and above. Such a scale could still be natural on the hyperbolic branch of radiative breaking of the electroweak symmetry [113]. Thus the proton lifetime exhibits a sensitive dependence on the Higgs boson mass [114]. Using the precise value of the Higgs boson mass one finds for the proton decay mode $\overline{\nu} K^+$ a lifetime range of $3 \times 10^{34} - 2 \times 10^{35}$ years for mSUGRA and $3 \times 10^{34} - 10^{36}$ years for SUGRA models with non-universal soft breaking (NUSUGRA) consistent with analyses that a heavy SUSY spectrum might revive the minimal $SU(5)$ GUT [102, 108, 115–119]. Further, SUSY Charge Conjugation (CP) phases enter in proton decay and can lead to cancellations in the decay rate enhancing the lifetime [120]. Similar cancellations due to specific flavor mixings are possible and can suppress proton decay rate, see, e.g., [121, 122]. The cancellation mechanism is quite general and can apply to wide class of unified models including SO(10) [123]. Additionally, higher-dimensional operators can affect proton decay textures which are in general different from the textures for the fermion masses and affect proton lifetime [124, 125] as well as can easily increase the triplet mass and thus increase the proton lifetime significantly, see, e.g. [122, 126, 127]. Recently, proton decay in minimal SUSY $SU(5)$ has been revisited in [110] (see also [128]) where various SSB conditions are imposed and uncertainties associated with numerous phenomenological inputs in the calculation of the proton lifetime are analyzed. For example, in constraint MSSM (cMSSM) case, assuming sparticle masses $\lesssim O(10)$ TeV, the proton lifetime is found to be $\tau_p(p \to \overline{\nu} K^+) \lesssim (2 - 6) \times 10^{34}$ years which can be tested in the near future.

We emphasize that unusual decay modes, such as $p \to \mu^+ \pi^0$ and $p \to \mu^+ K^0$, can also be within the reach of the future experiments even in the minimal SUSY SU(5), if there exists flavor violation in sfermion mass matrices [116]. These decay modes can also be enhanced in flipped SU(5) GUTs with R symmetry, as recently discussed in [129, 130].

• **$SO(10)$ GUTs:** GUTs based on $SO(10)$ gauge symmetry [18, 19] are especially attractive since all SM fermions of each family are unified into a single irreducible **16**-dimensional

representation. Additionally, **16** contains a right-handed neutrino which naturally leads to non-zero neutrino mass via a type-I seesaw mechanism. Furthermore, $SO(10)$ is free of gauge anomalies, whereas, in contrast, in $SU(5)$, the gauge anomaly due to the $\mathbf{5}_R$ cancels the anomaly due to the $\mathbf{10}_L$ of fermions (separately for each generation). The unification of all fermions of each generation into a single multiplet suggests that $SO(10)$ may serve as a fertile ground for addressing the flavor puzzle. In fact, it turns out that $SO(10)$ GUTs are very predictive and have only a limited number of parameters to fit charged fermion as well as neutrino masses and mixings, which have been extensively analyzed in the literature [131–152]. As shown in [147], the most economical Yukawa sector with only $SO(10)$ gauge symmetry consists of a *real* $\mathbf{10_H}$, a *real* $\mathbf{120_H}$, and a *complex* $\overline{\mathbf{126}}_\mathbf{H}$ Higgs fields. Another widely studied class of models [131], with minimal Yukawa sector, utilizes a *complex* $\mathbf{10_H}$ and a *complex* $\overline{\mathbf{126}}_\mathbf{H}$ fields, which relies on the additional Peccei–Quinn symmetry exterior to the $SO(10)$ gauge symmetry. Moreover, from decays of the heavy right-handed neutrinos, the matter-antimatter asymmetry of the Universe [8, 153, 154] can also be generated [155] in $SO(10)$ GUTs.

Since the $SO(10)$ group has rank 5, whereas the SM has rank 4, there are various possible pathways for the GUT symmetry to break down to the SM as demonstrated in figure 3. Depending on which Higgs multiplet is employed to break the GUT symmetry, at the classical level, there are typically four possibilities with minimal Higgs content for the intermediate gauge symmetry [20, 156]: (a) $G_{422} \times D$, (b) G_{422}, (c) $G_{3221} \times D$, and (d) G_{3221}. Here G_{422} is the PS group $SU(4)_C \times SU(2)_L \times SU(2)_R$ and G_{3221} is the group of the left–right symmetric model $SU(3)_c \times SU(2)_L \times SU(2)_R \times U(1)_{B-L}$. PS symmetry with (without) D-parity [157] is obtained if GUT symmetry is broken by a **54** [158, 159] (**210** [160–162]) Higgs representation, whereas left–right symmetry with (without) D-parity is achieved if a **210** [160–162] (**45** + **54** [163–165]) Higgs is used. Depending on the intermediate gauge symmetry, these models with predominant decay mode $p \to e^+\pi^0$ predict a lifetime in a wide range that varies in between 10^{28} and 10^{40} years [156]. For a recent study along similar lines using a non-minimal Higgs sector in generic $SO(10)$ models see [166, 167]. In these works, amounts of threshold corrections required to be consistent with present bounds on proton decay for various intermediate breaking chains are quantified. In [168], a minimal renormalizable model with a symmetry breaking sector consisting of Higgs fields in the $\mathbf{10} + \mathbf{54} + \overline{\mathbf{126}}$ is analyzed and shown to have an upper limit on the lifetime $\tau_p(p \to e^+\pi^0) \lesssim 5 \times 10^{35}$ years. A variant of this framework with the adjoint **45** scalar instead of **54** has been studied thoroughly in [169, 170] due to its very special quantum structure [171–173] and particular robustness with respect to the leading Planck-scale effects.

Recently, a minimal non-renormalizable version of $SO(10)$ GUT utilizing **10**+**16**+**45** Higgs multiplets in the symmetry breaking sector was proposed in [176]. To be consistent with the current proton decay bounds, three scalar multiplets—a scalar quark doublet, a weak triplet, and a color octet—must remain lighter than $\mathcal{O}(10)$ TeV. With this spectrum, maximum unification scale and proton lifetime are found to be $M_{GUT} \lesssim 10^{16}$ GeV and $\tau_p \lesssim 10^{35}$ years, respectively.

For another model that uses a combination of type I and type II seesaw for neutrino masses and leads to a prediction of proton lifetime in the accessible range is in [177]. The model solves also the baryogenesis and DM problems of the SM.

- **SUSY $SO(10)$ GUTs:** In SUSY $SO(10)$ GUTs, if the intermediate symmetry is broken by a $\overline{\mathbf{126}}$ Higgs that breaks $B-L$ by two units, in addition to giving large masses to the right-handed neutrinos (that in turn generates tiny neutrino masses), R-parity of the MSSM automatically emerges from within the $SO(10)$ symmetry. Therefore, SUSY $SO(10)$ GUTs are highly attractive as they naturally provide a DM candidate and prohibit $d = 4$ BNV operators

without any additional symmetry assumptions. The minimal renormalizable model [131, 200, 201] with a symmetry breaking sector consisting of $\mathbf{10} + \mathbf{126} + \overline{\mathbf{126}} + \mathbf{210}$ was found to be very successful in fitting fermion data [133–137, 139–144]. Soon after, it was realized [140, 202–204] that the intermediate symmetry breaking scale that is required to be of order $10^{12}-10^{13}$ GeV from fits to light neutrino masses, subsequently leads to certain colored particles from various Higgs fields with masses of order 10^{10} GeV that spoil the successful perturbative gauge coupling unification. Besides that, current proton decay limits completely rule out this version of the model with TeV scale SUSY spectrum.

These caveats can be resolved by extending the minimal version of the SUSY $SO(10)$ GUT. Without introducing any new parameter in the Yukawa sector, it was shown in [149] that a minimal realistic extension is to add a **54** multiplet to the symmetry breaking sector. This setup allows the intermediate breaking scale of order 10^{12}–10^{13} GeV to fit neutrino data, yet preserves perturbative gauge coupling unification. The viability of this model requires a mini-split SUSY spectrum with sfermion masses of order 100 TeV using the current experimental lower bound $\tau_p(p \to \overline{\nu}K^+) > 6.6 \times 10^{33}$ years. Even though squarks and sleptons are far beyond the reach of LHC, the model can be tested at colliders with the discovery of LSP (Wino) along with its charged partners. Improvement of the proton lifetime limits in the channel $p \to \overline{\nu}K^+$ by one order of magnitude will highly disfavor this version of the model (expected upper limit on the proton lifetime with $O(100)$ TeV sfermions is $\tau_p \lesssim 6 \times 10^{34}$ years). On the other hand, implementation of Peccei–Quinn (PQ) symmetry [205] to solve the strong CP problem (for a recent review see [206]) in renormalizable SUSY $SO(10)$ with minimal Yukawa sector allows TeV scale sfermion masses as shown in [150]. This is possible since Higgsino mediated proton decay rate is strongly suppressed by an additional factor of $(M_{\rm PQ}/M_{\rm GUT})^2$ [150, 207] and the expected proton lifetime in this framework is $\tau_p \approx 10^{33}$–10^{36} years. This scenario is exciting since the proton decay suppression mechanism is inherently linked to the solution to the strong CP problem.

The axion solution to the strong CP problem is particularly interesting since axion can be a cold DM candidate. Models in which the axion field is embedded into a scalar representation responsible for breaking the GUT symmetry show an interesting correlation between the proton decay rate and the axion mass. Models of this type were first proposed in the context of $SU(5)$ in [208] and $SO(10)$ in [209]. For recent works along this line, see, e.g. [83, 210–213].

Another option to accommodate low scale SUSY in the $SO(10)$ context is to permit more parameters in the Yukawa sector by introducing a **120** multiplet on top of $\mathbf{10} + \overline{\mathbf{126}}$ [189, 214]. With new parameters in the Yukawa sector, it is possible to realize some cancellations to save the theory from too rapid proton decay even with a TeV scale SUSY spectrum. As shown in [189], type-II seesaw case is highly disfavored by the current proton decay lower limit, whereas for type-I scenario, the proton lifetime for the channel $p \to \overline{\nu}K^+$ can reach up to 10^{37} years.

SUSY $SO(10)$ GUTs that adopt small Higgs representations, to be specific, **16** instead of $\overline{\mathbf{126}}$, do not guarantee automatic R-parity, but they still provide quite simply matter-parity which keeps the LSP stable to serve as DM. Nevertheless, models of this class (consisting of $\mathbf{16} + \overline{\mathbf{16}}$, **10**, and **45** Higgs fields) are particularly interesting, not only because doublet-triplet splitting occurs naturally but also an interesting correlation of the decay rates between the two major proton decay modes $p \to \overline{\nu}K^+$ and $p \to e^0\pi^+$ emerges [215]. This interdependence shows that the empirical lower limit on the lifetime for $p \to \overline{\nu}K^+$ provides a constrained upper limit on the lifetime for $p \to e^+\pi^0$ mode and vice versa. Based on this correlation, estimated upper limits for proton lifetimes have been obtained in the context of an updated version of [215] (to be published; private communications from the authors of [215]; see also section 7.2 of [216]). This updated version takes two factors into account: (a) the current LHC

constraints on SUSY spectrum by allowing for an inverted hierarchy of the sfermion masses with a light stop (∼800 GeV to 1 TeV) and lighter higgsino/bino (∼700–800 GeV), together with heavy masses (∼18–20 TeV) for the sfermions of the first two generations on the one hand, and (b) the appropriate normalization factors in the definitions of certain effective couplings involving identical fields, which were missed in [215], on the other hand. With this updating, the correlation mentioned above yields conservative estimates for the upper limits of $\tau_p(p \to e^+\pi^0)$ less than about $(2-10)\times 10^{34}$ years, and $\tau_p(p \to \overline{\nu}K^+)$ less than about $(1-8)\times 10^{34}$ years. These upper limits are within the reach of the Hyper-K and Dune detectors including their planned upgrades respectively.

Moreover, GUT models with family symmetries (for an incomplete list of references, see, e.g. [217–231]) are particularly interesting since they tend to explain the flavor puzzle. An important aspect of this class of models is that Yukawa couplings emerge dynamically from minimization of the flavon potential, thereby reducing the number of parameters considerably. For example, assuming S_4 flavor symmetry on top of $SO(10)$ gauge symmetry, in [196], in addition to explaining the hierarchies in the charged fermion masses and mixings, neutrino observables are also predicted (such as $\theta_{13} \sim 9^\circ$). Furthermore, the proton decay mode $p \to \overline{\nu}K^+$ in this model is found to have a lifetime of $\sim 10^{34}$ years, which is within reach of the upcoming experiments.

It should be noted that unified models such as $SO(10)$ with appropriate symmetry breaking that produce the SM gauge group are also constrained by electroweak physics. It is then of interest to investigate the consistency of the unified models (such as Yukawa coupling unification) with the recent result from the Fermilab E989 experiment [12] on the muon anomalous magnetic moment. The Fermilab experiment has measured $a_\mu = (g_\mu - 2)/2$ with a significantly greater accuracy than the previous Brookhaven [232] experiment and the combined Fermilab and Brookhaven experimental data gives a 4.2σ deviation [233] from the SM. An investigation of the Yukawa coupling unification for the third generation in a class of SUSY $SO(10)$ unified models [234, 235] shows that the $SO(10)$ model is fully consistent with the Fermilab result.

Finally we mention two new classes of $SO(10)$ models not discussed thus far. As noted above, $SO(10)$ models require several Higgs representations to break the GUT symmetry to the SM gauge group. Thus a **16** or a **126** of Higgs field is needed to change rank, and one of **45**, **54** or a **210** is needed to break the symmetry down further, and to achieve EWSB and to generate quark and lepton masses an additional **10** dimensional representation is also needed. Recently a class of $SO(10)$ models have been proposed consisting of $\mathbf{144} + \overline{\mathbf{144}}$ of Higgs fields [236, 237] which can break the symmetry down to $SU(3)_c \times U(1)_{em}$. Proton decay analysis in this model exhibits a cancellation mechanism consistent with the current experimental constraints and the possibility of observation in future experiment [123]. Another class of $SO(10)$ models relates to the doublet-triplet splitting problem which as noted earlier is quite generic in grand unified models. One way to resolve it is the so called missing VEV mechanism [238, 239] (see also [192, 215, 240]) where the VEU of a **45** Higgs field which breaks the $SO(10)$ symmetry lies in the $(B-L)$-preserving direction, and generates masses for the Higgs triplets but not for the Higgs doublets from a **10**-plet. This mechanism works in $SO(10)$ and has no analog in SU(5). A second approach is the missing partner mechanism [234, 241, 242]. For $SO(10)$ it leads to a variety of models discussed in [234]. $B-L=-2$ violating dimension-7 and dimension-9 operators have been computed in this class of models [243]. Thus previous analyses using a bottom up effective low energy operator approach can now be extended to a top down one [243] for GUT scale baryogenesis and for $B-L=-2$ proton decay such $p \to \nu\pi^+$, $n \to e^-\pi^+$, e^-K^+ and $n-\bar{n}$ oscillations.

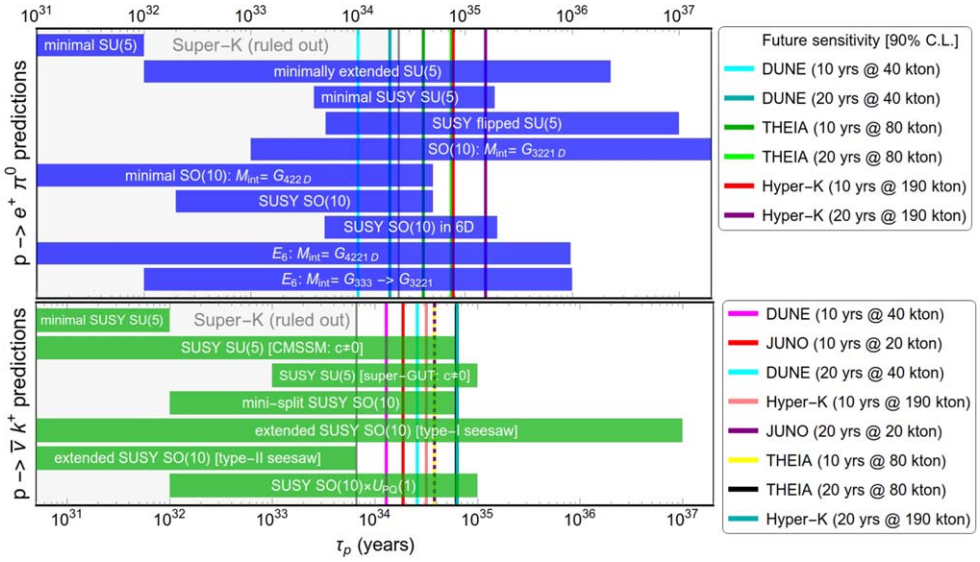

Figure 2. Theoretical predictions of proton lifetime for representative GUT models are presented (for the underlying assumptions, see text). (c here represents the coefficient of a Planck suppressed dimension-5 operator, for details, see [110].) Current Super-K data rule out the gray shaded regions. Future projections/sensitives from JUNO, DUNE, THEIA, and Hyper-K are also specified in the diagram (see section 3 for details). For these proton decay modes, the current and the future sensitivities (after 10 years of operation) are summarized in table 1. Future sensitivities after 20 years of operation are also presented, which are simply estimated as twice the sensitivities of 10 years of operation.

In short, well-motivated non-SUSY and SUSY GUTs generically predict rates of BNV processes that can be probed by next-generation experiments if not already ruled out by the current experimental data. A sketch of theoretical predictions for selected models and experimental reach of upcoming detectors are depicted in figure 2 for non-SUSY and SUSY GUTs. Furthermore, nucleon decay predictions for a wide range of models are summarized in table 2. For details on theoretical assumptions associated with each model's predictions, the readers are referred to the original literature.

As a cautionary remark, it is worth noting that none of the predictions in figure 2 or in table 2 is actually sharp; one typically encounters ranges stretching over several orders of magnitude. This has to do with a number of theoretical uncertainties affecting the precision of the calculations at various levels of significance. These can be loosely divided into three main classes corresponding to different ways the quantitative estimates based on diagrams in figure 1 are influenced: (i) uncertainties in the determination of the masses of the relevant leptoquark fields (i.e. the GUT scale), (ii) uncertainties in the couplings (gauge, Yukawa) governing the GUT-scale dynamics and (iii) uncertainties in the relevant hadronic or nuclear matrix elements. As for the first class, the most prominent of these effects are the uncertainties related to the generally unknown shape of the GUT-scale spectrum of the models at stakes, to the proximity of the GUT and the Planck scales enhancing the uncontrolled corrections from higher-dimensional operators (for instance those due to gravity effects) [244–246] and to the limited precision attainable in the perturbative accounts (see e.g. [173]), all inflicting uncertainties in the GUT-scale matching conditions. The second class corresponds to the

Table 2. Synopsis of the expected nucleon lifetime in various representative GUT models (see also [199]). NR here stands for non-renormalizable. For details, see text.

Model	Decay modes	τ_N ($N = p, n$) [years]	References
Non-SUSY minimal $SU(5)$	$p \to e^+\pi^0$	10^{30}–10^{32}	Georgi, Glashow [16]
Non-SUSY minimally extended $SU(5)$ (neutrino mass: 1-loop)	$p \to e^+\pi^0$	$\lesssim 2.3 \times 10^{36}$	Doršner, Saad [81]
Non-SUSY minimally extended $SU(5)$ (neutrino mass: 1-loop)	$p \to e^+\pi^0$	10^{32}–10^{36}	Perez, Murgui [73]
	$p \to \bar{\nu}K^+$	10^{34}–10^{37}	
Non-SUSY Minimal $SU(5)$ [NR] (neutrino mass: type-II seesaw)	$p \to \nu + (K^+, \pi^+, \rho^+)$	10^{31}–10^{38}	Doršner, Perez [63]
	$n \to \nu + (\pi^0, \rho^0, \eta^0, \omega^0, K^0)$		
Non-SUSY Minimal $SU(5)$ [NR] (neutrino mass: type-III+I seesaw)	$p \to e^+\pi^0$	$\lesssim 10^{36}$	Bajc, Senjanović [64]
Non-SUSY Extended $SU(5)$ (neutrino mass: 2-loop)	$p \to e^+\pi^0$	10^{34}–10^{40}	Saad [79]
Minimal flipped non-SUSY $SU(5)$	$p \to e/\mu^+\pi^0$	10^{38}–10^{42}	Arbeláez, Kolešová, Malinský [178]
Non-SUSY Minimal $SO(10)$	$p \to e^+\pi^0$	$\lesssim 5 \times 10^{35}$	Babu, Khan [168]
Minimal $SO(10)$ with 45 Higgs	$p \to e^+\pi^0$	$\lesssim 10^{36}$	Bertolini, Di Luzio, Malinský [179]
Minimal non-Renormalizable $SO(10)$	$p \to e^+\pi^0$	$\lesssim 10^{35}$	Preda, Senjanović, Zantedeschi [176]
Non-SUSY Generic $SO(10)$	$p \to e^+\pi^0$		Chakrabortty, King, Maji [167]
M_{int}: G_{422}		10^{34}–10^{46}	
M_{int}: G_{422D}		10^{31}–10^{34}	
M_{int}: G_{3221}		10^{36}–10^{46}	
M_{int}: G_{3221D}		10^{33}–10^{43}	
Non-SUSY Generic E_6	$p \to e^+\pi^0$		Chakrabortty, King, Maji [167]
M_{int}: G_{4221}		10^{27}–10^{36}	
M_{int}: G_{4221D}		10^{27}–10^{36}	
M_{int}: $G_{333} \to G_{3221}$		10^{32}–10^{36}	
M_{int}: $G_{4221D} \to G_{421}$		10^{26}–10^{48}	
M_{int}: $G_{4221} \to G_{421}$		10^{25}–10^{48}	
Minimal SUSY $SU(5)$	$p \to \bar{\nu}K^+$		Dimopoulos, Georgi [42], Sakai [103]
	$n \to \bar{\nu}K^0$	10^{28}–10^{32}	Hisano, Murayama, Yanagida [102]

Table 2. (Continued.)

Model	Decay modes	τ_N ($N = p, n$) [years]	References
Minimal SUSY $SU(5)$	$p \to \bar{\nu}K^+$	$\lesssim(2-6) \times 10^{34}$	Ellis *et al* [110]
(cMSSM)	$p \to e^+\pi^0$	$10^{35}-10^{40}$	
Minimal SUSY $SU(5)$	$p \to \bar{\nu}K^+$	$\lesssim 4 \times 10^{33}$	Babu, Bajc, Tavartkiladze [180]
($\mathbf{5} + \bar{\mathbf{5}}$ matter fields)	$p \to \mu^+\pi^0/K^0$, $n \to \bar{\nu}\pi^0/K^0$	$10^{33}-10^{34}$	
SUGRA $SU(5)$	$p \to \bar{\nu}K^+$	$10^{32}-10^{34}$	Nath, Arnowitt [106, 181]
mSUGRA $SU(5)$ (Higgs mass constraint)	$p \to \bar{\nu}K^+$	$3 \times 10^{34} - 2 \times 10^{35}$	Liu, Nath [114]
NUSUGRA $SU(5)$ (Higgs mass constraint)	$p \to \bar{\nu}K^+$	$3 \times 10^{34} - 10^{36}$	
SUSY $SU(5)$ or $SO(10)$	$p \to e^+\pi^0$	$\sim 10^{34.9\pm1}$	Pati [182]
MSSM ($d = 6$)			
Flipped SUSY $SU(5)$ (cMSSM)	$p \to e/\mu^+\pi^0$	$10^{35}-10^{37}$	Ellis *et al* [183–185]
Split SUSY $SU(5)$	$p \to e^+\pi^0$	$10^{35}-10^{37}$	Arkani-Hamed, *et. al.* [186]
SUSY $SU(5)$ in 5D	$p \to \mu^+K^0$	$10^{34}-10^{35}$	Hebecker, March-Russell[187]
	$p \to e^+\pi^0$		
SUSY $SU(5)$ in 5D variant II	$p \to \bar{\nu}K^+$	$10^{36}-10^{39}$	Alciati *et al* [188]
Mini-split SUSY $SO(10)$	$p \to \bar{\nu}K^+$	$\lesssim 6 \times 10^{34}$	Babu, Bajc, Saad [149]
SUSY $SO(10) \times U(1)_{\rm PQ}$	$p \to \bar{\nu}K^+$	$10^{33}-10^{35}$	Babu, Bajc, Saad [150]
Extended SUSY $SO(10)$	$p \to \bar{\nu}K^+$		
Type-I seesaw		$10^{30}-10^{37}$	Mohapatra, Severson [189]
Type-II seesaw		$\lesssim 6.6 \times 10^{33}$	Mohapatra, Severson [189]
Inverse seesaw		$\lesssim 10^{34}$	Dev, Mohapatra [190]
SUSY $SO(10)$	$p \to \bar{\nu}K^+$		Shafi, Tavartkiladze [191]
with anomalous	$n \to \bar{\nu}K^0$	$10^{32}-10^{35}$	
flavor $U(1)$	$p \to \mu^+K^0$		
SUSY $SO(10)$	$p \to \bar{\nu}K^+$	$10^{33}-10^{34}$	Lucas, Raby [192], Pati [182]
MSSM	$n \to \bar{\nu}K^0$	$10^{32}-10^{33}$	
SUSY $SO(10)$	$p \to \bar{\nu}K^+$	$10^{33}-10^{34}$	Pati [182]
ESSM		$\lesssim 10^{35}$	
SUSY $SO(10)/G(224)$	$p \to \bar{\nu}K^+$	$\lesssim 2 \times 10^{34}$	Babu, Pati, Wilczek [193–195],

Table 2. (Continued.)

Model	Decay modes	τ_N ($N = p, n$) [years]	References
MSSM or ESSM	$p \to \mu^+ K^0$		Pati [182]
(new $d = 5$)	$B \sim (1 - 50)\%$		
SUSY $SO(10) \times S_4$	$p \to \bar{\nu} K^+$	$\lesssim 7 \times 10^{33}$	Dev, Mohapatra, Dutta, Severson [196]
SUSY $SO(10)$ in 6D	$p \to e^+ \pi^0$	10^{34}–10^{35}	Buchmuller, Covi, Wiesenfeldt [197]
GUT-like models from	$p \to e^+ \pi^0$	$\sim 10^{36}$	Klebanov, Witten [198]
Type IIA string with D6-branes			

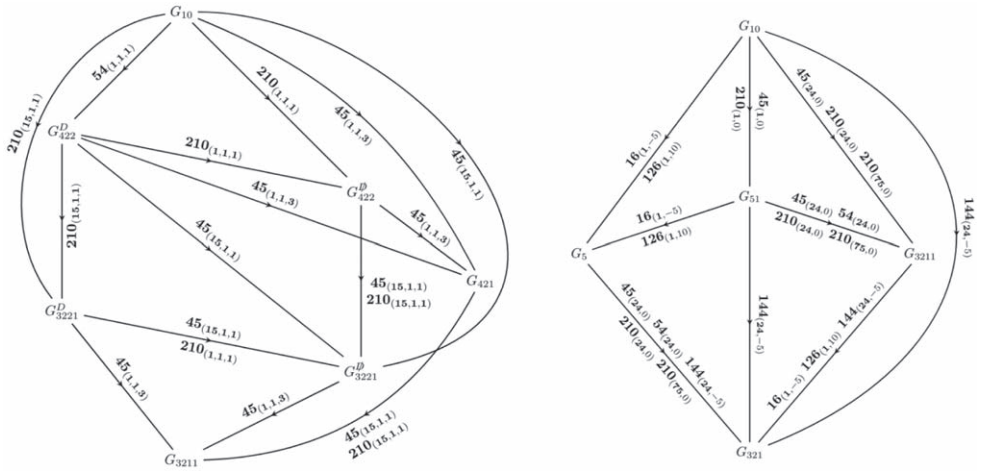

Figure 3. Various symmetry breaking chains [174] in $SO(10)$ GUTs (reproduced from [175]). The left (right) diagram shows breaking chains along the PS GG route.

limits in our understanding of the flavor structure of the relevant B- and L-violating charged currents (see [247, 248]) which, indeed, gets only partially reflected in the flavor observables accessible at low energies (the quark and lepton masses and mixings). It is also worth mentioning that unknown CP phases in the GUT Yukawa couplings [249] can change the proton decay rate significantly (see, e.g. [250] and [110]). The third class concerns the general difficulty with *ab initio* QCD calculations in the strongly coupled low-energy regime. While the modern lattice techniques have recently brought enormous progress in point (iii), see Section 2.9, (i) and (ii) still represent a formidable challenge to any precision calculations with rather limited prospects for any significant near-future improvement.

Thus far, we have discussed gauge-mediated proton decay, which dominates if the mass scale of vector-bosons and scalar-bosons are of a similar order. This happens for the latter contribution because the first-generation Yukawa couplings suppress the scalar-mediated proton decay. Naively, color-triplet scalar contributions become significant only if $M_S \lesssim \mathcal{O}(10^{-4})M_V$. It should be emphasized that the scalar-mediated contributions depend highly on the Yukawa sector of the theory and are model-dependent to a large extent. For minimal $SO(10)$ GUTs, using typical Yukawa coupling structures, color-triplet masses need to be heavier than about 10^{10}–10^{11} GeV [251]. In the context of a minimal model based on $\mathbf{10}_H$ and 126_H with Peccei–Quinn symmetry, when scalar-mediated contributions dominate, the proton decay spectrum is found to be quite different from the one typically anticipated [251]. For example, (i) proton dominantly decays into $\overline{\nu}K^+$ or μ^+K^0 for lighter $(\overline{3},\ 1,\ 1/3)$ or $(3,\ 1,\ -1/3)$, respectively, and (ii) $BR(p \to \mu^+\pi^0) \gg BR(p \to e^+\pi^0)$ is expected. Both these features are distinct from gauge-mediated proton decays; hence, if scalar-mediated contributions dominate, proton decay can provide very useful insight into the Yukawa structure of the theory.

• **GUTs in extra spatial dimensions:** Extra spatial dimensions provide a useful avenue for GUT model building in which some of the usual problems of four-dimensional GUTs can be addressed. For example, some versions of orbifold GUTs [187, 252–254] use compactification to break the unified gauge symmetry avoiding the doublet-triplet splitting problem. Moreover, localizing fermion fields appropriately in the bulk of extra dimension, a natural understanding of hierarchical fermion mass spectrum can be achieved in certain versions of

GUTs [255–257]. In 6D GUTs, the origin of multiple families of matter fields can be realized by quantization of flux in torus constructed from the compact extra two dimensions [258–260]. In these classes of GUTs, the Yukawa couplings become calculable parameters and the quarks and lepton spectrum can be obtained from a very small number of parameters. In the extra-dimensional GUT models, proton decay can have distinct features. For example, in a class of 5D models, the proton decay mediated by vector bosons has an additional suppression due to the wave-function profiles of first-generation fermions and the underlying vector bosons in the bulk [188, 253, 261, 262]. In SUSY orbifold GUTs, the dimension-5 operators are often suppressed due to $U(1)_R$ symmetry [188, 262]. In 6D models with flux compactification, the proton decay also receives a non-trivial contribution from the higher Kaluza–Klein modes of the vector bosons [263]. This, along with the special flavour structure of these theories, implies proton dominantly decaying into $\mu^+\pi^0$ which is otherwise suppressed in the 4D GUT models.

The absence of indication of low energy supersymmetry in the experimental searches so far has inspired investigations of the GUTs in the regime of split [141] or high scale SUSY [264]. Gauge coupling unification in this class of models is achieved by keeping only a part of SUSY spectrum at the intermediate energy scale while the remaining MSSM fields stay close to the GUT scale. Despite having most of the spectrum at intermediate or at very high energies, this class of theories are still reasonably constrained from the perspectives of Higgs mass, stability of the electroweak vacuum, flavour transitions, DM and proton decay [265–268]. It has been shown that if TeV scale Higgssino forms almost all of the DM of the Universe then it leads to particular ranges for the unified couplings and the scale of unification which in turn put an upper bound on the proton decay requiring the proton lifetime less than 7×10^{35} years [267, 268].

Finally, we point out that a public software package `SusyTCProton` for nucleon decay calculations in non-SUSY and SUSY GUTs is available, which includes, e.g., the full loop-dressing at the SUSY scale; for details, see [269].

2.3. PS partial unification

The first step towards unification was made in [14] (see also [15, 216, 270]) that are based on partial unification with non-Abelian gauge group $G_{422} = SU(4)_C \times SU(2)_L \times SU(2)_R$. By proposing the G_{422} symmetry, this work [14] introduced many new concepts into the literature, which include: (i) Quark-lepton unification; (ii) The first realistic model of matter and its three interactions which quantized electric charge, and thus (as was realized later) the first quantum-theoretically consistent model of magnetic monopoles; (iii) The first left–right symmetric gauge structure providing a compelling reason for the existence of the right-handed neutrino and the right-handed gauge-boson W_R; and (iv) The first model that questioned baryon number conservation and proton stability in the context of higher unification; while this was in the context of integer-charge quarks, nevertheless it served to remove partly the major conceptual barrier against BNV violation and proton instability that existed in the community in the early 1970s.

In this PS model, unlike $SO(10)$, there is no gauge-mediated proton decay. In fact in the original PS model, proton decay appears only if the quarks are chosen to have integer charges. This is why PS symmetry can be realized at rather low energy scales. In minimal models, the PS breaking scale can be as low as $v_R \gtrsim 10^3$ TeV [271, 272], which is coming from experimental limits on the branching ratios for $K_L^0 \to \mu^\pm e^\mp$ mediated by the new gauge bosons X_μ carrying $4/3$ charge under $B - L$. However, in the extended models, where additional fermionic degrees of freedom are introduced, the PS symmetry can even break down close to the

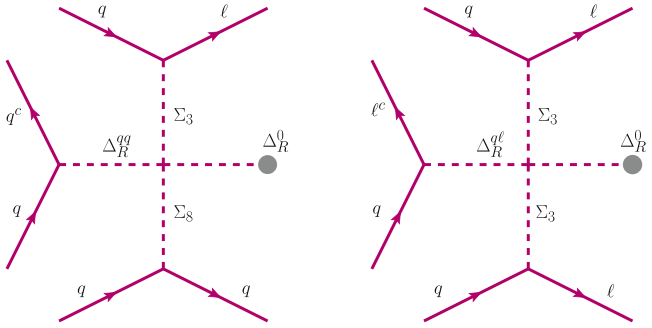

Figure 4. Nucleon decay modes in the $SU(4)_C \times SU(2)_L \times SU(2)_R$ model with inclusion of color sextet Higgs fields Δ_R a la [287]. Here the scalar sub-multiplets Δ_R^{qq}, Σ_8, and $\{\Sigma_3, \Delta_R^{q\ell}\}$ are color sextet, di-quark, and leptoquarks, respectively; moreover, Δ_R^0 is SM singlet that acquires a VEV and breaks $B-L$ by two units. The Feynman diagram on the left (right) leads to nucleon decay of the type $3q \to \ell q\overline{q}$ ($3q \to \ell\ell\overline{\ell}$).

TeV scale that has the potential to be directly probed at colliders; for a recent study, see, e.g. [273]. In light of recent anomalies [274–277] in the beauty-meson decays, low scale PS models have gained a lot of attention. Within this setup, the vector leptoquark X_μ is an attractive candidate to explain some of the flavor anomalies [278–286].

Even though baryon number violation does not proceed through gauge bosons, such processes naturally arise via the scalar sector, even with the minimal Higgs content [287–290]. In the minimal model, to generate a realistic charged fermion mass spectrum, the presence of both $\Phi(1, 2, 2)$ and $\Sigma(15, 2, 2)$ Higgs fields are required. Furthermore, $\Delta_R(10, 1, 3)$ multiplet breaks the PS symmetry to the SM group and generates non-zero neutrino mass via type-I seesaw. In this PS version, quartic terms of the form $\Sigma^2\Delta_R^2$ in the scalar potential lead to BNV decays which are distinct from the proton decay modes discussed above (such as $p \to e^+\pi^0$) that realize the $\Delta(B-L)=0$ selection rule. On the contrary, these BNV nucleon decay modes correspond to dimension-9 operators and obey a selection rule $\Delta(B-L)=-2$ [53, 289–297]. There are two types of such decays: (i) a single lepton p, $n \to \ell +$ mesons (such as $p \to e^-\pi^+\pi^+$, $e^-\pi^+K^+$, $\mu^-\pi^+K^+$, $\nu\pi^+$ etc) and (ii) three leptons p, $n \to \ell\ell\overline{\ell}+$ mesons (such as $n \to e^-e^+\nu$, $e^-\mu^+\nu$, $e^-\nu\overline{\nu}\pi^+$ as well as $p \to \nu e^+\nu$, $e^-e^+\nu\pi^+$, $e^-\nu\overline{\nu}\pi^+\pi^+$ etc) in the final state as shown in figure 4, where $\ell$and $\overline{\ell}$ are lepton and antilepton, respectively.

The difference between the left and the right Feynman diagrams in figure 4 is: the right-diagram is obtained from the left-diagram by replacing the di-quark Σ_8 by a leptoquark Σ_3. A priori, the amplitudes for these alternative decay modes could compete with each other. It is interesting to note that, in a certain region of the parameter space of the theory, the three lepton final states can dominate over single lepton final states; moreover, all these BNV processes can be within the observable range. Stringent limits on three-body decays $p \to e^+(\mu^+)\overline{\nu}\nu$ have been set by the Super-Kamiokande experiment, with $\tau > 2 \times 10^{32}$ years [298]. Unlike two-body nucleon decay channels, phase space alone provides only a crude approximation for the resulting particle spectra from these processes. For the trilepton modes, dynamics and phase space can be approximately accounted for using a general effective Fermi theory formalism of electroweak muon decay $\mu \to e^+\overline{\nu}\nu$ [299]. Searches for nucleon decay in other channels have also been conducted and typically have present lower bounds in the range of $10^{31}-10^{33}$ years [13].

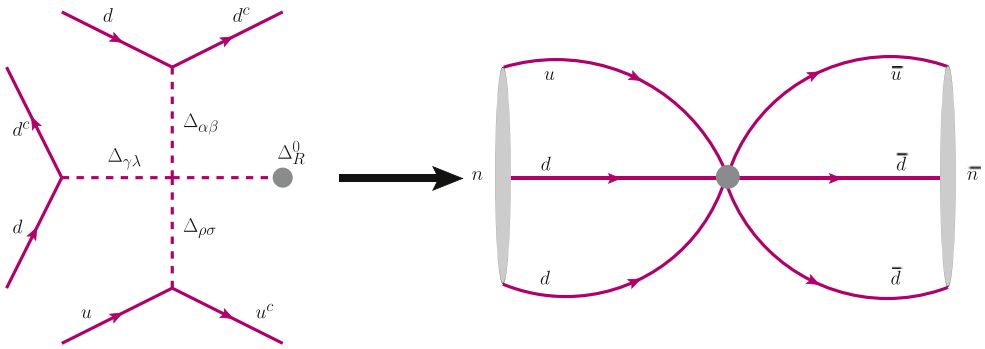

Figure 5. Feynman diagram for $n - \bar{n}$ oscillation in the model of [287]. Here, sub-multiplets $\Delta_{R,ab}$ are color sextets and Δ^0_R acquires a VEV that breaks $SU(4)_C \times SU(2)_L \times SU(2)_R$ symmetry to the SM.

2.4. Neutron-antineutron oscillation

Oscillations of electrically neutral particles are well-known phenomena; for example, neutrino oscillations and neutral meson ($K^0 - \overline{K}^0$, $B^0 - \overline{B}^0$, $D^0 - \overline{D}^0$) oscillations are all experimentally well established. Therefore, one would naturally expect to observe neutron-anti-neutron ($n - \bar{n}$) oscillations. However, the conservation of baryon number forbids the transition from a neutron (with one unit of baryon number) to an antineutron (with negative one unit of baryon number). As already pointed out, in the SM there is a global symmetry which forbids baryon number violation. However, once we go BSM, there is no obvious reason to expect baryon number conservation to hold. Indeed, baryon number violation is one of the necessary conditions noted by Sakharov for the generation of a baryon asymmetry in the Universe [300]. It was observed by Kuzmin that n–$\bar{n}$ oscillations might provide a source of baryon number violation connected with this generation of baryon asymmetry in the Universe [301]. Proton decay is mediated by four-fermion operators, which have coefficients of the dimensional form $1/M^2$, whereas n-$\bar{n}$ oscillations are mediated by six-quark operators, which have coefficients of the dimensional form $1/M^5$. Consequently, if there were only one high scale M responsible for baryon number violation, one might expect that n–$\bar{n}$ oscillations would be suppressed relative to proton (and bound neutron) decay. However, there are theories BSM where BNV nucleon decays are absent or highly suppressed and n-$\bar{n}$ oscillations are the main manifestation of baryon number violation [287, 302]. Observation of $n - \bar{n}$ transition would show that baryon number is violated by two units $|\Delta B| = 2$, which can be naturally expected within GUTs and other extensions of the SM. However, the selection rule $|\Delta B| = 2$ is again very different from $p \to e^+\pi^0$ that follows $\Delta B = -1$ (and $\Delta L = -1$, hence $\Delta(B-L) = 0$). Nucleon decay with a selection rule $\Delta B = -1$ are induced by dimension-6 (or dimension-5) operators and, therefore, would correspond to the existence of new physics at an energy scale of about 10^{15} GeV, whereas $n - \bar{n}$ transitions with $|\Delta B| = 2$ are induced by dimension-9 operators, and therefore, would imply new physics around the 100 TeV scale. Some early studies of n-$\bar{n}$ oscillations include [287, 303–307]. Some recent reviews include [308, 309].

Although, in general, a theory may violate L without violating B, in most of the well-motivated extensions of the SM, these two are connected via fundamental symmetries. As an example, within left–right symmetric models, $U(1)_{B-L}$ is promoted to a gauge symmetry [310]. As long as this symmetry is exact, $\Delta B = \Delta L$ is realized. This is highly motivating

since the existence of $|\Delta L| = 2$ generates the Majorana neutrino mass term, which is then connected to the existence of $|\Delta B| = 2$ operators. Therefore, $n - \bar{n}$ oscillation may be directly linked to neutrinoless double beta decay processes; see section 2.8.1.

It was shown in [287] that if the Higgs multiplet that breaks the $SU(4)_C \times SU(2)_L \times SU(2)_R$ group to the SM group is $\Delta_R(10, 1, 3)$ (instead of the Higgs set chosen in the original PS model), it generates Majorana neutrino mass via $|\Delta L| = 2$ processes while at the same time yielding $n - \bar{n}$ transition via $|\Delta B| = 2$ processes at an observable rate, keeping the proton stable. A term of the form Δ_R^4 in the scalar potential gives rise to a cubic term among three color sextet scalars once the $B-L$ violating VEU of the neutral component of Δ_R is inserted, which causes $n - \bar{n}$ oscillations [287, 308] as shown in figure 5. The $n - \bar{n}$ oscillations arising in this class of models with TeV scale color sextet scalars have an *upper limit* of $\tau_{n\bar{n}} \lesssim 10^{10-11}$ sec [311, 312], within the reach of the next-generation experiments; see figure 19. This upper bound is a consequence of the model requirements to satisfy the neutrino oscillation data via type-II seesaw, observed baryon asymmetry via the post-sphaleron baryogenesis mechanism [313], as well as the low-energy flavor changing neutral current (FCNC) constraints. Besides, TeV scale color sextets have rich phenomenology and can be uniquely probed at the hadron colliders [314–320]. There exist other simplified models of $n - \bar{n}$ [321–323], which, however, do not have an upper limit on $\tau_{n\bar{n}}$, although they can still be tested using the collider probes of colored particles.

An interesting class of BSM theories hypothesizes that our usual four spacetime dimensions are embedded in a space with higher (spatial) dimensions, such that SM fermions have strongly localized wave functions in the extra dimensions [324]. It has also been shown that in these extra-dimensional models, neutron-anti-neutron oscillations can occur at an observable rate while baryon-number-violating nucleon decays are suppressed far below experimental limits keeping the proton stable [302, 325, 326]. The BNV nucleon decays are suppressed by separating quark wave function centers sufficiently far from lepton wave function centers in the extra dimensions, but this does not suppress n–$\bar{n}$ oscillations since the operators that mediate these oscillations only involve quarks. These models can also produce a seesaw mechanism with naturally light neutrino masses and viable DM candidates [327, 328]. Another study of baryon-number violation without proton decay is [329].

An experimental search for n–$\bar{n}$ oscillations was carried out using neutrons from a reactor at the Institut Laue-Langevin (ILL) and obtained a lower limit $\tau_{n\bar{n}} > 0.86 \times 10^8$ s (90 % CL) [330]. Neutron-antineutron oscillations also lead to instability of matter with associated $\Delta B = -2$ dinucleon decays yielding mainly multi-pion final states. These have been searched for in deep underground nucleon decay detectors, most recently in Super-Kamiokande [331, 332], obtaining a lower limit on a lifetime characterizing such matter instability of $\tau > 3.6 \times 10^{32}$ years, which, when converted to a corresponding free neutron oscillation time, is $\tau_{n\bar{n}} > 4.7 \times 10^8$ s. This difference is due to the suppression of $n - \bar{n}$ oscillations in matter as a result of nuclear potential differences. The oscillation time is matter (τ_m) is related to free neutron oscillation time ($\tau_{n-\bar{n}}$) as $\tau_m = R\, \tau_{n-\bar{n}}^2$, with the conversion factor R for Oxygen evaluated to be about $0.5 \times 10^{23}\,\mathrm{s}^{-1}$ [333]. Upcoming experiments at the ESS (European Spallation Source) and Deep Underground Neutrino Experiment (DUNE) plan to improve these bounds to $\tau_{n\bar{n}} \gtrsim 10^{9-10}$ sec [334–336]. These oscillation times can be translated into new physics scales of roughly $(\tau_{n\bar{n}} \Lambda_{\mathrm{QCD}}^6)^{1/5} \sim O(100 - 1000)$ TeV, which are well above energies directly accessible at colliders. For recent reviews on this subject, see [308, 309]. Existing upper bounds on the rates for the dinucleon decays $nn \to \pi^0\pi^0$, $nn \to \pi^+\pi^-$, and $np \to \pi^+\pi^0$ imply upper bounds on the rates for dinucleon decays to dileptons $nn \to e^+e^-$,

$nn \to \mu^+\mu^-$, $nn \to \nu\bar{\nu}$, and $np \to \ell^+\nu_\ell$, where $\ell = e,\ \mu$. These have been calculated in [302, 337].

2.5. Other B−L violating processes

Nonzero neutrino masses, if these are Majorana fermions, are evidence for new physics that violates lepton number by two units. GUTs, as argued earlier, will ultimately lead to a connection between lepton-number and baryon-number violating new physics. While the details depend on both the mechanism behind nonzero neutrino masses and the underlying GUT, it is often the case that the lepton number violating physics is a subset of different phenomena correlated with $\Delta(B-L) = 2$ phenomena. Some connections have been explored at the effective operator level, in a number of papers; e.g. [307, 338].

Other than neutrinoless double-beta-decay ($\Delta L = 2$) and $n\bar{n}$-oscillations ($\Delta B = 2$), there are several other physics processes that are mediated by $\Delta(B-L) = 2$ new physics. For example, there are $|\Delta L| = 2$ meson decays, such as $K^+ \to \pi^-\mu^+\mu^+$ and $K^+ \to \pi^-\mu^+e^+$. Initial upper bounds on these decays were set in [339] and searches for them have been carried out at BNL [340, 341] and recently by the NA62 experiment at CERN [342, 343], yielding the upper limits $BR(K^+ \to \pi^-\mu^+\mu+) < 4.2 \times 10^{-11}$ and $BR(K^+ \to \pi^-\mu^+e^+) < 4.2 \times 10^{-11}$ (90 % CL). $|\Delta L| = 2$ baryon decays include, e.g. $\Xi^- \to p\mu^-\mu^-$, on which an initial upper bound was set in [344]. A Fermilab experiment searched for this decay and set the upper limit $BR(\Xi^- \to p\mu^-\mu^-) < 4.0 \times 10^{-8}$ [345] (90% CL). Other decays violating B and L include $B \to LM$ where B is a baryon, L is a lepton (neutrino or negatively-charged lepton) and M is a mesonic state. These include $n \to \mu^-\pi^+$, $p \to \nu\pi^+$, $n \to \nu\rho^0$, and $p \to e^-\pi^+K^+$.

The strongest bounds on these $\Delta(B-L) = 2$ processes come from searches for nucleon decay. These are nicely summarized in [13], and some are very strong, of order 10^{32} years. It is also the case that all of the strongest bounds on $\Delta(B-L) = 2$ neutron and proton decay come from twentieth century experiments, including Frejus [346] and IMB [347, 348], keeping in mind that it is not possible to distinguish a nucleon decay into a neutrino from that into an antineutrino. The DUNE experiment, thanks to its tracking, calorimetric, and particle-ID capabilities, is well positioned to be sensitive to $\Delta(B-L) = 2$ with lifetimes that approach 10^{34} years [57].

2.6. Effective field theory of B violation

The most suitable framework for studying low-energy, below electroweak-scale phenomena is the low energy effective field theory (LEFT) [349], which differs from the SM with respect to the internal symmetry as well as the degrees of freedom. In going from the SM to the LEFT, the heavy degrees of freedom namely, the Higgs boson h, the electroweak gauge bosons $W_\mu^\pm$ and Z_μ and the top-quark t are integrated out, whereas the internal symmetry is spontaneously broken from $SU(3)_C \times SU(2)_L \times U(1)_Y$ to $SU(3)_C \times U(1)_{\rm em}$.

LEFT operators can describe a wide variety of fermion-fermion interactions, also encompassing the BNV ones. The best examples are operators describing the proton decay into mesons and leptons or entirely into three charged leptons [350, 351]. In the SM baryon and lepton number conservation emerge as accidental symmetries. This suggests that the violation of these symmetries within the LEFT is a sign of BSM physics. The backdrop for conducting analyses on and to test the veracity of BSM models is the SM effective field theory (SMEFT) and it also acts as the necessary bridge between the low and the high energy sectors.

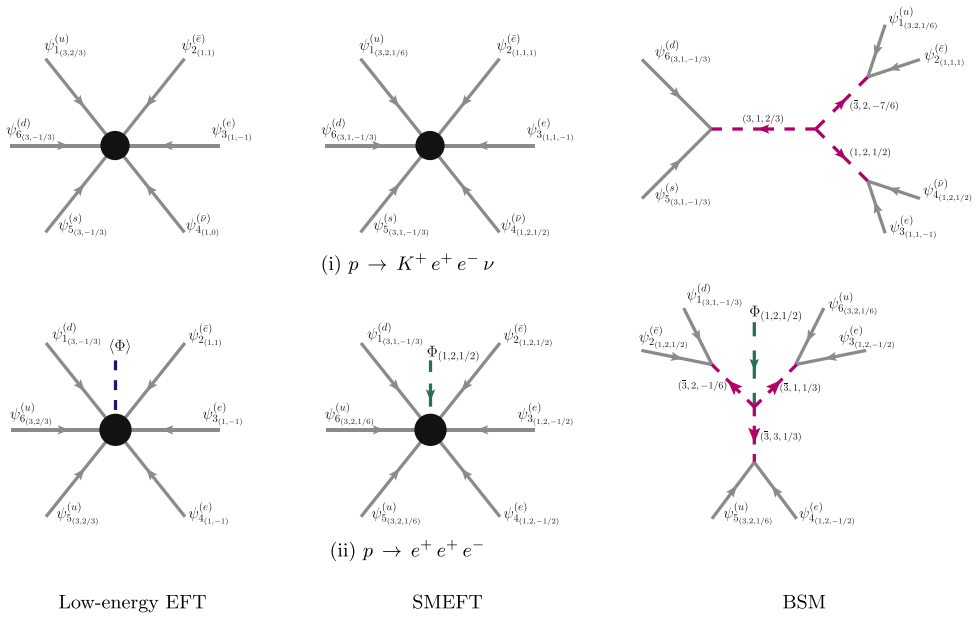

Figure 6. The low-energy EFT contact interactions of mass dimension 9 enveloping two distinct modes of proton decay, the corresponding SMEFT counterparts, and their realizations in terms of BSM propagators. For the LEFT diagrams, $\psi^{(f)}_{(R_C,Q)}$ denotes the light fermions $f \in \{\nu, e, u, d, s, c, b\}$ with R_C being the $SU(3)$ representation, and Q is the electromagnetic charge. For the SMEFT diagrams, $\psi^{(f)}_{(R_C,R_L,Y)}$ denotes the SM fermions $f \in \{q, l, e, d, u\}$ with R_L being the $SU(2)$ representation, and Y is the hypercharge. Φ is the SM Higgs and $\langle\Phi\rangle$ is its VEU.

A complete matching between a BSM model and the LEFT would involve an intricate and meticulous multi-step procedure of integrating out heavy fields and matching parameters. But a simpler way to catch a glimpse of possible BSM origins of the rare processes encapsulated by LEFT operators is to find their embedding within SMEFT operators and then based on symmetry arguments unfurl them into Feynman diagrams consisting of heavy propagators [352].

We have highlighted two examples in figure 6, where the first column presents LEFT contact operators of mass dimension 9 describing proton decay processes $(i)\, p \to K^+ e^+ e^- \nu$ and $(ii)\, p \to e^+ e^+ e^-$ The second column shows the relevant SMEFT operators of the same or higher mass dimension that describe the same contact interaction as the LEFT ones [352]. Finally, the last column reveals the BSM heavy field propagators that can mediate such processes.

The $\Delta B \neq 0$ operators of the SMEFT provide a model-independent framework for exploring B-violation, both for B-violating nucleon decay [53, 294, 295, 353] and for n-$\bar{n}$ oscillations [287, 304, 306, 307, 354]. The flavor structure of the operators at different dimensions allows one to establish nucleon decay-mediating processes that can dominate. This has been explored in further detail in more recent works such as [285, 325, 355–359]. In SMEFT, $\Delta B = 1$ appears at dimension-6. Any flavor $\Delta B = 1$ term leads to nucleon decay, including particles heavier than the proton such as charm or the tau lepton that can induce proton decay through off-shell contributions (see e.g. [360]). These contributions are strongly

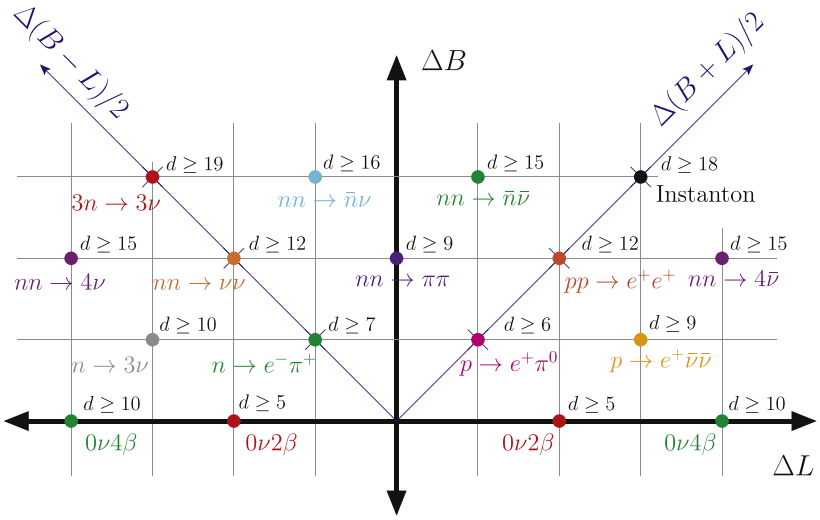

Figure 7. Process examples with baryon and lepton number violation by ΔB and ΔL units, respectively. 'Instanton' refers to processes that break the same quantum numbers as non-perturbative electroweak instantons. $0\nu2(4)\beta$ refers to neutrinoless double (quadruple) beta decay. The minimal mass dimension d of the underlying effective operator is shown. Operators also carry flavor. Reproduced from [358].

constrained by two-body nucleon decays such as $p \to e^+\pi^0$. At dimension > 6, non-trivial lepton number $\Delta L \neq 0$ allows to enforce dominance of some operators (e.g. [295]). ΔB and ΔL are connected through the dimensionful operators (e.g. [307, 357]). Higher dimensional operators can also often lead to multi-body channels, such as $n \to K^+\mu^+e^-e^-$ at dimension-9, or multi-nucleon decays with $\Delta B > 1$ [358]. One can use limits on rates for $p \to \ell^+M$ and $n \to \bar{\nu}M$, where M denotes a pseudoscalar or vector meson to obtain indirect limits on rates for $p \to \ell^+\ell'^+\ell'^-$, $n \to \bar{\nu}\ell^+\ell'^-$, $p \to \ell^+\nu\bar{\nu}$, and $n \to \bar{\nu}\bar{\nu}\nu$ [361]. Figure 7 displays characteristic examples of processes with distinct ΔB and ΔL structures.

2.7. Discrete symmetries and supersymmetry

B-violation processes appear in many extensions of the SM, a notable example being supersymmetric (SUSY) theories. Already in the MSSM realization nucleon decay-mediating dimension-4 operators QLd^c and $u^cd^cd^c$ appear, where Q, L are left-chiral quark and lepton doublets and u^c, d^c are the u-type, d-type superfields, respectively. To forbid rapid proton decay through these interactions, models often impose a Z_2 symmetry called R-parity (matter parity) (e.g. [41]). However, at dimension-5, one encounters nucleon decay-mediating $QQQL$, which can be forbidden by 'proton hexality' Z_6 symmetry that contains R-parity as a subgroup [362]. Since all global symmetries are expected to be violated at some level [363], it is appealing to consider discrete gauge symmetries. Such symmetries can appear as remnants of spontaneously broken local $U(1)$ symmetries [364]. Thus, care must be taken to ensure anomaly cancellation. Favorable discrete symmetries that allow for rich phenomenology, resolve theoretical puzzles (e.g. μ-problem) and forbid dangerously rapid nucleon decay have been identified, such as those of [362, 365–368]. Discrete (gauge) symmetries can also be considered in the context of GUT models.

Unlike the SM, the baryon and lepton numbers are no longer accidental symmetries of the classical Lagrangian in the MSSM. In the most general supersymmetric theory, gauge-invariant terms that violate baryon and lepton numbers are allowed, which are

$$W_{\Delta L=1} = \lambda_{ijk} L_i L_j \bar{e}_k + \lambda'_{ijk} L_i Q_j \bar{d}_k + \mu'_i L_i H_u, \tag{2}$$

$$W_{\Delta B=1} = \lambda''_{ijk} \bar{d}_i \bar{d}_j \bar{u}_k, \tag{3}$$

where standard notation of chiral superfields of the MSSM are used and i, j, k are family indices. The chiral supermultiplets carry baryon (lepton) numbers $B = +1/3$ for Q_i and $B = -1/3$ for $\bar{u}$, $\bar{d}$ ($L = +1$ for L_i and $L = -1$ for $\bar{e}_i$). Subsequently, the terms in equation (2) violate total lepton number by one unit, and terms in equation (3) violate total baryon number by one unit. If both λ' and λ'' are present and are unsuppressed, then the lifetime of the proton would be extremely short. In the low-energy MSSM model, one forbids these terms by imposing a new discrete symmetry, known as '*R*-parity' [369]. One can allow some of the R-parity-violating (RPV) terms while still avoiding excessively rapid proton decay, and these could lead to $|\Delta L| = 2$ decays such as $K^+ \to \pi^- \mu^+ \mu^+$ and $K^+ \to \pi^- \mu^+ e^+$; thus upper bounds on the branching ratios for these decays can be used to obtain upper bounds on the coefficients of certain RPV terms [341].

Here we consider the possibility of only baryon number violation. Therefore, the only non-zero term in the above superpotential we allow is $\bar{d}_i \bar{d}_j \bar{u}_k$. The associated coupling λ''_{ijk} is antisymmetric in the first two flavor indices, leading to in total nine couplings λ''_{dsu}, λ''_{dbu}, and so on. Due to this antisymmetric nature, coupling to three quarks of the first generation is absent; this is why $n - \bar{n}$ oscillation is highly suppressed. However, there exist stringent bounds on these couplings coming from dinucleon decay [370–376]. For example, let us consider the coupling λ''_{dsu}, which violates baryon number by one unit and strangeness by one unit; however, it conserves $B - S$. Hence it is easy to understand that the best bound comes from dinucleon decay into two mesons of identical strangeness via dimension-9 operators. Using the current limits of dinucleon decay to two kaons, $pp \to K^+ K^+$ for instance, Super-K provides a lower limit of $>1.7 \times 10^{32}$ years [377] (for pion final states, limits of similar order exist from Super-K [378]), and one obtains the following constraint on the RPV,

$$\lambda''_{dsu} < 10^{-16} \left(\frac{m_S}{\Lambda} \right)^{5/2}, \tag{4}$$

where m_S represents a common mass scale of SUSY particles and Λ is the hadronic scale. Dinucleon decays also appear in non-SUSY models, e.g., dinucleon decay to two kaons and dinucleon decay to leptons occur in a class of models studied in [329].

2.8. Implications of BNV for other BSM physics

2.8.1. Majorana nature of neutrinos. All fermions in the SM are charged, except neutrinos. Therefore, charged fermions are Dirac particles, whereas the nature of the neutrinos, whether Dirac or Majorana, is an unresolved question in particle physics. As is well known, observation of neutrinoless double beta decay would unambiguously establish the Majorana nature of neutrinos by virtue of the 'black box theorem' [379]; for a recent review on the status and prospects of neutrinoless double beta decay see [380]. However, if neutrinos have normal mass ordering with non-degenerate eigenvalues, the prospects of observing such decays are bleak in the near-future experiments. Interestingly, observation of BNV processes can independently confirm the Majorana nature of neutrinos. This provides additional motivation for experiments searching for nucleon decays and neutron-antineutron oscillation.

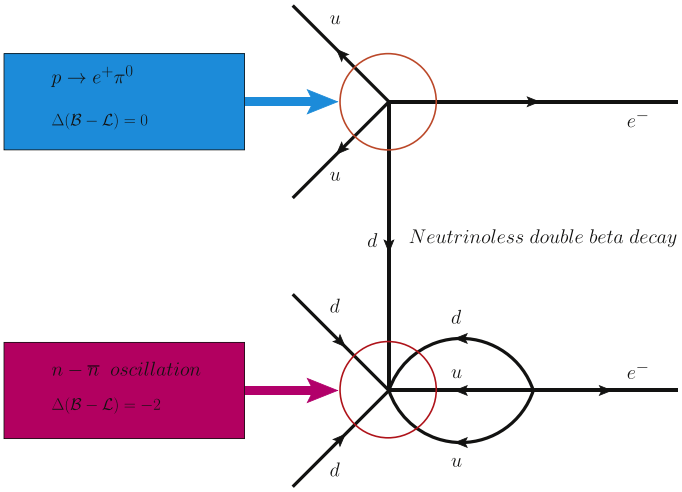

Figure 8. Neutrinoless double beta decay diagram originating from the BNV processes of proton decay and $n-\bar{n}$ oscillation obeying selection rules $\Delta(B-L)=0$ and $\Delta(B-L)=-2$, respectively. Observation of the latter two BNV processes would guarantee the Majorana nature of neutrinos.

As suggested in [381], baryon number violation in two processes with at least one obeying the selection rule $\Delta(B-L)=\pm 2$ can infer Majorana nature of neutrinos. As an example, consider two BNV processes: (i) $p\to e^+\pi^0$ ($|\Delta B|=1$) and (ii) $n-\bar{n}$ oscillation ($|\Delta B|=2$). The former and the latter processes correspond to $\Delta(B-L)=0$ and $\Delta(B-L)=-2$, respectively. Suppose both these BNV processes are observed in the experiments. In that case, neutrinoless double beta decay is guaranteed to exist just by combining these two vertices as depicted in figure 8. This would subsequently confirm the Majorana character of neutrinos. One can get to the same conclusion if instead (i) $p\to e^+\pi^0$ ($\Delta(B-L)=0$) and (ii) $n\to e^-\pi^+$ ($\Delta(B-L)=-2$) processes are considered [381]. In general, this is true for $p\to \ell^+ M^0$ and $n\to \ell^- M^+$, with ℓbeing e or μ and M being any light meson. The $0\nu\beta\beta$ lifetime arising from these BNV operators can be extremely long:

$$\tau_{0\nu\beta\beta} < \frac{\tau(p\to e^+\pi^0)}{10^{34}\ \mathrm{yr}}\frac{\tau(n\to e^-\pi^+)}{10^{32}\ \mathrm{yr}}\times 10^{113}\ \mathrm{yr}, \tag{5}$$

But the point is that it is finite, provided that $p\to e^+\pi^0$ and $n\to e^-\pi^+$ are observed. It is the finiteness of $\tau_{0\nu\beta\beta}$ that is essential to establish the Majorana nature of the neutrino. Other contributions to $0\nu\beta\beta$ generally exist, which would dominate over the nucleon decay mediated ones. However, these may still be below the experimental sensitivity (e.g. for normal ordering of neutrino masses), in which case the observation of the BNV processes mentioned above can be useful to infer the Majorana nature of the neutrinos.

Realistic SO(10) GUT models where both $B-L$ conserving and $B-L$ changing (by two units) decays of the nucleon are present can be found in [355, 356, 381]. It is also possible to get good fits to neutrino oscillation data in these models. Since nucleon decay in these well-motivated GUT models is within reach of ongoing and upcoming experiments, one can hope to resolve this outstanding puzzle (i.e. Majorana versus Dirac nature of neutrinos) by observing BNV processes, even if neutrinoless double beta decay is not directly observed by then.

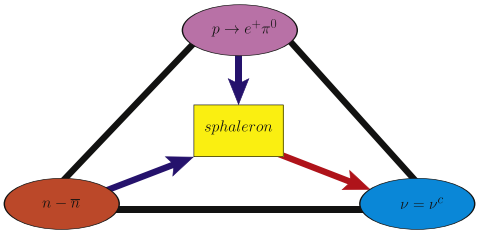

Figure 9. $B - L$ triangle [381] demonstrating how Majorana mass for neutrinos can be confirmed if BNV processes are observed.

We conclude this subsection by pointing out an interesting connection between BNV and Majorana neutrino mass via the weak instanton effects. Non-perturbative instanton/sphaleron configurations of weak interactions that lead to solutions to an effective operator involving twelve SM doublet fermions can be written as: $[uddudd] \cdot [uude] \cdot [\nu\nu]$. Of this operator, the first, second, and third pieces correspond to $n - \overline{n}$ oscillation, proton decay $p \to e^+\pi^0$, and Majorana neutrino mass, respectively. Therefore, if $p \to e^+\pi^0$ and $n - \overline{n}$ oscillation are observed, the sphaleron configuration would imply that neutrinos have Majorana masses; this non-trivial connection known as the '$B - L$ triangle' [381] is demonstrated in figure 9.

2.8.2. Leptogenesis. In the SM, baryon number and lepton number are accidental symmetries of the classical Lagrangian. However, B and L are exactly conserved only in perturbation theory and are not respected by non-perturbative effects. Sphaleron processes which are effective non-perturbative interactions constructed out of twelve left-handed SM fermions are the key to leptogenesis [155]. These interactions change baryon number B and lepton number L by a multiple of three ($\Delta B = \Delta L = 3N_{CS}$, where the integer N_{CS} is the Chern–Simons number characterizing the sphaleron gauge field configuration), but on the contrary, preserve $B-L$. Sphaleron processes are in thermal equilibrium in a wide range of temperatures: $T_{\rm EW} \sim 10^2\,{\rm GeV} \lesssim T \lesssim T_{\rm sph} \sim 10^{12}\,{\rm GeV}$ [8]; owing to these interactions, in Sakharov's conditions [300] for baryogenesis, lepton number violation can replace baryon number violation.

The existence of sphaleron processes typically divides models of baryogenesis into three categories depending on the energy scale when asymmetry is generated: (i) Leptogenesis: high scale L asymmetry generation after inflation that is converted to B asymmetry through sphaleron processes [155], (ii) Electroweak baryogenesis: phase transition dynamics at the electroweak scale coupled with new physics CP-violating sources near the EW scale (for a recent review see [382]), (iii) Post-sphaleron baryogenesis: new physics B-violating interactions occurring below the electroweak phase transition scale [311–313, 383]. Here we briefly discuss leptogenesis scenarios (for reviews on leptogenesis, see, e.g. [384–392]) that are inherently connected to neutrino mass generation via the seesaw mechanism [94–98].

The seesaw mechanism is the most natural candidate to explain tiny neutrino masses within the GUT framework or BSM frameworks with a local $B-L$ symmetry [310]. In this scenario, tiny neutrino masses arise due to the heaviness of right-handed partners. The heavy right handed neutrinos have Majorana masses breaking $B-L$ by two units which then gives a Majorana masses of light neutrinos. Neutrino mass in type-I seesaw is given by,

$$m^\nu = -m_D M_R^{-1} m_D^T, \tag{6}$$

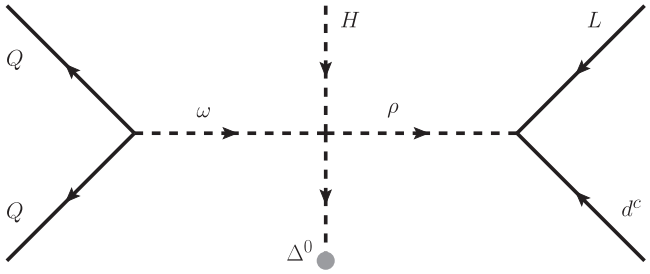

Figure 10. Effective $B-L$ violating dimension-7 nucleon decay operators induced by symmetric Yukawa couplings of **10** and $\overline{\mathbf{126}}$ Higgs fields of $SO(10)$.

where, $m_D = v/\sqrt{2}\ Y_\nu$ with Y_ν being the Dirac neutrino Yukawa coupling, and M_R is the right-handed neutrino mass. For order one Yukawa coupling for the neutrinos, one then obtains:

$$M_3 \sim 10^{15}\,\text{GeV} \sim M_{\text{GUT}}, \quad \Rightarrow m_3^\nu \sim 0.01\,\text{eV}, \tag{7}$$

consistent with neutrino oscillation data. In the vanilla leptogenesis scenario when N_1, the lightest of the right-handed neutrinos, decays into lepton-Higgs pairs, a lepton asymmetry in these CP-violating out-of-equilibrium decays are generated, which is then partially converted to baryon asymmetry by the sphaleron processes and the right amount [393] of matter-antimatter asymmetry of the Universe can be reproduced. Leptogenesis and its connection to absolute neutrino mass and neutrino mixing parameters in the context of $SO(10)$ GUTs are studied in [143, 394–396].

The CP-asymmetry from the right-handed neutrino decays can be estimated to be $\epsilon \sim m_\nu M_R/(16\pi v^2)$. A sufficiently large CP-asymmetry $\epsilon \gtrsim 10^{-7}$ to generate adequate baryon asymmetry imposes the so-called Davidson-Ibarra bound $M_R \gtrsim 10^9$ GeV [397]. However, if a pair of right-handed neutrinos are quasi-degenerate in mass, the CP asymmetry can be resonantly enhanced [398–400] (see also [399, 401–403]). Subsequently, the lower bound on M_R comes only from the requirement that sufficient baryon asymmetry is induced at $T > T_{sph}$. In this resonant leptogenesis scenario, right-handed neutrinos can have masses as low as sub-GeV to TeV range and low-scale seesaw models of this type have the virtue of being directly probed in experiments [390]. For implications of low-scale resonant leptogenesis from GUT, see e.g. [404].

2.8.3. Baryogenesis. The two leading proton decay modes, $p \to e^+\pi^0$ and $p \to \overline{\nu}K^+$ as extensively discussed above, both conserve $B-L$ symmetry (i.e. $\Delta(B-L) = 0$). For this reason, the minimal $SU(5)$ model does not have any way to explain the origin of matter even though it has both baryon number violation as well as CP violation. Sphaleron processes would wash out any baryon asymmetry generated in such models. However, going beyond these $d = 6$ operators, the next-to-leading BNV operators correspond to $d = 7$, an explicit computation of which for a class of $SO(10)$ models is given in [243], which break this symmetry by $\Delta(B-L) = -2$ and generate nucleon decay modes such as $p \to \nu\pi^+$, $n \to e^-\pi^+$, $n \to e^-K^+$. As mentioned above, spontaneous breaking of $B-L$ in $SO(10)$ GUTs is directly related to the neutrino mass generation. Intriguingly, in a class of $SO(10)$ GUTs (applicable to both non-SUSY and SUSY), these $d = 7$ nucleon decay modes for which the lifetime can be in the experimentally accessible range are inherently linked [355, 356] to the matter-antimatter asymmetry in the Universe. Due to their $B-L$ breaking nature, electroweak

Table 3. Possible DM candidates in $SO(10)$ GUTs. $SU(2)_L \times U(1)_Y$ multiplet that contains a neutral component is presented in the first column. The second (third) column lists representations that are even (odd) under P_M and contain a DM candidate are listed in the second (third) column. The triplet candidates with hypercharge ± 1 are shown for completeness; however, they are not viable as a DM candidates.

	Fermions	Scalars
DM multiplet $SU(2)_L \times U(1)_Y$	Even $SO(10)$ multiplet	Odd $SO(10)$ multiplet
1_0	**45**, **54**, **126**, **210**	**16**, **144**
$2_{\pm 1/2}$	**10**, **120**, **126**, **210**, **210′**	**16**, **144**
3_0	**45**, **54**, **210**	**144**
$3_{\pm 1}$	**54**, **126**	**144**

sphaleron processes would not wash out such a GUT-scale-induced baryon asymmetry; hence asymmetry generated would survive down to low temperatures. The VEV of $\overline{\mathbf{126}}$ Higgs breaks the $B-L$ generator of the $SO(10)$ and provides a large Majorana mass for right-handed neutrinos as well as generates trilinear scalar couplings that induce $d=7$ nucleon decay operators; an example diagram is presented in figure 10. In this figure, a trilinear coupling $\omega H \rho^*$ is induced via VEV insertion of a $\Delta(1, 1, 0)$ scalar that breaks the $B-L$ generator. Here, the quantum numbers of these fields are: $\omega(3, 1, -1/3)$, $H(1, 2, 1/2)$, $\rho(3, 2, 1/6)$ and this term originates from a quartic coupling in the scalar potential of the form 126^4, which is gauge invariant. From the left (right) vertex in the Feynman diagram figure 10, it can be understood that ω (ρ) has $B-L=-2/3$ ($B-L=+4/3$); this clearly dictates that the associated trilinear coupling leads to the decay $\omega \to H^* \rho$ which violates $B-L$ by -2. Thus, when tree as well as loop diagrams for the decay $\omega \to H^* \rho$ are combined, a net $B-L$ asymmetry is generated. This GUT-scale-induced baryon asymmetry in $\omega \to H^* \rho$ decay that has deep correlations with neutrino mass generation and nucleon decay is shown [355, 356] to correctly reproduce the observed baryon-to-entropy ratio in the Universe.

2.8.4. DM. The natural appearance of DM in SUSY GUTs has already been mentioned. Here we briefly discuss some DM candidates in non-SUSY GUTs. There are a large number of DM candidates in the literature, and a comprehensive review of these models is beyond the scope of this white paper.

It is remarkable that GUTs based on $SO(10)$ gauge symmetry automatically contain matter parity $P_M = (-1)^{3(B-L)}$, as a discrete subgroup that can naturally stabilize the DM without the need for imposing ad hoc symmetries by hand. To be specific, stability of the DM is guaranteed by the discrete subgroup $Z_2^{3(B-L)}$ of $U(1)_{B-L} \subset SO(10)$ [405–408] that typically arises when the intermediate group $G_{\rm int}$ breaks to the SM group $G_{\rm SM}$ [409]:

$$SO(10) \to G_{\rm int} \to G_{\rm SM} \times Z_2. \tag{8}$$

The smallest representation in SO(10) that can realize this symmetry breaking pattern (i.e. with a remnant Z_2 symmetry) is **126**, which can also be used to generate Majorana masses for right-handed neutrinos as discussed above.

Under the matter parity, only the **16**- and **144**-dimensional representations are odd, whereas the rest of them are even (here, we restrict ourselves to representations not bigger than **210**). Given the fact that the SM Higgs doublet residing in a **10**-dimensional representation is even while a **16**-dimensional representation containing fermions of each generation is odd, the lightest component of an additional even fermion or an odd scalar multiplet will be stable due to the residual Z_2 symmetry [175, 409–414]. However, this

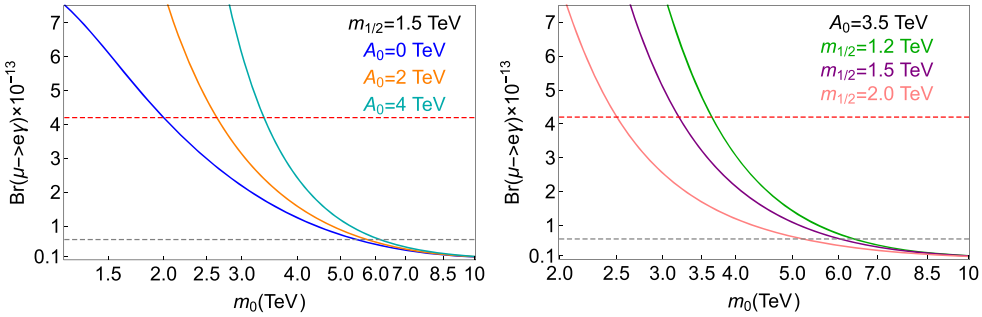

Figure 11. Branching ratio of $\mu \to e\gamma$ is presented for SUSY $SO(10) \times U(1)_{\rm PQ}$ model of [150]. The red horizontal dashed line corresponds to the current upper bound BR $(\mu \to e\gamma) < 4.2 \times 10^{-13}$ by the MEG experiment and the gray horizontal dashed line represents the projected sensitivity $\mathrm{BR}(\mu \to e\gamma) < 6 \times 10^{-14}$ by the MEG II experiment [419].

stability will be lost if a Higgs in the **16**-dimensional or **144**-dimensional representation acquires a VEV. This leads to the list of possible DM candidates in $SO(10)$ GUTs given in table 3. DM candidates have also been presented in the context of extra-dimensional models (e.g. [327, 328].

2.8.5. Flavor violation. It is widely known that low-energy SUSY models with arbitrary mixings in the soft breaking parameters would lead to unacceptably large flavor-violating effects (e.g. [415, 416]). It is essential to assume flavor universality in the mechanism that breaks SUSY to be consistent with experimental observations. Starting with flavor-universal SUSY breaking boundary conditions at a high scale, running effects of the renormalization group equations (RGEs) can still induce sizable flavor mixings in soft breaking parameters that lead to extensive flavor violations at low energies. Many constraining flavor-violating processes arise in the leptonic sector and are inherently connected to neutrino parameters. In $SO(10)$ GUTs, Dirac neutrino Yukawa couplings Y_ν induce observable lepton flavor violations (LFVs) that put strong constraints on SUSY breaking parameters [417, 418]. Present experimental bounds on some of the most important LFV processes are [13]:

$$\mathrm{BR}(\mu \to e\gamma) < 4.2 \times 10^{-13}, \quad \mathrm{BR}(\mu \to eee) < 1.0 \times 10^{-12}, \tag{9}$$

$$\mathrm{BR}(\tau \to e\gamma) < 3.3 \times 10^{-8}, \quad \mathrm{BR}(\tau \to eee) < 2.7 \times 10^{-8}, \tag{10}$$

$$\mathrm{BR}(\tau \to \mu\gamma) < 4.4 \times 10^{-8}, \quad \mathrm{BR}(\tau \to \mu\mu\mu) < 2.1 \times 10^{-8}. \tag{11}$$

In the RG evolution of the left-handed slepton soft-masses $(m^2_{\tilde{L}})_{ij}$, flavor violating off-diagonal entries are induced that are proportional to $Y_\nu Y_\nu^\dagger$:

$$(\Delta^{\ell}_{LL})_{ij} = -\frac{3m_0^2 + A_0^2}{8\pi^2} \sum_{k=3}^{3} (Y_\nu)_{ik} (Y_\nu^*)_{kj} \ln\left(\frac{M_{\rm GUT}}{M_{R_k}}\right), \tag{12}$$

where M_{R_k} are the heavy right-handed neutrino masses. Assuming scalar mass universality and gaugino mass unification as is usually done in cMSSM, there exist only a few parameters in the SUSY breaking sector: $\{m_0, m_{1/2}, A_0, \tan\beta, \mathrm{sgn}(\mu)\}$. Here m_0 and $m_{1/2}$ are the universal SSB scalar and gaugino masses, respectively; A_0 is the universal tri-linear coupling and μ the Higgs mass term, which is determined from EWSB condition. The fit to fermion

spectrum in a specific GUT fully determines $\tan\beta$ as well as Y_ν and the right-handed neutrino masses M_{R_k}. Consequently, one can compute the rates for LFV processes as functions of the remaining SUSY breaking parameters: $\{m_0, m_{1/2}, A_0\}$ (in this way, the gaugino, slepton, and squark masses are expressed in terms of $\{m_0, m_{1/2}, A_0\}$). Such correlations within a minimal $SO(10)$ GUTs are presented in figure 11; for details see [150]. Quark flavor violating processes such as $K^0 - \overline{K}^0$ mixing, $b \to s\gamma$, etc also put strong constraints on SUSY breaking parameters. For a systematic study of constraints on Yukawa couplings due to GUT relations and finding correlations between constraints on flavor violation between the lepton and quark sectors, see [418].

2.8.6. Gravitational wave production. After the great success of the direct observation of gravitational waves (GWs) by the LIGO collaboration [420], GW detection has been considered to be a powerful probe of new physics that complements experiments in particle physics. BNV effects are usually associated with new symmetries (e.g. those preserving $B-L$) at high scales. Spontaneous breaking of these symmetries may generate gravitational radiation in the early Universe, which appears as cosmic GW background today. The GW exploration will be very helpful to understand these processes and any new physics behind them. Here we discuss potential sources of GWs generated from BNV-related physics: GWs via cosmic strings generated from intermediate symmetry breaking in GUTs and those via first-order phase transition.

The production of cosmic strings is another important prediction for most GUTs in addition to proton decay. GUTs beyond $SU(5)$ provide a series of intermediate symmetries before breaking down to the SM. The spontaneous breaking of the GUT symmetry to the SM gauge symmetry occurs in several steps, and topological defects are produced accompanied by the symmetry breaking. Those defects include monopoles, domain walls and cosmic strings [421]. The former two are problematic as they would come to dominate the energy density of the Universe. This problem is solved by including a period of inflation after their production. The production of cosmic strings is usually associated with the breaking of a $U(1)$ symmetry, which appears as a subgroup of $SO(10)$ or larger groups [422]. These strings, if produced after inflation, evolve to a network. The network follows a scaling solution during the Hubble expansion and the energy density does not overclose the Universe [423–425].

Strings in the network intersect to form loops. Cusps and oscillations of loops release energy via gravitational radiation, which forms a stochastic background today [426–428]. The GW density parameter $\Omega_{\rm GW} \equiv \rho_{\rm GW}/\rho_c$, where ρ_c is the critical energy density of the Universe, appears with a characteristic spectrum that drops in the low frequency, peaks in the middle and flattens in the high frequency [429]. $\Omega_{\rm GW}$ is directly determined by the string tension μ, which represents the energy per unit length of the string. In the high frequency band, $\Omega_{\rm GW}$ follows a simple correlation with the string tension, $\Omega_{\rm GW}(f) \propto (G\mu)^{1/2}$, where G is the Newton constant [430]. In the future, a series of undergoing or planned GW observatories such as LIGO [431], SKA [432], LISA [433], Taiji [434], TianQin [435], BBO [436], DECIGO [437], Einstein Telescope [438] (ET), Cosmic Explorer [439] (CE), MAGIS [440], AEDGE [441], and AION [442] have the potential to explore $\Omega_{\rm GW}$ in a wide range $\sim 10^{-15}$–10^{-7}, referring to $G\mu \sim 10^{-19}$–10^{-11} and the new physics scale $\sim\sqrt{\mu} \sim 10^9 - 10^{13}$ GeV following the result of Nambu-Goto string simulation [429].

The measurement of the cosmic GW background provides a novel way to probe grand unification [443, 444]. It is worth mentioning that the new physics scale probed by GW measurements is usually not the GUT scale M_X, but an intermediate scale between M_X and the electroweak scale [445]. This scale is not arbitrary, but correlated with M_X via the unification

of gauge couplings. Measuring proton decay in neutrino experiments can determine both M_X and the intermediate scale as well as $G\mu$. For example, given the lower bound $\tau(p \to \pi^0 e^+) \gtrsim 1.6 \times 10^{34}$ years from Super-K [446], restrictions on $G\mu$ in the following typical breaking chains are obtained,

$$\begin{aligned} SO(10) &\to G_{3221}^{\not{D}} \to \mathcal{G}_{\rm SM}\colon\ G\mu \simeq 2.0 \times 10^{-17}, \\ SO(10) &\to G_{422}^{D} \to G_{3221}^{\not{D}} \to \mathcal{G}_{\rm SM}\colon\ G\mu \simeq 2.0 \times 10^{-17} - 8.4 \times 10^{-15}, \\ SO(10) &\to G_{422}^{D} \to G_{3221}^{D} \to G_{3221}^{\not{D}} \to \mathcal{G}_{\rm SM}\colon\ G\mu \simeq 2.0 \times 10^{-17} - 1.3 \times 10^{-10}, \end{aligned} \tag{13}$$

where D in the upper case refers the left–right matter parity symmetry and the minimal particle content consistent with the SM and neutrino masses have been considered [447]. Once any proton decay signal is confirmed in next-generation neutrino experiments, GW measurement provides a good opportunity to study the details of GUT breaking. Note that the the spontaneous breaking of the lowest intermediate gauge symmetries for all chains in equation (13) also leads to the U_{B-L} breaking. It provides a window to connect GW signals with the Majorana nature of neutrinos and to test leptogenesis via seesaw mechanism [448].

For the symmetry breaking scale below 10^8 GeV, a strong first-order phase transition might provide a compelling source of observable GW signals. During the phase transition, bubbles of the broken phase nucleate and expand in the Universe. The collision of the bubbles and the resulting motion of the ambient cosmic fluid provides a source of a stochastic background of GWs that can be observable at GW observatories [449].

The GW spectrum is in general given by the sum of three contributions: bubble wall collisions, sound waves and hydrodynamic turbulence (see [449, 450] for recent reviews). Despite the energy budget, the spectrum has a generic feature: a peak in the middle and polynomial suppressions in both low and high frequencies. It is distinguishable with that from cosmic strings as there is no plateau in the high frequency band. The frequency at the peak depends on the phase transition temperature linearly. In addition to the temperature, two more parameters are crucial to determine the GW spectrum: α the ratio of the released latent heat during the phase transition to the total energy density and $\beta/H_\star$ the ratio of the inverse duration of the phase transition to the Hubble rate. α dominates the GW strength. Enhancing α by one order of magnitude can enhance the GW strength by several orders of magnitude. $\beta/H_\star$ influences both the strength and frequency of GW. Faster the phase transition proceeding, higher frequency of the GW signal is expected. Theoretical efforts have been made to enhance $\alpha \to \mathcal{O}(0.1)$ and reduce $\beta/H_\star \to \mathcal{O}(10^2 - 10^3)$ such that part of the parameter space of B- or L-violating new physics can be reached by the exploration of next-generation GW interferometers (see, e.g. discussions in [451–457]).

2.9. Lattice developments

Rates of proton decays and neutron oscillations depend on nucleon and nuclear matrix elements of effective baryon number-violating operators. Prior to development of lattice QCD methods, these matrix elements were initially calculated with various nucleon models. However, eliminating theory uncertainties completely requires *ab initio* QCD calculations on a lattice with physical quark parameters. Calculations of proton decay amplitudes have been pursued since simulating nucleons on a lattice became possible, with methodology gradually improving over the last three decades. Neutron oscillation amplitudes were studied only relatively recently, when realistic lattice QCD calculations were already feasible.

Apart from the usual systematic effects inherent in lattice QCD calculations (discretization, finite volume, etc), calculations of BNV amplitudes are complicated by the need to preserve

chiral symmetry of the quarks. Since the effective proton decay and neutron oscillation operators contain chiral quark fields, using a simple fermion discretization such as Wilson action may lead to undesirable mixing of operators on a lattice. This mixing would complicate renormalization and introduce additional systematic effects. Fortunately, formidable progress has been made towards lattice calculations with chiral fermions at the physical point [458–460].

Amplitudes of $p \to \bar{\ell}\pi$, $p \to \bar{\ell}K$ decays may be computed on a lattice *directly* as matrix elements between the proton and a meson. Such calculations have initially been performed in quenched QCD with Wilson valence quarks [461] and DWF quarks [462], and later in unitary QCD with $N_f = 2 + 1$ flavors of DW fermions [463, 464]. All these calculations have been performed with unphysical masses of light quarks corresponding to pion masses $m_\pi \gtrsim 300\,\text{MeV}$, and required some form of chiral extrapolation to the physical point. Although these amplitudes did not exhibit strong pion mass dependence, applying chiral perturbation theory (ChPT) to baryons is often questioned, and proton decay amplitudes have not been computed in ChPT beyond the leading order. In the framework of the chiral-bag proton model, it has also been suggested that the proton decay matrix elements may depend dramatically on the light quark masses [465]. These deficiencies have been addressed in the recent work [466], in which the proton decay amplitudes have been calculated with 10%–20% precision using chirally symmetric DW fermions at the physical point, albeit with relatively coarse lattice spacing $a \gtrsim 0.14\,\text{fm}$. The physical-point results are largely in agreement with previous calculations, and no suppression at light-quark masses has been observed.

The proton-to-meson transition amplitudes can also be *'indirectly'* estimated from proton-to-vacuum proton decay constants α, β [467] using the leading-order chiral Lagrangian. These decay constants have been computed using quenched QCD with Wilson quarks [468–470] and Domain Wall quarks [462], as well as in unitary QCD with dynamical DW fermions [464, 466, 471]. The 'indirect' estimates of proton decay amplitudes are typically higher than the 'direct' results, which is likely attributable to pion loop effects. A calculation with next-to-leading order ChPT is highly desirable to understand this discrepancy. The proton-to-vacuum decay constants are also highly important to analysis of $p \to \mu^- e^+ e^+$ and $p \to e^- \mu^+ \mu^+$ proton decays.

A particular BSM theory yields predictions for the effective scale of the physics contributing to n-$\bar{n}$ oscillations and predictions for the coefficients of the various six-quark operators $\mathcal{O}_i$ contributing to these oscillations. To calculate the expected rate of n-$\bar{n}$ oscillations in a given model, one then needs to compute the matrix elements $\langle \bar{n}|\mathcal{O}_i|n\rangle$. These matrix elements have dimensions of $(\text{mass})^6$, and since at the hadronic level, the only important mass scale in the problem is $\Lambda_{QCD} \simeq 250\,\text{MeV}$, it follows that the matrix elements are $\sim\Lambda_{QCD}^6$. Early calculations of the n-$\bar{n}$ matrix elements were performed using the MIT bag model [306, 307]. Recently, these matrix elements have been calculated using lattice QCD [472, 473]. This calculation has been performed on a lattice with chirally symmetric action at the physical point, and the operators have been renormalized using two-loop perturbative anomalous dimension [474]. As examples, for one operator, denoted Q_5 in [472], the lattice QCD calculation (normalized at 2 GeV) yielded a value in agreement with the MIT (fit A) value, while for other operators, the lattice QCD calculation yielded values larger in magnitude by up to an order of magnitude. Since the general amplitude for n–$\bar{n}$ oscillations has contributions from several different operators and since the matrix elements of these operators have different signs, there can be destructive interference, so that one cannot make a statement about the overall size of the n-$\bar{n}$ transition amplitude from a knowledge of individual matrix elements of operators without knowing the details of a given UV model predicting which operators occur and the values of the coefficients of these operators. Nevertheless, the lattice

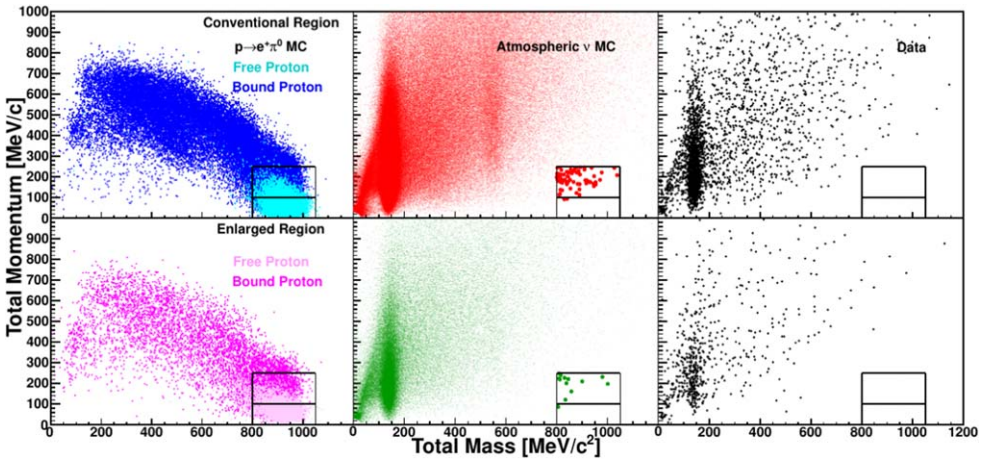

Figure 12. The search for $p \rightarrow e^{+}\pi^{0}$ in 450 kton-y of Super-Kamiokande data[55]. The leftmost panels show the results of simulated proton decay, where the nuclear effects that degrade the signal for proton decay in ^{16}O are distinct from the low momentum events from the decay of the free hydrogen nuclei. The center panels show the predicted background due to atmospheric neutrino interactions. The rightmost panels show the SK experimental data. The upper row represents the original fiducial volume, used in the majority of Super-K publications, requiring the interaction vertex to be 200 cm from the PMT plane. The lower row represents the additional fiducial volume that is between 100 cm and 200 cm from the PMT plane.

QCD calculations of these matrix elements are valuable inputs for the analysis of the predictions of a given BSM model for n–$\bar{n}$ oscillations.

Finally, lattice calculations of proton decay and neutron oscillation amplitudes inside nuclei may soon become feasible [475, 476]. Although lattice simulation of nuclei requires substantially more resources due to the sign problem, development of exascale computing resources over the next decade is expected to make *ab initio* calculations of nuclear matrix elements possible.

3. Experimental overview

This section summarizes results and sensitivities for baryon number violation searches for currently running, planned, and proposed neutrino detectors, as well as some avenues for potential improvement in nuclear modeling and detection techniques for future detectors. A comparison of current limits and future sensitivities for important modes are shown in table 1.

3.1. Super-K

The Super-Kamiokande neutrino detection experiment represents the 2nd generation of large water Cherenkov neutrino and nucleon decay experiments, following Kamiokande and IMB which ran in the 1980s and 1990s. Super-K (also SK) is currently running and has been in operation since 1996. The experiment addresses major neutrino topics such as atmospheric neutrino oscillation, solar neutrino oscillation, gravitational collapse supernova bursts in the Milky Way galaxy, searching for the diffuse background of supernova neutrinos, and indirectly searching for DM via annihilation or decay to neutrinos. The SK detector is also the

Table 4. Selected BNV searches by Super-Kamiokande.

Channel	Comment	Exposure	Limit	Reference
$p \to e^+\pi^0$	$d=6$ operators, e.g. SU(5)	450 kt·yrs	2.4×10^{34} years	[55]
$p \to \mu^+\pi^0$	flipped SU(5)	450 kt·yrs	1.6×10^{34} years	[55]
$p \to \nu K^+$	$d=5$ SUSY operators	260 kt·yrs	5.9×10^{33} years	[478]
$p \to \mu^+K^0$	SUSY SO(10)	173 kt·yrs	1.6×10^{33} years	[480]
$pp \to K^+K^+$	RPV SUSY	92 kt·yrs	1.7×10^{32} years	[377]
$p \to e^+e^+e^-$	lepton flavor symmetries	370 kt·yrs	3.4×10^{34} years	[481]
$n \to \bar{n}$	$\Delta B=2$	370 kt·yrs	3.6×10^{32} years	[332]
$np \to \tau^+\nu$	extended Higgs sector	273 kt·yrs	2.9×10^{31} years	[482]
$n \to \nu\gamma$	radiative	273 kt·yrs	5.5×10^{32} years	[482]
$p \to e^+\nu\nu$	Pati-Salam	273 kt·yrs	1.7×10^{32} years	[298]

far detector for the T2K long-baseline neutrino oscillation experiment. The interaction target is 22.5 to 27.2 ktons of ultrapure water in a cylindrical stainless steel tank located 1 km underground in the Kamioka mine in Japan. The target mass is viewed by 11, 000 50 cm photomultiplier tubes (PMTs), and is surrounded by an optically isolated active veto of roughly 2 m of water viewed by 1, 800 PMTs. Since 2020, the detector water system has been upgraded to allow gadolinium sulfate in solution to enhance the capture and detection of neutrons [477]. This Super-Kamiokande detector naturally enables the search for a variety of baryon number violation processes in the same target mass, with only atmospheric neutrinos as a competing background. Foremost are searches for nucleon decay, often cited as one of two possible meanings embedded in the Super-Kamiokande name: **N**ucleon **D**ecay **E**xperiment.

Unfortunately for fans of new physics, the SK experiment has not detected any signs of nucleon decay. The extensive exposure, 450 kt-yr in a recent publication, sets a high bar for future experiments to overcome. For example, the lifetime lower limit for $p \to e^+\pi^0$ is now at 2.4×10^{34} years based on a recent analysis that uses several improvements over older publications [55]. The improvements include: background reduction by tagging events where neutron capture on hydrogen is detected nearby the interaction, expansion of the fiducial volume from 22.5 to 27.2 ktons, and dividing the search region into a section where the nearly background-free decay of the free proton in H_2O is accentuated. The simplicity and clarity of this search is illustrated in the three-panels of figure 12, showing the low background region at high invariant mass and low net momentum (note the extremely low expected background of the free proton region), and the absence of any data events in that region.

Overall, the Super-K experiment has published leading limits on 30 BNV processes including: an extensive survey of antilepton plus meson final states that conserve $(B-L)$, dinucleon decay modes that violate baryon number by two units, and three-body decay modes including those with fully leptonic final states. Special attention has been given to decay channels favored by SUSY, which are distinguished by the presence of a kaon in the final state. The most recent published limit for the key decay mode $p \to \bar{\nu}K^+$ is 5.9×10^{33} years based on an exposure of 260 kt-yr [478], but a preliminary result of 8×10^{33} years has been reported in conferences. In addition, Super-K holds the leading limit on the interesting $\Delta B = 2$ process of neutron oscillation into anti-neutron within the oxygen nucleus [332]. This may be converted to an effective free $n - \bar{n}$ lifetime of 4.7×10^8 s, which is comparable to

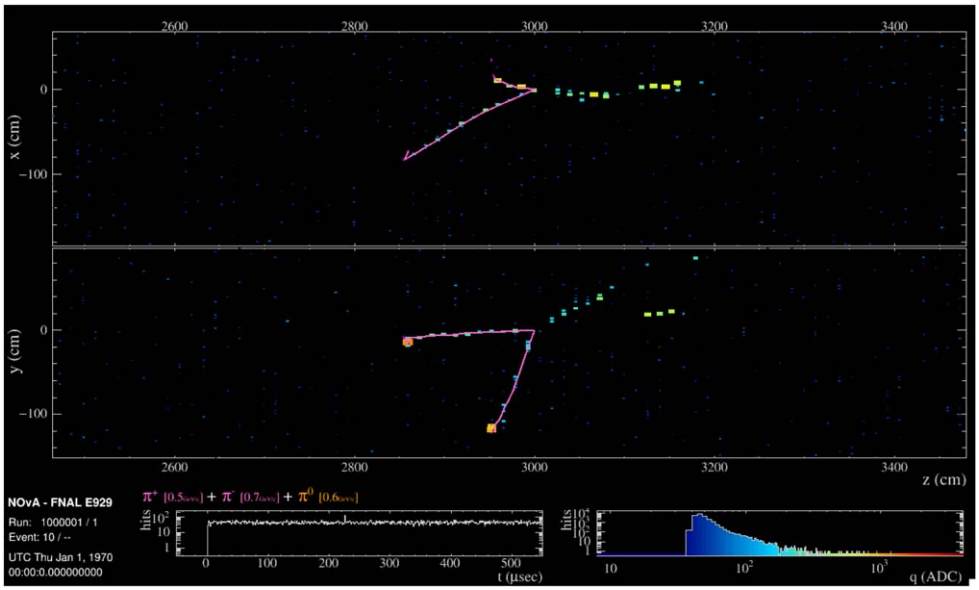

Figure 13. Simulation of neutron-antineutron oscillation in a carbon nucleus in the NOvA Far Detector, yielding $\pi^+\pi^-\pi^0$. The purple lines show the true trajectories of the charged pions.

(slightly exceeding) the leading free neutron experiment [479]. Table 4 lists a sample of published limits.

Major improvement in sensitivity to lifetimes much beyond the limits listed here await the next generation of more massive detectors. Until then, operation of the Super-K experiment with concomitant data analysis will provide incremental progress but valuable methodological developments. Ongoing studies of nucleon decay include continued development of reconstruction techniques, refinement of the intranuclear simulations relevant to both signal and background, first studies of algorithms for neutron capture on gadolinium, and new searches for novel modes.

3.2. Neutron-antineutron transformations in NOvA

The NOvA Far Detector is sensitive to the spontaneous conversion of neutrons to antineutrons. Since all neutrons in NOvA are bound in nuclei, the resulting antineutron would immediately annihilate on a neutron or proton, typically yielding three to six pions. The experimental signature is therefore a star with approximately zero net momentum and a visible energy typically between 0.8 and 1.5 GeV, depending on the mode (see figure 13).

Neutron-antineutron oscillations are suppressed in nuclei by a factor R such that $t_{\rm free} = \sqrt{t_{bound}/R}$, where $t_{\rm free}$ is the free neutron oscillation time. The suppression factor varies by nuclide. About half of the neutrons in NOvA are bound in carbon nuclei, with the majority of the remainder in chlorine. Although no calculations exist for these elements, one calculation of R for oxygen gives $0.517 \times 10^{23}\ \mathrm{s}^{-1}$ [331, 333]. Likely the suppression factor for carbon is somewhat lower than for the larger oxygen nucleus, so there is a possibility that the effective suppression for NOvA as a whole is lower than for a water-based detector, allowing NOvA to set stronger limits on $t_{\rm free}$, all other things being equal.

Table 5. The number of entities for each reconstruction and selection stage. The numbers are evaluated using a simulation sample that corresponds to roughly 10 times the MicroBooNE 372 s exposure. The selection efficiency indicates the ratio between the 'Events' and 'Events (after final-selection)'.

Entities	$n - \bar{n}$	Cosmic
Events	1633 525	1618 827
Reconstructed clusters	1684 516	14 857 224
Clusters (after pre-selection)	1455 214	1283 074
Clusters (after final-selection)	1207 153	142
Events (after final-selection)	1202 281	142
Selection efficiency (%)	73.6	8.77×10^{-3}

NOvA must confront a significant background due to its surface location with only 3.6 meters water-equivalent overburden. Since 2018, NOvA has run a dedicated trigger searching for neutron-antineutron-like events. By the end of the planned NOvA run in 2026, 112 kt-years of data will have been collected. To reduce background from cosmic rays, the trigger requires candidates to be contained, to have a similar extent in z as they do in y (unlike downward-going cosmic rays), to have only short tracks that could be produced by pions of the expected energy, to have a total physical size and number of hits consistent with a neutron-antineutron oscillation event, and finally to be symmetric between the xz and yz views.

Backgrounds to this search include atmospheric neutrinos and cosmic rays. On the surface, cosmic rays are the more challenging background. We expect that the most difficult to exclude will be from neutrons and gammas produced in the overburden or rock berms adjacent the detector. Two approaches are being pursued to study these backgrounds: first, a data-driven approach using the energy sidebands above and below the expected signal visible energy, and second, a simulation using CORSIKA [483].

The analysis to search for neutron-antineutron events in triggered data is under development. Further information available to an offline event classifier includes more sophisticated measures of event symmetry, calibrated hit energies, event time duration, and various reconstructed track variables. Using a convolutional neural network (CNN) to distinguish between neutron annihilation events and cosmic rays, as is planned for DUNE [484], is also a possibility. If successful in suppressing cosmic ray backgrounds below the level of atmospheric neutrino backgrounds, NOvA will achieve a sensitivity on the free neutron oscillation time of somewhat longer than 10^8 s at 90% C.L.

3.3. MicroBooNE

The MicroBooNE detector is an 89 ton active Liquid Argon Time Projection Chamber (LArTPC) detector located on-surface and exposed to neutrinos from the Booster Neutrino Beamline and Neutrinos at Main Injector beamline at Fermilab. The excellent spatial and calorimetric resolution offered by MicroBooNE's LArTPC, also shared by the future DUNE, enables precise measurements of neutrino scattering as well as BSM searches, including intranuclear neutron-antineutron transitions. In a LArTPC, this process is characterized by a unique and striking star-like signature containing multiple final-state pions from the anti-neutron annihilation with a nearby nucleon. The pions are visible as tracks (from charged pions) or showers (from neutral pion electromagnetic decays) pointing back to the

Table 6. 90% C.L. sensitivity for argon-bound $n - \bar{n}$ transition lifetime assuming 372 s of exposure in MicroBooNE, considering only statistical uncertainties.

Source of Uncertainty	Sensitivity (Rolke)
Statistical-only	3.09 e + 25 years

annihilation vertex, with approximately zero net momentum and total energy of about twice the nucleon mass.

Although MicroBooNE is too small in size and too overwhelmed with cosmogenic background to perform a competitive search, it aims to perform the first ever search for neutron-antineutron ($n - \bar{n}$) transitions in a LArTPC, which will serve as a proof-of-principle demonstration of LArTPC capabilities in searching for this process. The analysis MicroBooNE has developed [485] makes use of state-of-the-art reconstruction tools, including deep learning methods developed for LArTPC image data analysis, to look for neutron-antineutron transition signatures in data collected during neutrino beam-off times. The signal events are simulated using the GENIE Neutrino MC Generator (GENIE) v.3.00.04 with hA-Local Fermi Gas (hA-LFG) as a default model, while backgrounds are expected to be contributed by cosmogenic activity during multiple 2.3 ms intervals of exposure (corresponding to a total of 372 s) and are evaluated using a data-driven approach. The signal interaction is simulated per one exposure interval of 2.3 ms, which also contains multiple reconstructed clusters of cosmogenic activity.

Pre-selection is applied to all clusters reconstructed during 2.3 ms intervals ('events') based on a Boosted Decision Tree (BDT) score, to control the background rate and remove obvious backgrounds (cosmics). The BDT is trained using only the topological information derived from the extent of the reconstructed clusters in channel and time space. As shown in table 5, pre-selection reduces the cosmic background clusters such that the number of $n - \bar{n}$ clusters and cosmic clusters per 2.3 ms interval become of the same order. The pre-selected clusters are subsequently used to train a sparse CNN to differentiate signal from background clusters. For this step, 2D projections of clusters from MicroBooNE's three planes (U, V, Y) are formatted in such a way so as to retain only the important pixels, out of the full image, in the form of a collection of spacepoints containing information of wire position, time-tick and charge deposition per spacepoint. Considering statistical-only sensitivity as a figure of merit, an optimized CNN selection provides $73.6 \pm 0.034\%$ signal efficiency and $8.77 \times 10^{-3} \pm 7.4 \times 10^{-4}\%$ cosmic background efficiency. As shown in table 5, the final selection highly suppresses the cosmic background clusters while the number of signal clusters remains high.

The preliminary sensitivity for MicroBooNE's $n - \bar{n}$ search is calculated assuming 372 seconds of exposure, corresponding to 3.13 neutron·years, and considering statistical uncertainties only, and is shown in table 6. The sensitivity is calculated using the frequentist-based Rolke method [486]. Although the $n - \bar{n}$ search in MicroBooNE is not competitive compared to existing limits from SNO or Super-Kamiokande, this analysis serves as a demonstration for the capability of future, larger and well-shielded LArTPC's, including the future DUNE, to perform such searches for baryon number violation with significantly higher exposure and thus higher sensitivity. The MicroBooNE analysis is ongoing, to incorporate effects of systematic uncertainties.

Table 7. Sensitivities at 90% C.L. to various single nucleon decay modes after 10 years of Hyper-Kamiokande operations and after 20 years in the case of dinucleon decay modes.

Mode	Sensitivity (90 % CL) [years]	Mode	Sensitivity (90 % CL) [years]
$p \to e^+\pi^0$	7.8×10^{34}	$p \to \overline{\nu}K^+$	3.2×10^{34}
$p \to \mu^+\pi^0$	7.7×10^{34}	$p \to \mu^+\eta^0$	4.9×10^{34}
$p \to e^+\rho^0$	0.63×10^{34}	$p \to \mu^+\rho^0$	0.22×10^{34}
$p \to e^+\nu\nu$	10.2×10^{32}	$p \to \mu^+\nu\nu$	10.7×10^{32}
$p \to e + X$	31.1×10^{32}	$p \to \mu^+X$	33.8×10^{32}
$np \to e^+\nu$	6.2×10^{32}	$np \to \mu^+\nu$	4.2×10^{32}
$np \to \tau^+\nu$	6.0×10^{32}	$n \to e^-K^+$	1.0×10^{34}

3.4. Hyper-K

Continuing the neutrino and nucleon decay physics program in Kamioka, Japan, HK is a third-generation water Cherenkov detector currently under construction roughly 8 km south of Super-Kamiokande. The detector will use a 187 kton water target, roughly 8 times that of its predecessor, and will observe natural neutrinos from the Sun, core collapse supernovae, and atmospheric neutrinos as well as a 1.3 MW neutrino beam from an upgraded J-PARC accelerator. The experiment is expected to begin operations in spring of 2027 and is expected to improve on BNV searches at SK (see section 3.1) by an order of magnitude or more using similar analysis techniques.

Importantly, HK will be instrumented with improved 50 cm PMTs with increased quantum and collection efficiencies, resulting in twice the photon detection efficiency of the sensors used in SK. Further, HK's sensors will have roughly half the timing resolution for single photoelectron signals. Both of these features positively impact searches for nucleon decays at HK. Notably, atmospheric neutrino backgrounds can be reduced by 30% relative to SK's achievement [55] by the augmented ability to tag the faint light from the 2.2 MeV gamma ray produced by neutron capture on hydrogen. Focusing specifically on the $p \to \overline{\nu}K^+$ mode, the improved PMT timing resolution allows HK to better separate light from the below-Cherenkov-threshold K^+'s decay products and that from photons produced by the recoiling oxygen nucleus. This improves the detection efficiency of the $K^+ \to \mu^+\nu_\mu$ mode from 9.1% [478] to 12.7% in HK [56]. Altogether HK's discovery potential after 10 years will exceed 3σ if the effective lifetime of the proton decay into this channel is less than 2×10^{34} years. For the other 'flagship' mode, $p \to e^+\pi^0$, a lifetime less than 6×10^{34} years, i.e. slightly more than twice the current SK limit, will lead to a 3σ detection.

Unified theories predict branching ratios for the various possible proton decay modes, indicating that observations of multiple channels and therefore comprehensive coverage of the possibilities is important for determining the symmetries of the underlying model. Table 7 lists HK's median sensitivity to several of these modes, including some $|\Delta(B-L)| = 2|$ and $\Delta B = 2$ modes. It should be noted that for modes in which the initial state cannot be fully reconstructed from the decay products, such as $p \to e^+\nu\nu$, the search becomes background limited. In such cases the sensitivity increases with only the root of the exposure, resulting in only a factor of a few improvement in existing limits. Accordingly, the challenge for HK going forward is to leverage its improved detector to reduce backgrounds to all modes. Currently efforts to reduce backgrounds include adoption of improved particle reconstruction algorithms, improved detector calibration and light collection with additional photosensors,

and introducing enhanced neutron tagging methods, either via algorithms or future gadolinium doping.

3.5. DUNE

The DUNE promises one of the largest highly instrumented fiducial detector masses of any future large underground facility ([487, 488]). With 40 kt of liquid argon (LAr) some 1500 m below Lead, South Dakota to shield against cosmic ray backgrounds, DUNE's immense wire readout particle ionization charge-collection system across four separate modules (that will eventually be in operation [489]) forms its three-dimensional LAr time projection chambers, allowing scientists to exploit bubble-chamber quality images ([490–492]) for world-leading precision physics studies of the SM and beyond. With potentially MeV-scale precision ([493]), the ability to distinguish γ and e species ([494]), low cosmic μ backgrounds, and very low LAr ionization kinetic energy thresholds for even heavy charged species such as protons (ps) ([57, 488]), the overall physics potential of DUNE goes far beyond its initial purpose as a ν detector built to better constrain and measure oscillation parameters such as δ_{CP}. Indeed, the bubble-chamber-like capabilities of DUNE allow for observation of complex event topologies with potentially high multiplicities. Combined with state of the art detector reconstruction and particle identification (PID) methodologies, as well as a gargantuan number of intranuclear nucleons, there is great potential for the DUNE far detector to unlock the secrets behind rare processes.

Sensitivity to several of these processes has been studied [59] using the full DUNE simulation and reconstruction analysis chain, including the impact of nuclear modeling and FSIs on a BDT-based selection algorithm. With an expected 30% signal efficiency, including anticipated reconstruction advances, and an expected background of one event per Mt·yr, a 90% confidence level (CL) lower limit on the proton lifetime in the $p \to \bar{\nu}K^+$ channel of 1.3×10^{34} years can be set, assuming no signal is observed for a 400 kt-year exposure. Another potential mode for a baryon number violation search is the decay of the neutron into a charged lepton plus meson, i.e., $n \to e^- K^+$. The lifetime sensitivity for a 400 kt-year exposure is estimated to be 1.1×10^{34} years. Neutron-antineutron ($n \to \bar{n}$) oscillation is a BNV process that has never been observed but is predicted by a number of BSM theories. The expected limit for the oscillation time of free neutrons for a 400 kt-year exposure is calculated to be 5.53×10^8 s.[33]

Reconstruction of these events, which have final state particle kinetic energy of order 100 MeV, is a significant challenge, made more difficult by FSIs, which generally reduce the energy of observable particles. The dominant background for these searches is from atmospheric neutrino interactions. For example, a muon from an atmospheric $\nu_\mu n \to \mu^- p$ interaction may be indistinguishable from a muon from $K \to \mu \to e$ decay chain from $p \to \bar{\nu}K^+$ decay, such that identification of the event relies on the kaon-proton discrimination. Neutron-antineutron oscillations can be detected via the subsequent antineutron annihilation with a neutron or a proton. The annihilation event will have a distinct, roughly spherical signature of a vertex with several emitted light hadrons (a so-called 'pion star'), with total energy of twice the nucleon mass and roughly zero net momentum. Reconstructing these hadrons correctly and measuring their energies is key to identifying the signal event. As with nucleon decay, nuclear effects and FSIs make the picture more complicated, as FSIs can reduce the multiplicity of pions and make the pions less energetic.

[33] This analysis used an intranuclear suppression factor for $n \to \bar{n}$ in ^{56}Fe [333] with a slightly inflated uncertainty rather than the suppression factor for ^{40}Ar, which has only recently been calculated [495] and will be applied in future analyses.

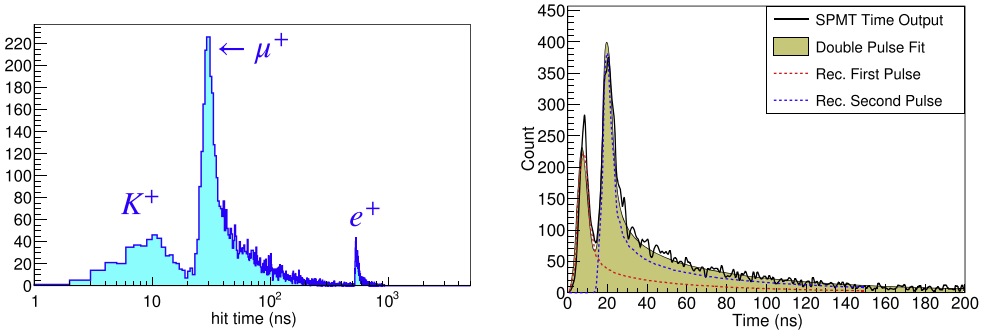

Figure 14. Left: Example of hit time distribution in JUNO for a $p \to \bar{\nu}K^+$ decay as seen with the 3-inch PMTs. Despite the proximity between the first two signals, the threefold coincidence is clearly visible. Right: Example of multi-pulse fitting in a case where the time separation between the two first pulses is 11 ns. Both images are obtained from [496].

3.6. JUNO

JUNO is a next-generation liquid scintillator detector under construction in southern China [60, 496]. It consists of a 20 kton liquid scintillator target inside an acrylic spherical vessel surrounded by 17, 612 20 inch and 25, 600 3 inch PMTs. Its choice of technology, which affords it a good timing resolution and a low energy threshold, combined with its large size, unprecedented for a detector of this type, give it unique capabilities in the search for nucleon decays.

JUNO will be particularly sensitive to the $p \to \bar{\nu}K^+$ decay channel. The main reason is that, as highlighted in section 3.7.2, this decay unleashes a three-fold sequence of events, each of which is detectable in a liquid scintillator detector such as JUNO: a prompt signal from the K^+'s loss of kinetic energy, a short delayed signal ($\tau = 12.4$ ns) from its decay daughter (most commonly a μ^+), and a long delayed signal from the daughter's decay (most commonly into a Michel positron with $\tau = 2.2$ μs). This threefold coincidence provides a powerful handle to suppress backgrounds, which in JUNO are dominated by atmospheric neutrino interactions.

The sensitivity to the $p \to \bar{\nu}K^+$ decay channel has been studied using JUNO's custom Monte Carlo simulation framework [497] including a realistic detector performance. A modified version of the GENIE 3.0 [498] generator that accounts for FSIs and residual nucleus de-excitations is used to generate $p \to \bar{\nu}K^+$ decays and atmospheric neutrino backgrounds. The short K^+ lifetime causes the energy depositions of the K^+ and its subsequent decay daughter to overlap in time. However, the 3 inch PMTs, whose transit time spread is around 1.5 ns, allow in many cases to disentangle these two signals after the time-of-flight correction has been applied, as illustrated on the left panel of figure 14. Fitting the two pulses simultaneously [499], as illustrated on the right panel of figure 14, allows to reconstruct their time separation and energy deposition. The distribution of the best-fit time separations is broader for the signal than for the atmospheric neutrino background, allowing to discriminate between these two with high efficiency [500].

There are additional handles that further enhance the signal-to-background separation. Among them is the use of a fiducial volume cut, the consideration of a muon veto to suppress cosmogenic backgrounds, and the consideration of the visible energy of the candidate signals, among others. A preliminary selection using all these criteria yields an efficiency of 31% to $p \to \bar{\nu}K^+$ decays, with only 0.3 background events in a period of 10 years. A

Table 8. Detection efficiency and background rates for the three considered modes of nucleon decay in THEIA.

Signal	Efficiency	Bkg [/Mton·yr]
$p \to e^+\pi^0$	40%	0.3
$p \to \bar{\nu}K^+$	55%	2.5
$n \to 3\nu$	44%	95.6

Feldman-Cousins [501] estimation of the sensitivity to this decay mode yields a lower limit for the proton lifetime of 8.34×10^{33} years at 90% C.L. with 10 years of data, in absence of a signal.

It is worth noting that JUNO is also expected to have good sensitivity to other decay modes, namely $p \to \mu^+\mu^+\mu^-$ and the $n \to 3\nu$ invisible mode. JUNO will have an energy resolution of 3% at 1 MeV, which is unprecedented for a liquid scintillator detector. This will be an important asset in those searches where the signal is a mono-energetic energy deposition, as explained in section 3.7.3. JUNO's sensitivity to these modes is still under evaluation, and the results are expected to be released soon.

3.7. THEIA

THEIA is a detector concept that utilizes advances in photon detection technology (fast timing, chromatic separation) with water-based liquid scintillator to create a highly scalable detector (up to the 100 kton scale) with better energy resolution than a pure water detector. Due to the large mass and presence of scintillation light, THEIA would have sensitivity to several modes of nucleon decay that is either comparable with or better than next-generation detectors see figure 15 and table 8. Additional details are available in [502].

3.7.1. $p \to e^+\pi^0$ and related modes. Decay modes which have pions in the final state are subject to inelastic intranuclear scattering for bound protons, which causes the pion to be reabsorbed about 60% of the time. This dominates the total efficiency to see this decay mode in water as well as water-based liquid scintillator. For THEIA the dominant background comes from atmospheric neutrino interactions, and is independent of depth. Compared with other water Cherenkov detectors, THEIA would have improved neutron tagging (90% efficiency), better energy resolution, and sensitivity to below-Cherenkov threshold charged particles. These features can be all used to better reject atmospheric neutrino backgrounds.

3.7.2. $p \to \bar{\nu}K$ and related modes. Kaon decay modes are less affected by intranuclear effects and produce a three-fold coincidence signal in the detector through the subsequent decays of their daughter particles [13].

- $K^+ \to \mu^+\nu_\mu$ (63.56%)
- $K^+ \to \pi^+\pi^0$ (20.67%)
- $K^+ \to \pi^+\pi^+\pi^-$ (5.58%)
- $K^+ \to \pi^0 e^+\nu_e$ (5.07%)
- $K^+ \to \pi^+\pi^0\pi^0$ (1.76%)

In a pure water Cherenkov detector the kaon is below the energy Cherenkov threshold and does not produce a detectable signal; however, the multiple pions can produce identifiable multi-ring signals, and the subsequent decays of the pions and muon create a coincidence

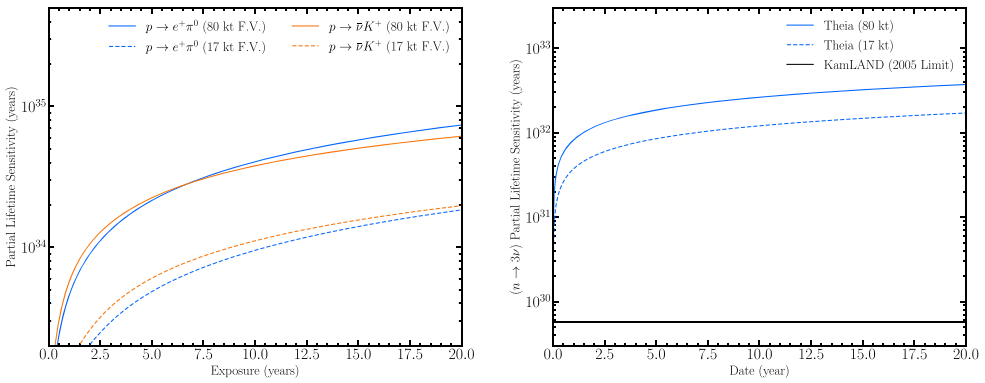

Figure 15. (Left) Median sensitivity curves for $p \to e^+\pi^0$ and $p \to \bar{\nu}K^+$, and (Right) $n \to 3\nu$ for the two considered THEIA fiducial volumes.

trigger. In THEIA, the kaon would produce scintillation light as well, though much of the kaon signal would overlap with it is decay products due to it is 12 ns lifetime [60]. Since these first two signals would be difficult to distinguish, it is safe to assume that THEIA would perform no better than JUNO (pure scintillator) in terms of signal efficiency, but could be built to a much larger scale.

3.7.3. $n \to 3\nu$ and related modes. Finally, THEIA would have sensitivity to a class of low-energy modes known as 'invisible' modes, where all of the final state particles cannot produce light emissions (such as all-neutrino final states). When these occur in a multi-nucleon nucleus then the nucleus will often be left in an excited state and will release deexcitation γs and nucleons. In an ^{16}O nucleus this manifests as a 6.18 MeV γ with a relatively high branching ratio (44%). The primary background for this signal comes from solar neutrinos, internal radioactivity, and cosmogenic activation of oxygen to ^{16}N. THEIA would be the only large-scale water Cherenkov detector available to look for this decay due to its large mass and great depth. Leading limits on invisible neutron and dineutron decay are set by KamLAND [503], and on invisible proton and diproton decay by SNO+ [504].

3.8. Detection techniques in LArTPCs

The search for baryon number violation is a prime goal of particle physics and is being carried out in large underground detectors. Most of the current lifetime limits are affected by backgrounds, predominantly from the 100 events per kiloton year which arise from atmospheric neutrino interactions. The current best limits come from water detectors, but a promising way to reduce backgrounds is with a large liquid argon time projection chamber (LArTPC), almost all ^{40}Ar. Large LArTPCs provide the capability to image charged particles with mm-scale resolution and thus explore signatures from particle and nuclear physics at the same time [505]. The concurrent detection of light in a photo-detector system provides an opportunity to identify signatures from nucleon decay that are not present in neutrino interactions. Analysis strategies can then be tuned to both reduce background and increase efficiency. A photon-detection system can also measure energy calorimetrically, working as a crosscheck of the energy measured by the ionizing particles in a TPC and thus improving the energy resolution when both measurements are used together. There are about one hundred nucleon decay modes accessible to large underground liquid argon TPCs, similar to the

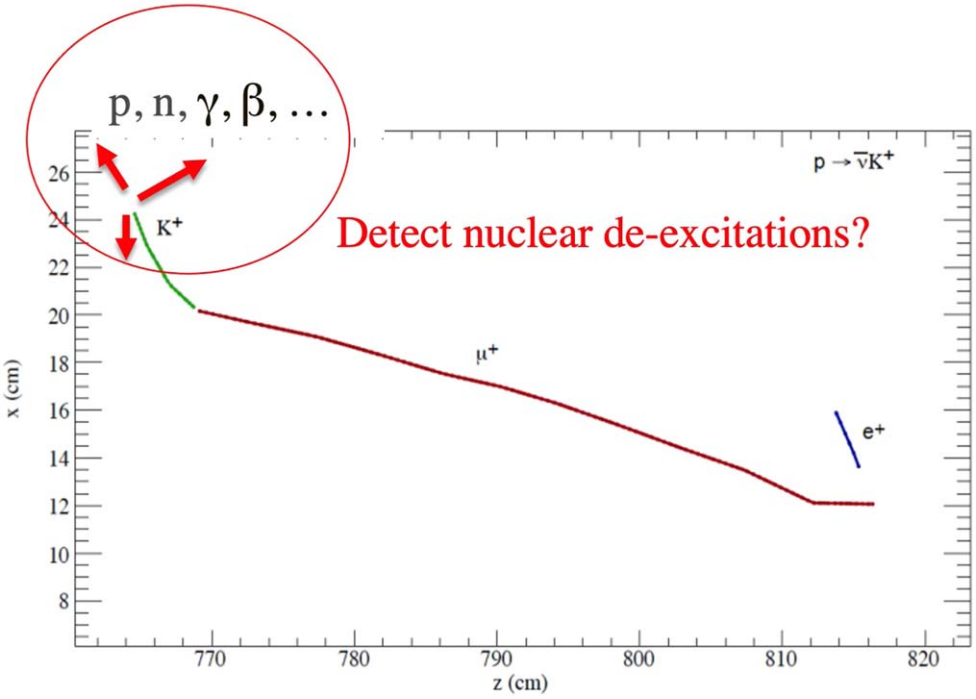

Figure 16. Search for the decay products from nuclear de-excitation of the residual radioactive daughter nuclei left after the disappearance of proton from ^{40}Ar nucleus.

DUNE Far Detector [487], or to the considered module of opportunity liquid argon TPCs, under consideration [506], such as Q-Pix based LArTPC [507]. We see a valuable opportunity to combine signatures from particle and nuclear physics and take advantage of the fast and precise timing capabilities of a photon-detection system and the detailed pattern recognition capabilities of a LArTPC [491, 508] to improve the sensitivity of future nucleon decay searches. As an example, consider the mode $p \to \bar{\nu}K^+$ [478]. For this mode, one looks for the K^+ signature via a short ionization track, followed primarily by $K^+ \to \mu^+\nu\mu$ decay which makes an observable μ^+ track. The μ^+ decays to an observable positron. There are also other less likely K^+ decay modes. The kaon and its decay products can be reconstructed as images and the decay chain could be tested for kinematic consistency. Three potential backgrounds include 1) the large number of quasi-elastic atmospheric ν_μ interactions where the recoil proton is misidentified as a K^+, 2) production of K^+ by atmospheric neutrinos, and 3) neutrino production of K_L outside the detector which enter the LArTPC and charge exchange to a K^+.

There are several additional signatures of $p \to \bar{\nu}K^+$ decay to investigate, mostly requiring LArTPC mm-scale resolution and a low-energy charge detection threshold ideally combined with a fast timing from the photon system:

- The ^{40}Ar could often become an excited state of ^{39}Cl, with emission of de-excitation gamma rays. This nuclear process needs additional studies since any proton inside the ^{40}Ar can decay. The proton that decays might be deeply bound within the nucleus and the nucleus would be, at a minimum, left with an excitation energy much higher than the neutron separation energy and maybe even other separation energies. There is a possibility of even higher excitation if part of the decay energy is transferred to the

nucleus. On the LArTPC response side, the detection of MeV-scale gamma-rays was demonstrated ([493]) with efficiency of 50% and energy resolution of 24% at 0.5 MeV, and with an efficiency of almost 100% and energy resolution of 14% at 0.8 MeV. If the gammas from $^{40}\mathrm{Ar} \rightarrow {}^{39}\mathrm{Cl}$ de-excitation are measured by the photon system, in addition to the TPC charge detection, we would have a new unique time-tag of the proton decay process, see figure 16.

- The product ^{39}Cl decays with a 56 min half life to ^{39}Ar (feasible to tag in a deep detector). Then, ^{39}Ar decays 93% of the time to excited states and will give you characteristic gamma rays, roughly 54% of the time a 1.27 MeV gamma, 39% of the time a 1.52 MeV gamma and 46% of the time a 250 keV gamma (this one typically comes with the 1.27 MeV gamma).
- The K^+ lifetime is 12 ns, and a photon system with good timing could distinguish it from its decay products, as well as improve the identification of Michel electrons, from the 2 μs decay of μ's. In recently published results of the ProtoDUNE-SP liquid argon time projection chamber performance ([493]), a time resolution of 14 ns was achieved in the case of a single photon-detector channel. It is expected that photon-detector time resolution will improve as a square root of the number of independent channels, driving the resolution well-below the 12 ns lifetime of K^+.
- Bound neutron decay to excited states of ^{39}Ar might also make de-excitation gamma.

Our intent is, therefore, to further study these signatures and to examine how the signal sensitivity will be further enhanced, and how backgrounds could be rejected more efficiently with additional information from nuclear de-excitations and with precise timing from photon-detectors in TPCs.

3.9. Effect of different nuclear model configurations on sensitivity to intranuclear neutron-antineutron transformations

Sensitivity studies for BNV processes are currently relegated to simulations using generated Monte Carlo (MC) event samples. For example, using the GENIE MC event generator [509] and DUNE detector simulation and reconstruction software packages such as LArSoft [510], a first foray into sensitivity investigations for separating intranuclear $n \rightarrow \bar{n}$ from (predominately neutral-current) atmospheric neutrino backgrounds in the DUNE far detector was considered in [336]. However, there remains much work to be done [511]. The dependencies of CNN's and other automated (machine learning) methods such as multivariate boosted decision trees' (BDTs') responses to various topological inputs is not entirely clear. The nature of these algorithms' responses to underlying choices in what are generally considered to be broadly consistent nuclear model configurations (NMCs) must be further studied to assess effective uncertainties, including those originating from disparate models of nuclear Fermi motion and FSIs from (non)stochastic intranuclear cascades [495, 512]. Given that the event triggers for $n \rightarrow \bar{n}$ will likely utilize the signal's expected region of interest (ROI) as informed primarily by the MC simulation of the process and its separation from background via automated methods, such dependencies are highly important, particularly when physical correlations are being ignored; this is but one important component of the larger, still developing paradigm, which should include improved reconstruction and PID.

To explain this particular aspect in some detail, let us begin by stating the obvious: there is actual importance in the maintaining of particularly relevant physical correlations in MC simulations which act to inform the detection of unknown (rare) processes. To illustrate this, consider figures 17 [495]. Some correlations which have gone previously unexplored include the expected position of the intranuclear $\bar{n}$ annihilation following $n \rightarrow \bar{n}$ conversion, as

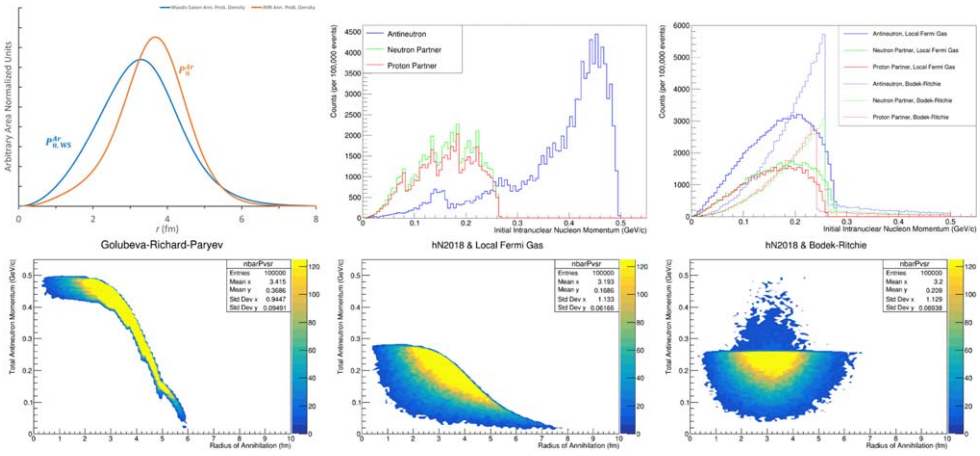

Figure 17. Top Left: Two curves are shown for various generator assumptions. In blue is the naive intranuclear radial position of $\bar{n}$ annihilation, a probability distribution generated by a Woods–Saxon nuclear density as presented in GENIE [509]. In orange is the modern, quantum-mechanically derived intranuclear radial position of annihilation probability distribution as developed in ([495]). The vertical scale is arbitrary. **Top Center**: The initial (anti)nucleon momentum distributions are shown using a local Fermi gas (LFG) model with an additional $\bar{n}$ potential ([495]). **Top Right**: The same for the GENIEv3.0.6 [509], showing an LFG model and the default nonlocal Bodek-Ritchie (BR) model. **Bottom Left**: A two dimensional plot of intranuclear $\bar{n}$ momentum-radius correlation is shown using an LFG and the newly-derived annihilation position distribution [495] (top left, orange). **Bottom Center**: The same using GENIEv3.0.6's [509] LFG model of (anti)nucleon momentum and a Woods–Saxon nuclear density (top left, blue), showing good correlation. **Bottom Right**: The same using GENIEv3.0.6's ([509]) *nonlocal* BR nuclear model of (anti)nucleon momentum and a Woods–Saxon nuclear density (top left, blue), showing no positional correlation, and thus over-selecting high momenta.

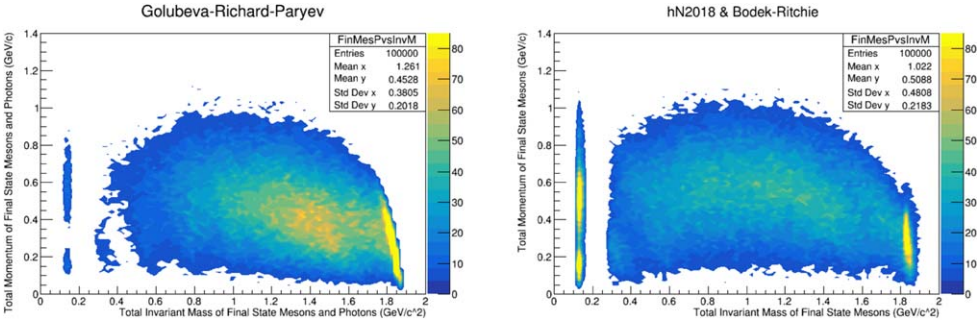

Figure 18. The final state mesonic/pionic parameter space (total momentum versus invariant mass) [331] after stochastic intranuclear transport of $\bar{n}$ annihilation generated mesons, compared for a few NMCs, not including detector effects. The ROI is generally considered to the be 'hot-spot' in the lower right hand corner, implying the expected low Fermi momentum and high invariant mass derived from the annihilation of two nucleons creating a topologically spherical π-star; differences in these may lead to different detector signal efficiencies via automated methods. **Left**: an LFG model with an additional $\bar{n}$ potential and a full intranuclear cascade [495, 512]. **Right**: GENIEv3.0.6 [509] using the default nonlocal BR relativistic Fermi gas and a full intranuclear cascade via the 2018 hN Intranuke model (hN).

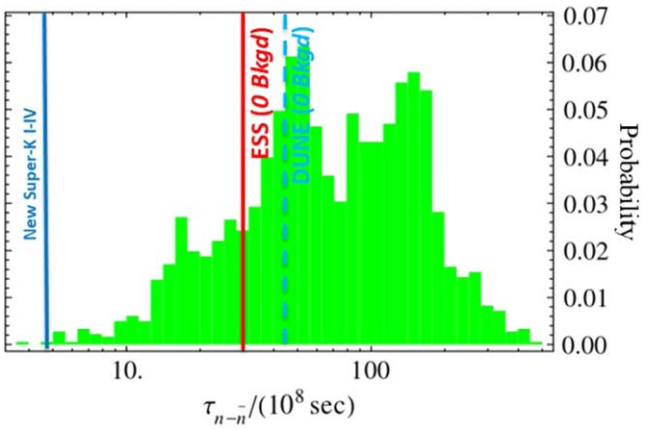

Figure 19. A reproduction of figure 9 in [312] is shown with sensitivity estimates for DUNE–assuming a 25% efficiency–and ESS NNBAR–assuming an ILL-like efficiency [330]–each in a case of zero background compared to the Super-Kamiokande I–IV limit [332].

shown at top left. Considering the $\{n, \bar{n}\}$ mass splitting which suppresses $n \to \bar{n}$ lessens as one hypothetically decreases the binding energy, a radial dependence is expected in the transformation probability beyond the simplistic assumption of the assumed Woods–Saxon nuclear density–indeed, such transformations are expected to occur predominately near the nuclear surface where n binding is low. Further, and as illustrated in the top central figure, given the strength of the annihilation cross section, the optical potential describing the Fermi motion of a previously converted $\bar{n}$ is expected to be deeper than that of normal nuclear matter, imbuing the converted $\bar{n}$ with higher available momentum. Similarly, due to $n \to \bar{n}$ occurring predominately on the surface of the nucleus, one may expect a reduction in the available Fermi motion-derived momentum; thus, simulations which are inherently *nonlocal* in their assumptions of Fermi motion (as is the case in the GENIE [509] default nuclear model) can lead to biases in any particular ROI. The (non)locality of a given nuclear model is shown by a decrease in (anti)nucleon momentum as one moves further out toward the nuclear envelope ($r \to R$), as shown in the bottom figures for two generators; if a hemicircular region is occupied in this parameter space, then no momentum-radius correlations are preserved.

The investigation in maintaining these physically relevant correlations can go even further, as one may expect fewer FSIs to be experienced by annihilation-generated mesons due to reduced views on intranuclear scattering centers near the nuclear periphery. Also, when evaluating the $n \to \bar{n}$ signal's ROI (before consideration of further skewing due detector effects), choices across models of these FSIs can have a critical role in determining signal efficiencies through topological selection of high multiplicity events involving knock-out *p*s, which may be overproduced ([495]). When considering outgoing mesons only, the nature of the ROI can be seen to remain disparate through the comparison of various NMCs across multiple (and single) generators, as shown in figures 18.

The importance of these correlations goes beyond the signal simulation; indeed, the same NMCs and correlations should be respected consistently across atmospheric neutrino background simulations. Iterating across the available NMCs, between and within single generators (for instance, GENIE [509]), and intermixing these together allows for the evaluation of uncertainties in a 'universe' style approach, though going beyond simple knob turning; a

project of this scale requires massive automated analysis techniques to be successful, especially given the nonreweightable nature of some of the more theoretically well-motivated stochastic FSIs models employed. Such uncertainty evaluations will permit a better understanding of the signal to background ratio, informing the final expected sensitivities to $n \to \bar{n}$: if this ratio remains stable across NMCs, then the minutia of certain physical correlations in simulation will be shown to be unnecessary; however, the opposite is the more likely case. One study showed that a change in the NMC reduced the sensitivity by roughly 40% all else being equal [511]. Thus, this greatly encourages not only the evaluation of dependencies of automated analyses' (CNNs, BDTs) responses, but also the necessity of improved reconstruction. DUNE has had successes in machine learning being applied to PID [59], which was not included in [336]; implementing a CNN score describing the probability of particular track's PID could better discriminate signal from background considering the unique high-multiplicity π-star expected to emanate from a nucleus after $\bar{n}$ annihilation.

From these discussions, one may hypothesize as to the regions of $\tau_{n\bar{n}}$ parameter space probed by DUNE [59], Super-Kamiokande [332], and ESS NNBAR [309]. In the context of post-sphaleron baryogenesis [312, 313], one can compare potential lower limits to model predictions, as shown in figure 19. A spread in the expected values of $\tau_{n\bar{n}}$ given various NMCs is *concerning*, especially as the underlying nuclear physics, though well constrained [511], is not definitively known.

By considering the above in greater detail into the future, sensitivities to $B-L$-violating $\Delta B = 2$ processes such as $n \to \bar{n}$ and related dinucleon decay modes are expected to greatly improve through enhanced physical modeling, reconstruction, and PID. Uncertainties due to specific NMC choices remain under investigation, potentially lowering the sensitivities without other improvements. These steps are required in order to pursue truly complementary physics goals beyond proton decay and neutrino oscillation studies, enabling the broader particle physics community to fully utilize future large underground detectors to better search for BSM physics, potentially informing us of our universe's origins.

3.10. Inclusive nucleon decay searches

As summarized in section 2, B-violating processes are associated with a broad variety of theories and can manifest through distinct nucleon decay channels. The strongest limits can be set on particular exclusive nucleon decay processes, motivated by specific theoretical models. However, as discussed in section 2.5, higher order operators leading to complicated processes can readily dominate over typical two-body nucleon decay channels. With increased complexity of interactions, performing exclusive experimental searches for all specific nucleon decay channels becomes unfeasible beyond the simplest realizations.

These considerations highlight the importance of inclusive nucleon decay searches and set limits on classes of baryon number-violating processes simultaneously. Such searches can be classified as follows [358]:

- *model-independent and invisible mode searches*
  model-independent searches probe all nucleon decays simultaneously, unconstrained by specific final states. These searches also constitute the primary approach for studying invisible channels such as $n \to invisible$. Invisible channels such as $n \to 3\nu$ could become significant in models based on extra-dimensions (e.g. [513]). Analysis of $p \to invisible$ will also serve as a test of charge conservation. Prominent searches of this class include isotope fission products as well as signatures of nuclear de-excitation, with current limits being $\tau \gtrsim 10^{30}$ years. The latter method is expected to be a promising target for future neutrino experiments such as JUNO, HK and DUNE.

- $N \to X +$ anything-allowing for model-independence while also taking advantage of precise particle identification in current and upcoming large neutrino experiments, such as Super-Kamiokande (see related searches of [482]), motivates $N \to X +$ anything searches, where X is a SM particle of unknown energy. These include:
  (A) $N \to (e^{\pm},\ \mu^{\pm},\ \pi^{\pm},\ K^{\pm},\ \rho^{\pm},\ K^{*,\pm}) + anything$: primary decay charged particles are often directly visible with high efficiency in experimental searches. From electric-charge conservation any proton decay will eventually result in at least one positron, albeit potentially space-time-delayed if it is originated from the decay of a heavier charged final-state particle.
  (B) $N \to (\pi^0,\ K^0,\ \eta,\ \rho,\ \omega,\ K^{*,0}) + anything$: searches involving neutral mesons rely on the electromagnetically interacting daughter particles for detection (e.g. $\pi^0 \to \gamma\gamma$).
  (C) $N \to \gamma + anything$: assuming multi-body nucleon decays, the emission of a photon will typically be suppressed compared to the same multi-body channel without a photon.
  (D) $N \to \nu + anything$: similar to other invisible searches, can also be studied through neutrino flux measurements from accumulation of nucleon decays inside the Earth.
- $\Delta B > 1$ processes
  inclusive searches also offer prospects for $\Delta B > 1$ processes. Note that inclusive $\Delta B = 1$ searches also constrain $\Delta B > 1$. The increased available energy for final state particles in multi-nucleon decay processes modifies the search compared to single-body decays.

4. Conclusion and outlook

We have discussed the current status and future prospects of baryon number violation searches with large underground detectors for neutrino experiments. These detectors used for next-generation neutrino experiments have the capability to improve the existing limits on nucleon lifetime by up to an order of magnitude. A broad class of GUT models (both non-supersymmetric and supersymmetric) can be probed. Some of them predict an upper limit on the nucleon lifetime, which might be fully within reach of the future experiments. Apart from the $|\Delta B| = 1$ nucleon decay, there exist other interesting BNV observables as well, such as neutron-antineutron oscillation ($|\Delta B| = 2$) and $B \to LM$ decays ($|\Delta(B{-}L)| = 2$), which also have promising prospects for underground detectors to be used in future neutrino experiments. The discovery of baryon number violation will be an unambiguous signal of new physics, and therefore, it is important to search for as many BNV channels as possible.

For the most crucial proton decay modes (see table 1), the future searches will improve the existing limits by a factor of few with 10 years of operation and up to an order of magnitude with 20 years of operation. Implications of these improvements in the measurements on GUT model building can be profound. The proton decay mode $p \to e^+\pi^0$, mediated by the superheavy gauge bosons, is the most significant one since it is generically present in GUTs with or without supersymmetry. The decay channel $p \to \overline{\nu}K^+$, on the other hand, is the most promising one in probing supersymmetric GUTs. Well-motivated models, such as minimal non-supersymmetric $SO(10)$ GUTs with intermediate PS symmetry [168], in their simplest versions can be ruled out (or discovered!) by only a few years of operations of HK. Moreover, 20 years of operations of HK will probe almost the entire parameter space of minimal non-supersymmetric $SU(5)$ GUT [82]. Another notable proton decay channel is $p \to \mu^+\pi^0$. If such decays are observed, it can play an important role in selecting the types of GUT models. For example, non-supersymmetric $SU(5)$ GUT with vectorlike fermions containing minimal representations predicts [84] that if the proton decay channel $p \to e^+\pi^0$ is not observed, then the decay mode $p \to \mu^+\pi^0$ must be seen by HK in its 20 years of operations. Concerning the

supersymmetric framework, two of the most attractive scenarios, namely the minimal superysmmetric $SU(5)$ and $SO(10)$ GUTs, both predict $\tau_p(p \to \overline{\nu}K^+) \lesssim 6 \times 10^{34}$ years with sparticle masses $\lesssim\mathcal{O}(10)$ TeV [110] and $\lesssim\mathcal{O}(100)$ TeV [149], respectively. Therefore, HK, as well as THEIA, will thoroughly probe these scenarios within their 20 years of operations. A discovery of this kind may also suggest somewhat high-SUSY. It is intriguing to note that such high-scale masses of the supersymmetric partners are far beyond the reach of current LHC.

While proton decay remains the poster-child of BNV processes, other BNV processes, such as dinucleon decays and neutron-antineutron oscillation, are also equally important to search for. They could give us key insights on the outstanding issues of the SM. For instance, the next-generation $n - \bar{n}$ experiments could probe a big chunk of the post-sphaleron baryogenesis parameter space [312]. Similarly, a simultaneous observation of $B-L$ conserving and violating (by two units) decays would necessarily imply the Majorana nature of neutrinos [381].

In conclusion, next-generation large-volume neutrino experiments provide an excellent opportunity for improved the baryon number violation searches—a promising tool for exploring new physics up to the GUT scale.

Acknowledgments

We thank Borut Bajc, Ilja Doršner, Natsumi Nagata, Jogesh Pati, Stuart Raby, Zurab Tavartkiladze, and Cem Salih Un for useful comments on the manuscript. The work of PSBD is supported in part by the US Department of Energy under grant No. DE-SC0017987. This research was supported in part by the National Science Foundation under Grant No. NSF PHY-1748958. S Syritsyn is supported by the National Science Foundation under CAREER Award PHY-1847893. VT is supported by the World Premier International Research Center Initiative (WPI), MEXT, Japan. The work of RNM is supported by the US National Science Foundation grant no. PHY-1914631. The work of MM is supported by the Grant Agency of the Czech Republic (GAČR) through contract number 20-17490S and from the Charles University Research Center UNCE/SCI/013. The work of RS is supported in part by NSF Grant NSF-PHY-22-10533.

Data availability statement

All data that support the findings of this study are included within the article (and any supplementary files).

ORCID iDs

P S B Dev https://orcid.org/0000-0003-4655-2866
L W Koerner https://orcid.org/0000-0002-9544-5349
S Saad https://orcid.org/0000-0003-3784-3776
S Antusch https://orcid.org/0000-0001-6120-9279
M Askins https://orcid.org/0000-0002-6951-7994
K S Babu https://orcid.org/0000-0001-6147-5155
J L Barrow https://orcid.org/0000-0002-7319-3339
J Chakrabortty https://orcid.org/0000-0001-8709-916X

A de Gouvêa https://orcid.org/0000-0002-9835-7731
Z Djurcic https://orcid.org/0000-0002-5472-216X
S Girmohanta https://orcid.org/0000-0003-4209-1118
I Gogoladze https://orcid.org/0000-0003-3373-4564
M C Goodman https://orcid.org/0000-0003-1439-1551
A Higuera https://orcid.org/0000-0001-9310-2994
D Kalra https://orcid.org/0000-0002-6124-3941
G Karagiorgi https://orcid.org/0000-0001-6915-3732
E Kearns https://orcid.org/0000-0002-1781-150X
V A Kudryavtsev https://orcid.org/0000-0002-7018-5827
M Malinský https://orcid.org/0000-0003-0415-662X
D A Martinez Caicedo https://orcid.org/0000-0001-8270-8907
R N Mohapatra https://orcid.org/0000-0003-0128-9160
P Nath https://orcid.org/0000-0001-9879-9751
J P Ochoa-Ricoux https://orcid.org/0000-0001-7376-5555
V Pec https://orcid.org/0000-0003-4104-829X
A Rafique https://orcid.org/0000-0001-8057-4087
R Shrock https://orcid.org/0000-0001-6541-0893
H W Sobel https://orcid.org/0000-0001-5073-4043
T Stokes https://orcid.org/0000-0002-9353-6343
M Strait https://orcid.org/0000-0001-5708-8734
R Svoboda https://orcid.org/0000-0001-8297-0905
S Syritsyn https://orcid.org/0000-0003-1189-2940
V Takhistov https://orcid.org/0000-0003-2647-3431
Y-T Tsai https://orcid.org/0000-0001-7011-3551
R A Wendell https://orcid.org/0000-0002-0969-4681
Y-L Zhou https://orcid.org/0000-0002-3664-9472

References

[1] Weyl H 1929 Electron and Gravitation. 1. (In German) *Z. Phys.* **56** 330
[2] Stückelberg E C 1938 Interaction energy in electrodynamics and in the field theory of nuclear forces *Helv. Phys. Acta* **11** 225
[3] Stueckelberg E 1938 Forces of interaction in electrodynamics and in the field theory of nuclear forces (parts ii and iii) *Helv. Phys. Acta* **11** 299
[4] Wigner E P 1949 Invariance in physical theory *Proc. Am. Phil. Soc.* **93** 521
[5] Hooft G 't 1976 Symmetry breaking through bell-jackiw anomalies *Phys. Rev. Lett.* **37** 8
[6] Hooft G 't 1976 Computation of the quantum effects due to a four-dimensional pseudoparticle *Phys. Rev.* D **14** 3432
[7] Manton N S 1983 Topology in the weinberg-salam theory *Phys. Rev.* D **28** 2019
[8] Kuzmin V, Rubakov V and Shaposhnikov M 1985 On the anomalous electroweak baryon number nonconservation in the early universe *Phys. Lett.* B **155** 36
[9] CMS collaboration 2012 Observation of a new boson at a mass of 125 Gev with the CMS experiment at the LHC *Phys. Lett.* B **716** 30
[10] ATLAS collaboration 2012 Observation of a new particle in the search for the standard model higgs boson with the ATLAS detector at the LHC *Phys. Lett.* B **716** 1
[11] LHCb collaboration 2022 Test of lepton universality in beauty-quark decays *Nat. Phys.* **18** 277
[12] Muon G-2 collaboration 2021 Measurement of the positive muon anomalous magnetic moment to 0.46 ppm *Phys. Rev. Lett.* **126** 141801
[13] Particle Data Group collaboration 2020 Review of particle physics *PTEP* **2020** 083C01
[14] Pati J C and Salam A 1973 Is baryon number conserved? *Phys. Rev. Lett.* **31** 661
[15] Pati J C and Salam A 1974 Lepton number as the fourth color *Phys. Rev.* D **10** 275

[16] Georgi H and Glashow S L 1974 Unity of all elementary particle forces *Phys. Rev. Lett.* **32** 438
[17] Georgi H, Quinn H R and Weinberg S 1974 Hierarchy of interactions in unified gauge theories *Phys. Rev. Lett.* **33** 451
[18] Georgi H 1975 The state of the art—gauge theories *AIP Conf. Proc.* **23** 575
[19] Fritzsch H and Minkowski P 1975 Unified interactions of leptons and hadrons *Ann. Phys.* **93** 193
[20] Langacker P 1981 Grand unified theories and proton decay *Phys. Rept.* **72** 185
[21] Reines F and Crouch M F 1974 Baryon conservation limit *Phys. Rev. Lett.* **32** 493
[22] Croon D, Gonzalo T E, Graf L, Košnik N and White G 2019 GUT physics in the era of the lHC *Front. in Phys.* **7** 76
[23] Rosen S P 1975 Another method of searching for proton decay *Phys. Rev. Lett.* **34** 774
[24] Bennett C L 1981 Limitations on proton decay modes from a passive detection scheme *2nd Workshop on Grand Unification* pp 120–4
[25] Backenstoss G *et al* 1960 An investigation of the stability of nucleons *Nuovo Cim.* **16** 749–55
[26] Learned J, Reines F and Soni A 1979 Limits on nonconservation of baryon number *Phys. Rev. Lett.* **43** 907
[27] Cherry M L, Deakyne M, Lande K, Lee C K, Steinberg R I and Cleveland B T 1981 Experimental test of baryon conservation: a new limit on the nucleon lifetime *Phys. Rev. Lett.* **47** 1507
[28] Perkins D H 1984 Proton decay experiments *Ann. Rev. Nucl. Part. Sci.* **34** 1
[29] NUSEX collaboration 1989 Experimental study of atmospheric neutrino flux in the NUSEX experiment *Europhys. Lett.* **8** 611
[30] Frejus collaboration 1990 A study of atmospheric neutrino oscillations in the FREJUS experiment *Phys. Lett.* B **245** 305
[31] Soudan-2 collaboration 1994 Contained neutrino events observed in SOUDAN-2 *Nucl. Phys.*B **35** 427
[32] Irvine-Michigan-Brookhaven collaboration 1983 A search for proton decay into e+ pi0 *Phys. Rev. Lett.* **51** 27
[33] Hirata K S *et al* 1988 Observation in the kamiokande-II detector of the neutrino burst from supernova SN 1987a *Phys. Rev.* D **38** 448
[34] Kamiokande-II collaboration 1987 Observation of a neutrino burst from the supernova SN 1987a *Phys. Rev. Lett.* **58** 1490
[35] Bionta R M *et al* 1987 Observation of a neutrino burst in coincidence with supernova SN 1987a in the large magellanic cloud *Phys. Rev. Lett.* **58** 1494
[36] Super-Kamiokande collaboration 1999 Measurement of the flux and zenith angle distribution of upward through going muons by Super-Kamiokande *Phys. Rev. Lett.* **82** 2644
[37] Super-Kamiokande collaboration 2001 Solar B-8 and hep neutrino measurements from 1258 d of Super-Kamiokande data *Phys. Rev. Lett.* **86** 5651
[38] Super-Kamiokande collaboration 2001 Constraints on neutrino oscillations using 1258 d of super-kamiokande solar neutrino data *Phys. Rev. Lett.* **86** 5656
[39] Wess J and Zumino B 1974 Supergauge transformations in four-dimensions *Nucl. Phys.* B **70** 39
[40] Witten E 1981 Dynamical breaking of supersymmetry *Nucl. Phys.* B **188** 513
[41] Dimopoulos S, Raby S and Wilczek F 1981 Supersymmetry and the scale of unification *Phys. Rev.* D **24** 1681
[42] Dimopoulos S and Georgi H 1981 Softly broken supersymmetry and SU(5) *Nucl. Phys.* B **193** 150
[43] Sakai N 1981 Naturalness in supersymmetric guts *Z. Phys.*C **11** 153
[44] Veltman M J G 1981 The infrared—ultraviolet connection *Acta Phys. Polon.*B **12** 437
[45] Dimopoulos S and Raby S 1981 Supercolor *Nucl. Phys.* B **192** 353
[46] Dine M, Fischler W and Srednicki M 1981 Supersymmetric technicolor *Nucl. Phys.* B **189** 575
[47] Nilles H P 1984 Supersymmetry, supergravity and particle physics *Phys. Rept.* **110** 1
[48] Nath P and Fileviez Perez P 2007 Proton stability in grand unified theories, in strings and in branes *Phys. Rept.* **441** 191
[49] Babu K S *et al* 2013 Working group report: baryon number violation *Community Summer Study 2013: Snowmass on the Mississippi* **11** arXiv:1311.5285
[50] Hewett J L *et al* 2014 Planning the future of us particle physics (snowmass 2013): chapter 2: intensity frontier *Community Summer Study 2013: Snowmass on the Mississippi* **1** arXiv:1401.6077
[51] Dorsner I 2012 A scalar leptoquark in SU(5) *Phys. Rev.* D **86** 055009

[52] Weinberg S 1982 Supersymmetry at ordinary energies: 1. masses and conservation laws *Phys. Rev.* D **26** 287
[53] Wilczek F and Zee A 1979 Operator analysis of nucleon decay *Phys. Rev. Lett.* **43** 1571
[54] Fileviez Perez P 2004 Fermion mixings versus $d = 6$ proton decay *Phys. Lett.* **B595** 476
[55] Super-Kamiokande collaboration 2020 Search for proton decay via $p \to e^+\pi^0$ and $p \to \mu^+\pi^0$ with an enlarged fiducial volume in Super-Kamiokande I–IV *Phys. Rev.* D **102** 112011
[56] Hyper-Kamiokande collaboration Hyper-Kamiokande design report arXiv:1805.04163
[57] DUNE collaboration Deep underground neutrino experiment (DUNE), far detector technical design report, volume II: DUNE physics arxiv:2002.03005
[58] Super Kamiokande collaboration 2016 Recent nucleon decay results from Super Kamiokande *J. Phys. Conf. Ser.* **718** 062044
[59] DUNE collaboration 2021 Prospects for beyond the standard model physics searches at the deep underground neutrino experiment *Eur. Phys. J.* C **81** 322
[60] JUNO collaboration 2016 Neutrino physics with JUNO *J. Phys. G* **43** 030401
[61] Randall L and Csaki C 1995 The doublet—triplet splitting problem and higgses as pseudogoldstone bosons *Int. Workshop on Supersymmetry and Unification of Fundamental Interactions (SUSY 95)* vol 3, pp 99–109
[62] Yamashita T 2011 Doublet-triplet splitting in an SU(5) grand unification *Phys. Rev.* D **84** 115016
[63] Dorsner I and Fileviez Perez P 2005 Unification without supersymmetry: neutrino mass, proton decay and light leptoquarks *Nucl. Phys.* **B723** 53
[64] Bajc B and Senjanovic G 2007 Seesaw at LHC *J. High Energy Phys.* JHEP08(2007)014
[65] Dorsner I and Perez P Fileviez 2007 Upper bound on the mass of the type iii seesaw triplet in an SU(5) model *J. High Energy Phys.* JHEP06(2007)029
[66] Perez P Fileviez 2007 Renormalizable adjoint SU(5) *Phys. Lett.*B **654** 189
[67] Bajc B, Nemevsek M and Senjanovic G 2007 Probing seesaw at LHC *Phys. Rev.* **D76** 055011
[68] Dorsner I and Mocioiu I 2008 Predictions from type II see-saw mechanism in SU(5) *Nucl. Phys.* **B796** 123
[69] Schnitter K 2013 Higgs mass spectrum in non-SUSY SU(5) *J. High Energy Phys.* JHEP05(2013)151
[70] Di Luzio L and Mihaila L 2013 Unification scale versus electroweak-triplet mass in the $SU(5) + 24_F$ model at three loops *Phys. Rev.* **D87** 115025
[71] Dorsner I, Fajfer S and Mustac I 2014 Light vector-like fermions in a minimal SU(5) setup *Phys. Rev.* **D89** 115004
[72] Tsuyuki T 2015 Bottom-tau unification by neutrinos in a nonsupersymmetric SU(5) model *PTEP* **2015** 011B01
[73] Fileviez Perez P and Murgui C 2016 Renormalizable SU(5) Unification *Phys. Rev.* **D94** 075014
[74] Hagedorn C, Ohlsson T, Riad S and Schmidt M A 2016 Unification of gauge couplings in radiative neutrino mass models *J. High Energy Phys.* JHEP09(2016)111
[75] Babu K S, Khanov A and Saad S 2017 Anarchy with hierarchy: a probabilistic appraisal *Phys. Rev.*D **95** 055014
[76] Doršner I, Fajfer S and Košnik N 2017 Leptoquark mechanism of neutrino masses within the grand unification framework *Eur. Phys. J.* **C77** 417
[77] Kumericki K, Mede T and Picek I 2018 Renormalizable SU(5) Completions of a Zee-type Neutrino Mass Model *Phys. Rev.* **D97** 055012
[78] Fileviez Pérez P, Gross A and Murgui C 2018 Seesaw scale, unification, and proton decay *Phys. Rev.* **D98** 035032
[79] Saad S 2019 Origin of a two-loop neutrino mass from SU(5) grand unification *Phys. Rev.* **D99** 115016
[80] Klein C, Lindner M and Vogl S 2019 Radiative neutrino masses and successful SU(5) unification *Phys. Rev.* **D100** 075024
[81] Doršner I and Saad S 2020 Towards minimal SU(5) *Phys. Rev.* D **101** 015009
[82] Doršner I, Džaferović-Mašić E and Saad S 2021 Parameter space exploration of the minimal SU(5) unification *Phys. Rev.* D **104** 015023
[83] Antusch S, Doršner I, Hinze K and Saad S 2023 Fully testable axion dark matter within a minimal SU(5) GUT *Phys. Rev.* D **108** 015025
[84] Antusch S, Hinze K and Saad S 2023 Minimal SU(5) GUTs with vectorlike fermions *Phys. Rev.* D **108** 095010

[85] Antusch S, Hinze K and Saad S 2023 Viable quark-lepton Yukawa ratios and nucleon decay predictions in SU(5) GUTs with type-II seesaw *Nucl. Phys.* B **986** 116049
[86] Antusch S, Hinze K and Saad S 2023 Quark-lepton Yukawa ratios and nucleon decay in SU(5) GUTs with type-III seesaw *Nucl. Phys.* B **991** 116195
[87] Georgi H and Jarlskog C 1979 A new lepton—quark mass relation in a unified theory *Phys. Lett.* B **86** 297
[88] Ellis J R and Gaillard M K 1979 Fermion masses and higgs representations in SU(5) *Phys. Lett.* **88B** 315
[89] Magg M and Wetterich C 1980 Neutrino mass problem and gauge hierarchy *Phys. Lett.* B **94** 61
[90] Schechter J and Valle J W F 1980 Neutrino masses in $SU(2) \times U(1)$ theories *Phys. Rev.* **D22** 2227
[91] Lazarides G, Shafi Q and Wetterich C 1981 Proton lifetime and fermion masses in an SO(10) model *Nucl. Phys.* B **181** 287
[92] Mohapatra R N and Senjanovic G 1981 Neutrino masses and mixings in gauge models with spontaneous parity violation *Phys. Rev.* D **23** 165
[93] Foot R, Lew H, He X G and Joshi G C 1989 Seesaw neutrino masses induced by a triplet of leptons *Z. Phys. C* **44** 441
[94] Minkowski P 1977 $\mu \to e\gamma$ at a rate of one out of 10^9 muon decays? *Phys. Lett.* **67B** 421
[95] Yanagida T 1979 Horizontal gauge symmetry and masses of neutrinos *Conf. Proc.* **C7902131** 95
[96] Glashow S 1980 The future of elementary particle physics *NATO Sci. Ser.*B **61** 687
[97] Gell-Mann M, Ramond P and Slansky R 1979 Complex spinors and unified theories *Conf. Proc.* C **790927** 315
[98] Mohapatra R N and Senjanovic G 1980 Neutrino mass and spontaneous parity nonconservation *Phys. Rev. Lett.* **44** 912
[99] Antusch S and Spinrath M 2009 New GUT predictions for quark and lepton mass ratios confronted with phenomenology *Phys. Rev.* D **79** 095004
[100] Antusch S, King S F and Spinrath M 2014 GUT predictions for quark-lepton Yukawa coupling ratios with messenger masses from non-singlets *Phys. Rev.* D **89** 055027
[101] Antusch S and Hinze K 2022 Nucleon decay in a minimal non-SUSY GUT with predicted quark-lepton Yukawa ratios *Nucl. Phys.* B **976** 115719
[102] Hisano J, Murayama H and Yanagida T 1993 Nucleon decay in the minimal supersymmetric SU(5) grand unification *Nucl. Phys.* B **402** 46
[103] Sakai N and Yanagida T 1982 Proton decay in a class of supersymmetric grand unified models *Nucl. Phys.* B **197** 533
[104] Dimopoulos S, Raby S and Wilczek F 1982 Proton decay in supersymmetric models *Phys. Lett.* B **112** 133
[105] Ellis J R, Nanopoulos D V and Rudaz S 1982 GUTs 3: SUSY GUTs 2 *Nucl. Phys.* B **202** 43
[106] Nath P, Chamseddine A H and Arnowitt R L 1985 Nucleon decay in supergravity unified theories *Phys. Rev.* D **32** 2348
[107] Nath P and Arnowitt R L 1988 Limits on photino and squark masses from proton lifetime in supergravity and superstring models *Phys. Rev.* D **38** 1479
[108] Goto T and Nihei T 1999 Effect of RRRR dimension five operator on the proton decay in the minimal SU(5) SUGRA GUT model *Phys. Rev.* D **59** 115009
[109] Murayama H and Pierce A 2002 Not even decoupling can save minimal supersymmetric SU(5) *Phys. Rev.* D **65** 055009
[110] Ellis J, Evans J L, Nagata N, Olive K A and Velasco-Sevilla L 2020 Supersymmetric proton decay revisited *Eur. Phys. J.* C **80** 332
[111] Chamseddine A H, Arnowitt R L and Nath P 1982 Locally supersymmetric grand unification *Phys. Rev. Lett.* **49** 970
[112] Akula S, Altunkaynak B, Feldman D, Nath P and Peim G 2012 Higgs boson mass predictions in SUGRA unification, recent LHC-7 results, and dark matter *Phys. Rev.* D **85** 075001
[113] Chan K L, Chattopadhyay U and Nath P 1998 Naturalness, weak scale supersymmetry and the prospect for the observation of supersymmetry at the Tevatron and at the CERN LHC *Phys. Rev.* D **58** 096004
[114] Liu M and Nath P 2013 Higgs boson mass, proton decay, naturalness, and constraints of the LHC and Planck data *Phys. Rev.* D **87** 095012
[115] Hisano J, Kobayashi D, Kuwahara T and Nagata N 2013 Decoupling can revive minimal supersymmetric SU(5) *J. High Energy Phys.* JHEP07(2013)038

[116] Nagata N and Shirai S 2014 Sfermion flavor and proton decay in high-scale supersymmetry *J. High Energy Phys.* JHEP03(2014)049
[117] Bajc B, Lavignac S and Mede T 2016 Resurrecting the minimal renormalizable supersymmetric SU(5) model *J. High Energy Phys.* JHEP01(2016)044
[118] Babu K S, Gogoladze I and Un C S 2022 Proton lifetime in minimal SUSY SU(5) in light of LHC results *J. High Energy Phys.* JHEP02(2022)164
[119] Hisano J Proton decay in SUSY GUTs arxiv:2202.01404
[120] Ibrahim T and Nath P 2000 Effects of large CP phases on the proton lifetime in supersymmetric unification *Phys. Rev.* D **62** 095001
[121] Bajc B, Fileviez Perez P and Senjanovic G 2002 Proton decay in minimal supersymmetric SU(5) *Phys. Rev.* D **66** 075005
[122] Bajc B, Fileviez Perez P and Senjanovic G 2002 Minimal supersymmetric SU(5) theory and proton decay: where do we stand? *Conf. on Physics Beyond the Standard Model: Beyond the Desert 02* vol 10, pp 131–9
[123] Nath P and Syed R M 2008 Suppression of Higgsino mediated proton decay by cancellations in GUTs and strings *Phys. Rev.* D **77** 015015
[124] Nath P 1996 Hierarchies and textures in supergravity unification *Phys. Rev. Lett.* **76** 2218
[125] Nath P 1996 Textured minimal and extended supergravity unification and implications for proton stability *Phys. Lett.* B **381** 147
[126] Bachas C, Fabre C and Yanagida T 1996 Natural gauge coupling unification at the string scale *Phys. Lett.* B **370** 49
[127] Chkareuli J L and Gogoladze I G 1998 Unification picture in minimal supersymmetric SU(5) model with string remnants *Phys. Rev.* D **58** 055011
[128] Evans J L and Yanagida T T Upper limit on the proton lifetime in minimal supersymetric SU(5) arxiv:2109.12505
[129] Hamaguchi K, Hor S and Nagata N 2020 R-symmetric flipped SU(5) *J. High Energy Phys.* JHEP11(2020)140
[130] Mehmood M, Rehman M U and Shafi Q 2021 Observable proton decay in flipped SU(5) *J. High Energy Phys.* JHEP02(2021)181
[131] Babu K S and Mohapatra R N 1993 Predictive neutrino spectrum in minimal SO(10) grand unification *Phys. Rev. Lett.* **70** 2845
[132] Bajc B, Senjanovic G and Vissani F 2001 How neutrino and charged fermion masses are connected within minimal supersymmetric SO(10) *PoS* **HEP2001** 198
[133] Bajc B, Senjanovic G and Vissani F 2003 *b*—tau unification and large atmospheric mixing: a case for noncanonical seesaw *Phys. Rev. Lett.* **90** 051802
[134] Fukuyama T and Okada N 2002 Neutrino oscillation data versus minimal supersymmetric SO(10) model *J. High Energy Phys.* JHEP11(2002)011
[135] Goh H S, Mohapatra R N and Ng S-P 2003 Minimal SUSY SO(10), *b* tau unification and large neutrino mixings *Phys. Lett.* B **570** 215
[136] Goh H S, Mohapatra R N and Ng S-P 2003 Minimal SUSY SO(10) model and predictions for neutrino mixings and leptonic CP violation *Phys. Rev.* D **68** 115008
[137] Bertolini S, Frigerio M and Malinsky M 2004 Fermion masses in SUSY SO(10) with type II seesaw: a non-minimal predictive scenario *Phys. Rev.* D **70** 095002
[138] Bertolini S and Malinsky M 2005 On CP violation in minimal renormalizable SUSY SO(10) and beyond *Phys. Rev.* D **72** 055021
[139] Babu K S and Macesanu C 2005 Neutrino masses and mixings in a minimal SO(10) model *Phys. Rev.* D **72** 115003
[140] Bertolini S, Schwetz T and Malinsky M 2006 Fermion masses and mixings in SO(10) models and the neutrino challenge to SUSY GUTs *Phys. Rev.* D **73** 115012
[141] Bajc B, Dorsner I and Nemevsek M 2008 Minimal SO(10) splits supersymmetry *J. High Energy Phys.* JHEP11(2008)007
[142] Joshipura A S and Patel K M 2011 Fermion masses in SO(10) models *Phys. Rev.* D **83** 095002
[143] Altarelli G and Meloni D 2013 A non supersymmetric SO(10) grand unified model for all the physics below $M_{\rm GUT}$ *J. High Energy Phys.* JHEP08(2013)021
[144] Dueck A and Rodejohann W 2013 Fits to SO(10) grand unified models *J. High Energy Phys.* JHEP09(2013)024
[145] Fukuyama T, Ichikawa K and Mimura Y 2016 Revisiting fermion mass and mixing fits in the minimal SUSY *SO*(10) GUT *Phys. Rev.* D **94** 075018

[146] Babu K S, Bajc B and Saad S 2016 New class of SO(10) models for flavor *Phys. Rev.* D **94** 015030
[147] Babu K S, Bajc B and Saad S 2017 Yukawa sector of minimal SO(10) unification *J. High Energy Phys.* JHEP02(2017)136
[148] Saad S 2017 SO(10) models for flavor with vector-like fermions *AIP Conf. Proc.* **1900** 020010
[149] Babu K S, Bajc B and Saad S 2018 Resurrecting minimal Yukawa sector of SUSY SO(10) *J. High Energy Phys.* JHEP10(2018)135
[150] Babu K S, Fukuyama T, Khan S and Saad S 2019 Peccei–Quinn symmetry and nucleon decay in renormalizable SUSY SO(10) *J. High Energy Phys.* JHEP06(2019)045
[151] Ohlsson T and Pernow M 2019 Fits to non-supersymmetric SO(10) models with Type I and II Seesaw mechanisms using renormalization group evolution *J. High Energy Phys.* JHEP06(2019)085
[152] Babu K S and Saad S 2021 Flavor hierarchies from clockwork in SO(10) GUT *Phys. Rev.* D **103** 015009
[153] Shaposhnikov M E 1986 Possible Appearance of the baryon asymmetry of the Universe in an electroweak theory *JETP Lett.* **44** 465
[154] Shaposhnikov M E 1987 Baryon asymmetry of the universe in standard electroweak theory *Nucl. Phys.* **B287** 757
[155] Fukugita M and Yanagida T 1986 Baryogenesis without grand unification *Phys. Lett.* B **174** 45
[156] Lee D-G, Mohapatra R N, Parida M K and Rani M 1995 Predictions for proton lifetime in minimal nonsupersymmetric SO(10) models: an update *Phys. Rev.* D **51** 229
[157] Chang D, Mohapatra R N and Parida M K 1984 Decoupling parity and SU(2)-R breaking scales: a new approach to left–right symmetric models *Phys. Rev. Lett.* **52** 1072
[158] Lazarides G, Magg M and Shafi Q 1980 Phase transitions and magnetic monopoles in SO(10) *Phys. Lett.* B **97** 87
[159] Uzhinsky V and Galoyan A Description of the Totem experimental data on elastic pp-scattering at $\sqrt{s} = 7$ TeV in the framework of unified systematic of elastic scattering data arXiv:1111.4984
[160] Chang D and Kumar A 1986 Symmetry breaking of SO(10) by 210-dimensional Higgs Boson and the Michel's conjecture *Phys. Rev.* D **33** 2695
[161] Basecq J, Meljanac S and O'Raifeartaigh L 1989 Stability of spontaneous symmetry breaking in a class of SO(10) Models *Phys. Rev.* D **39** 3110
[162] He X G and Meljanac S 1989 Stability of spontaneous symmetry breaking in a class of SO(10) Models *Phys. Rev.* D **40** 2098
[163] Kaymakcalan O, Michel L, Wali K C, McGlinn W D and O'Raifeartaigh L 1986 Absolute minima of a SO(10) invariant Higgs potential *Nucl. Phys.* B **267** 203
[164] Thornburg R J and Mcglinn W D 1986 Extrema of SO(N) invariant Higgs potentials and their associated mass eigenstates *Phys. Rev.* D **33** 2991
[165] Kuchimanchi R 1993 Absolute minima, stability and mass spectrum for one step breaking of SO(N) *Phys. Rev.* D **47** 685
[166] Meloni D, Ohlsson T and Pernow M 2020 Threshold effects in SO(10) models with one intermediate breaking scale *Eur. Phys. J.* C **80** 840
[167] Chakrabortty J, Maji R and King S F 2019 Unification, proton decay and topological defects in non-SUSY GUTs with thresholds *Phys. Rev.* D **99** 095008
[168] Babu K S and Khan S 2015 Minimal nonsupersymmetric SO(10) model: gauge coupling unification, proton decay, and fermion masses *Phys. Rev.* D **92** 075018
[169] Bertolini S, Di Luzio L and Malinsky M 2013 Light color octet scalars in the minimal SO(10) grand unification *Phys. Rev.* D **87** 085020
[170] Kolešová H and Malinský M 2014 Proton lifetime in the minimal SO(10) GUT and its implications for the LHC *Phys. Rev.* D **90** 115001
[171] Bertolini S, Di Luzio L and Malinsky M 2010 On the vacuum of the minimal nonsupersymmetric SO(10) unification *Phys. Rev.* D **81** 035015
[172] Gráf L, Malinský M, Mede T and Susič V 2017 One-loop pseudo-Goldstone masses in the minimal SO(10) Higgs model *Phys. Rev.* D **95** 075007
[173] Jarkovská K, Malinský M, Mede T and Susič V Quantum guts of the minimal potentially realistic SO(10) Higgs model arXiv:2109.06784
[174] Chang D, Mohapatra R N, Gipson J, Marshak R E and Parida M K 1985 Experimental Tests of New SO(10) Grand Unification *Phys. Rev.* D **31** 1718

[175] Ferrari S, Hambye T, Heeck J and Tytgat M H G 2019 SO(10) paths to dark matter *Phys. Rev.* D **99** 055032
[176] Preda A, Senjanovic G and Zantedeschi M SO(10): a Case for Hadron Colliders arXiv:2201.02785
[177] Parida M K, Nayak B P, Satpathy R and Awasthi R L 2017 Standard coupling unification in so(10), hybrid seesaw neutrino mass and leptogenesis, dark matter, and proton lifetime predictions *J. High Energy Phys.* JHEP04(2017)075
[178] Arbeláez Rodrí C, Kolešová H and Malinský M 2014 Witten's mechanism in the flipped SU(5) unification *Phys. Rev.* D **89** 055003
[179] Bertolini S, Di Luzio L and Malinsky M 2012 Seesaw scale in the minimal renormalizable SO(10) grand unification *Phys. Rev.* D **85** 095014
[180] Babu K S, Bajc B and Tavartkiladze Z 2012 Realistic fermion masses and nucleon decay rates in SUSY SU(5) with vector-like matter *Phys. Rev.* D **86** 075005
[181] Nath P and Arnowitt R L 1998 Grand unification and B and L conservation *Int. Symp. on Lepton and Baryon Number Violation* vol 4, pp 3–32
[182] Pati J C 2003 Link between neutrino oscillations, leptogenesis, and proton decay in supersymmetric grand unification *Int. Conf. on 20 Years of SUGRA and Search for SUSY and Unification (SUGRA 20)* vol 3, pp 299–321
[183] Ellis J R, Nanopoulos D V and Walker J 2002 Flipping SU(5) out of trouble *Phys. Lett.* B **550** 99
[184] Ellis J, Evans J L, Nagata N, Nanopoulos D V and Olive K A 2021 Flipped SU(5) GUT phenomenology: proton decay and $\mathbf{g}_{\mu} - \mathbf{2}$ *Eur. Phys. J.* C **81** 1109
[185] Ellis J, Garcia M A G, Nagata N, Nanopoulos D V and Olive K A 2020 Proton Decay: Flipped vs Unflipped SU(5) *J. High Energy Phys.* JHEP05(2020)021
[186] Arkani-Hamed N, Dimopoulos S, Giudice G F and Romanino A 2005 Aspects of split supersymmetry *Nucl. Phys.* B **709** 3
[187] Hebecker A and March-Russell J 2002 Proton decay signatures of orbifold GUTs *Phys. Lett.* B **539** 119
[188] Alciati M L, Feruglio F, Lin Y and Varagnolo A 2005 Proton lifetime from SU(5) unification in extra dimensions *J. High Energy Phys.* JHEP03(2005)054
[189] Mohapatra R N and Severson M 2018 Leptonic *CP* Violation and Proton Decay in SUSY SO(10) *J. High Energy Phys.* JHEP09(2018)119
[190] Bhupal Dev P S and Mohapatra R N 2010 Electroweak symmetry breaking and proton decay in SO(10) SUSY-GUT with TeV W(R) *Phys. Rev.* D **82** 035014
[191] Shafi Q and Tavartkiladze Z 2000 Flavor problem, proton decay and neutrino oscillations in SUSY models with anomalous U(1) *Phys. Lett.* B **473** 272
[192] Lucas V and Raby S 1997 Nucleon decay in a realistic SO(10) SUSY GUT *Phys. Rev.* D **55** 6986
[193] Babu K S, Pati J C and Wilczek F 1998 Suggested new modes in supersymmetric proton decay *Phys. Lett.* B **423** 337
[194] Babu K S, Pati J C and Wilczek F 2000 Fermion masses, neutrino oscillations, and proton decay in the light of Super-Kamiokande *Nucl. Phys.* B **566** 33
[195] Pati J C 2000 Discovery of proton decay: a must for theory, a challenge for experiment *AIP Conf. Proc.* **533** 37
[196] Bhupal Dev P S, Dutta B, Mohapatra R N and Severson M 2012 θ_{13} and proton decay in a minimal $SO(10) \times S_4$ model of flavor *Phys. Rev.* D **86** 035002
[197] Buchmuller W, Covi L, Emmanuel-Costa D and Wiesenfeldt S 2004 Flavour structure and proton decay in 6D orbifold GUTs *J. High Energy Phys.* **09** JHEP09(2004)004
[198] Klebanov I R and Witten E 2003 Proton decay in intersecting D-brane models *Nucl. Phys.* B **664** 3
[199] Bueno A, Dai Z, Ge Y, Laffranchi M, Melgarejo A J, Meregaglia A *et al* 2007 Nucleon decay searches with large liquid argon TPC detectors at shallow depths: Atmospheric neutrinos and cosmogenic backgrounds *J. High Energy Phys.* JHEP04(2007)041
[200] Aulakh C S and Mohapatra R N 1983 Implications of supersymmetric SO(10) grand unification *Phys. Rev.* D **28** 217
[201] Clark T E, Kuo T-K and Nakagawa N 1982 A SO(10) supersymmetric grand unified theory *Phys. Lett.* B **115** 26
[202] Aulakh C S 2005 MSGUTs from germ to bloom: Towards falsifiability and beyond *Workshop Ser. Theor. High Energy Phys.* **6** 1–40 arxiv:hep-ph/0506291

[203] Bajc B, Melfo A, Senjanovic G and Vissani F 2006 Fermion mass relations in a supersymmetric SO(10) theory *Phys. Lett.* B **634** 272
[204] Aulakh C S and Garg S K 2006 MSGUT: from bloom to doom *Nucl. Phys.* B **757** 47
[205] Peccei R D and Quinn H R 1977 CP Conservation in the presence of instantons *Phys. Rev. Lett.* **38** 1440
[206] Di Luzio L, Giannotti M, Nardi E and Visinelli L 2020 The landscape of QCD axion models *Phys. Rept.* **870** 1
[207] Hisano J, Murayama H and Yanagida T 1992 Peccei–Quinn symmetry and suppression of nucleon decay rates in SUSY GUTs *Phys. Lett.* B **291** 263
[208] Wise M B, Georgi H and Glashow S L 1981 SU(5) and the Invisible Axion *Phys. Rev. Lett.* **47** 402
[209] Lazarides G 1982 SO(10) and the Invisible Axion *Phys. Rev.* D **25** 2425
[210] Ernst A, Ringwald A and Tamarit C 2018 Axion predictions in $SO(10) \times U(1)_{PQ}$ Models *J. High Energy Phys.* JHEP02(2018)103
[211] Di Luzio L, Ringwald A and Tamarit C 2018 Axion mass prediction from minimal grand unification *Phys. Rev.* D **98** 095011
[212] Ernst A, Di Luzio L, Ringwald A and Tamarit C 2019 Axion properties in GUTs *PoS* **CORFU2018** 054
[213] Fileviez Pérez P, Murgui C and Plascencia A D 2020 Axion dark matter, proton decay and unification *J. High Energy Phys.* JHEP01(2020)091
[214] Dutta B, Mimura Y and Mohapatra R N 2005 Suppressing proton decay in the minimal SO(10) model *Phys. Rev. Lett.* **94** 091804
[215] Babu K S, Pati J C and Tavartkiladze Z 2010 Constraining proton lifetime in SO(10) with stabilized doublet-triplet splitting *J. High Energy Phys.* JHEP06(2010)08
[216] Pati J C 2017 Advantages of unity with SU(4)-Color: reflections through neutrino oscillations, baryogenesis and proton decay *Int. J. Mod. Phys.* A **32** 1741013
[217] Hagedorn C, Lindner M and Mohapatra R N 2006 S(4) flavor symmetry and fermion masses: Towards a grand unified theory of flavor *J. High Energy Phys.* JHEP06(2006)042
[218] Chen M-C and Mahanthappa K T 2007 CKM and Tri-bimaximal MNS matrices in a $SU(5)\times^{(d)}T$ model *Phys. Lett.* B **652** 34
[219] Hagedorn C, Schmidt M A and Smirnov A Y 2009 Lepton mixing and cancellation of the dirac mass hierarchy in SO(10) GUTs with flavor symmetries T(7) and sigma(81) *Phys. Rev.* D **79** 036002
[220] Ishimori H, Shimizu Y and Tanimoto M 2009 S(4) Flavor symmetry of quarks and leptons in SU(5) GUT *Prog. Theor. Phys.* **121** 769
[221] Joshipura A S, Kodrani B P and Patel K M 2009 Fermion masses and mixings in a mu-tau symmetric SO(10) *Phys. Rev.* D **79** 115017
[222] Dutta B, Mimura Y and Mohapatra R N 2010 An SO(10) grand unified theory of flavor *J. High Energy Phys.* JHEP05(2010)034
[223] King S F and Luhn C 2010 A Supersymmetric grand unified theory of flavour with PSL(2)(7) x SO(10) *Nucl. Phys.* B **832** 414
[224] Altarelli G and Feruglio F 2010 Discrete flavor symmetries and models of neutrino mixing *Rev. Mod. Phys.* **82** 2701
[225] Hagedorn C, King S F and Luhn C 2010 A SUSY GUT of flavour with S4 $\times$ SU(5) to NLO *J. High Energy Phys.* JHEP06(2010)048
[226] Antusch S, King S F and Spinrath M 2011 Measurable neutrino mass scale in $A_4 \times$ SU(5) *Phys. Rev.* D **83** 013005
[227] de Medeiros Varzielas I 2012 Non-Abelian family symmetries in Pati–Salam unification *J. High Energy Phys.* JHEP01(2012)097
[228] Antusch S, King S F and Spinrath M 2013 Spontaneous CP violation in $A_4 \times SU(5)$ with constrained sequential dominance 2 *Phys. Rev.* D **87** 096018
[229] Feruglio F 2015 Pieces of the flavour puzzle *Eur. Phys. J.* C **75** 373
[230] Meloni D 2017 GUT and flavor models for neutrino masses and mixing *Front. Phys.* **5** 43
[231] Xing Z-z 2020 Flavor structures of charged fermions and massive neutrinos *Phys. Rept.* **854** 1
[232] Muon g-2 collaboration 2006 Final report of the muon E821 anomalous magnetic moment measurement at BNL *Phys. Rev.* D **73** 072003
[233] Aoyama T *et al* 2020 The anomalous magnetic moment of the muon in the Standard Model *Phys. Rep.* **887** 1

[234] Babu K S, Gogoladze I, Nath P and Syed R M 2012 Variety of SO(10) GUTs with natural doublet-triplet splitting via the missing partner mechanism *Phys. Rev.* D **85** 075002
[235] Aboubrahim A, Nath P and Syed R M 2021 Yukawa coupling unification in an SO(10) model consistent with Fermilab $(g\text{-}2)_\mu$ result *J. High Energy Phys.* JHEP06(2021)002
[236] Babu K S, Gogoladze I, Nath P and Syed R M 2005 A unified framework for symmetry breaking in SO(10) *Phys. Rev.* D **72** 095011
[237] Babu K S, Gogoladze I, Nath P and Syed R M 2006 Fermion mass generation in SO(10) with a unified Higgs sector *Phys. Rev.* D **74** 075004
[238] Dimopoulos S and Wilczek F Incomplete Multiplets in Supersymmetric Unified Models
[239] Babu K S and Barr S M 1993 Natural suppression of Higgsino mediated proton decay in supersymmetric SO(10) *Phys. Rev.* D **48** 5354
[240] Barr S M and Raby S 1997 Minimal SO(10) unification *Phys. Rev. Lett.* **79** 4748
[241] Masiero A, Nanopoulos D V, Tamvakis K and Yanagida T 1982 Naturally massless higgs doublets in supersymmetric SU(5) *Phys. Lett.* B **115** 380
[242] Babu K S, Gogoladze I and Tavartkiladze Z 2007 Missing partner mechanism in SO(10) grand unification *Phys. Lett.* B **650** 49
[243] Nath P and Syed R M 2016 An analysis of B–L= −2 Operators from Matter-Higgs interactions in a class of supersymmetric SO(10) models *Phys. Rev.* D **93** 055005
[244] Hill C T 1984 Are there significant gravitational corrections to the unification scale? *Phys. Lett.* B **135** 47
[245] Shafi Q and Wetterich C 1984 Modification of GUT predictions in the presence of spontaneous compactification *Phys. Rev. Lett.* **52** 875
[246] Calmet X, Hsu S D H and Reeb D 2008 Grand unification and enhanced quantum gravitational effects *Phys. Rev. Lett.* **101** 171802
[247] Dorsner I and Perez P Fileviez 2005 Could we rotate proton decay away? *Phys. Lett.* B **606** 367
[248] Kolešová H and Malinský M 2019 Flavor structure of GUTs and uncertainties in proton lifetime estimates *Phys. Rev.* D **99** 035005
[249] Ellis J R, Gaillard M K and Nanopoulos D V 1979 On the effective lagrangian for baryon decay *Phys. Lett.* B **88** 320
[250] Ellis J, Evans J L, Mustafayev A, Nagata N and Olive K A 2016 The super-GUT CMSSM revisited *Eur. Phys. J.* C **76** 592
[251] Patel K M and Shukla S K Anatomy of scalar mediated proton decays in *SO*(10) models arXiv:2203.07748
[252] Kawamura Y 2001 Triplet doublet splitting, proton stability and extra dimension *Prog. Theor. Phys.* **105** 999
[253] Altarelli G and Feruglio F 2001 SU(5) grand unification in extra dimensions and proton decay *Phys. Lett.* B **511** 257
[254] Hall L J and Nomura Y 2001 Gauge unification in higher dimensions *Phys. Rev.* D **64** 055003
[255] Feruglio F, Patel K M and Vicino D 2014 Order and anarchy hand in hand in 5D SO(10) *J. High Energy Phys.* JHEP09(2014)095
[256] Feruglio F, Patel K M and Vicino D 2015 A realistic pattern of fermion masses from a five-dimensional SO(10) model *J. High Energy Phys.* JHEP09(2015)040
[257] Kitano R and Li T-j 2003 Flavor hierarchy in SO(10) grand unified theories via five-dimensional wave function localization *Phys. Rev.* D **67** 116004
[258] Buchmuller W, Dierigl M, Ruehle F and Schweizer J 2015 Split symmetries *Phys. Lett.* B **750** 615
[259] Buchmuller W and Schweizer J 2017 Flavor mixings in flux compactifications *Phys. Rev.* D **95** 075024
[260] Buchmuller W and Patel K M 2018 Flavor physics without flavor symmetries *Phys. Rev.* D **97** 075019
[261] Dermisek R and Mafi A 2002 SO(10) grand unification in five-dimensions: Proton decay and the mu problem *Phys. Rev.* D **65** 055002
[262] Alciati M L, Feruglio F, Lin Y and Varagnolo A 2006 Fermion masses and proton decay in a minimal five-dimensional SO(10) model *J. High Energy Phys.* JHEP11(2006)039
[263] Buchmuller W and Patel K M 2019 Proton decay in flux compactifications *J. High Energy Phys.* JHEP05(2019)196
[264] Joshipura A S and Patel K M 2012 Yukawa coupling unification in SO(10) with positive \mu\ and a heavier gluino *Phys. Rev.* D **86** 035019

[265] Bagnaschi E, Brümmer F, Buchmüller W, Voigt A and Weiglein G 2016 Vacuum stability and supersymmetry at high scales with two Higgs doublets *J. High Energy Phys.* JHEP03(2016)158
[266] Mummidi V S, P K V and Patel K M 2018 Effects of heavy neutrinos on vacuum stability in two-Higgs-doublet model with GUT scale supersymmetry *J. High Energy Phys.* JHEP08(2018)134
[267] Mummidi V S and Patel K M 2019 Pseudo-Dirac Higgsino dark matter in GUT scale supersymmetry *J. High Energy Phys.* JHEP01(2019)224
[268] Suryanarayana Mummidi V and Patel K M 2020 Precision unification and Higgsino dark matter in GUT scale supersymmetry *Phys. Rev.* D **101** 115008
[269] Antusch S, Hohl C and Susič V 2021 Employing nucleon decay as a fingerprint of SUSY GUT models using SusyTCProton *J. High Energy Phys.* JHEP06(2021)022
[270] Pati J C and Salam A 1973 Unified lepton–hadron symmetry and a gauge theory of the basic interactions *Phys. Rev.* D **8** 1240
[271] Valencia G and Willenbrock S 1994 Quark—lepton unification and rare meson decays *Phys. Rev.* D **50** 6843
[272] Smirnov A D 2007 Mass limits for scalar and gauge leptoquarks from $K_L^0 \to e^{\mp}\mu^{\pm}$, $B^0 \to e^{\mp}\tau^{\pm}$ decays *Mod. Phys. Lett.*A **22** 2353
[273] Dolan M J, Dutka T P and Volkas R R 2021 Lowering the scale of Pati-Salam breaking through seesaw mixing *J. High Energy Phys.* JHEP05(2021)199
[274] LHCb collaboration 2015 Measurement of the ratio of branching fractions $\mathcal{B}(\bar{B}^0 \to D^{*+}\tau^-\bar{\nu}_\tau)/\mathcal{B}(\bar{B}^0 \to D^{*+}\mu^-\bar{\nu}_\mu)$ *Phys. Rev. Lett.* **115** 111803
[275] LHCb collaboration 2017 Test of lepton universality with $B^0 \to K^{*0}\ell^+\ell^-$ decays *J. High Energy Phys.* JHEP08(2017)055
[276] LHCb collaboration 2014 Test of lepton universality using $B^+ \to K^+\ell^+\ell^-$ decays *Phys. Rev. Lett.* **113** 151601
[277] LHCb collaboration 2019 Search for lepton-universality violation in $B^+ \to K^+\ell^+\ell^-$ decays *Phys. Rev. Lett.* **122** 191801
[278] Assad N, Fornal B and Grinstein B 2018 Baryon number and lepton universality violation in leptoquark and diquark models *Phys. Lett.* B **777** 324
[279] Di Luzio L, Greljo A and Nardecchia M 2017 Gauge leptoquark as the origin of B-physics anomalies *Phys. Rev.* D **96** 115011
[280] Calibbi L, Crivellin A and Li T 2018 Model of vector leptoquarks in view of the B-physics anomalies *Phys. Rev.* D **98** 115002
[281] Bordone M, Cornella C, Fuentes-Martin J and Isidori G 2018 A three-site gauge model for flavor hierarchies and flavor anomalies *Phys. Lett.* B **779** 317
[282] Blanke M and Crivellin A 2018 *B* Meson anomalies in a Pati–Salam model within the Randall-Sundrum background *Phys. Rev. Lett.* **121** 011801
[283] Heeck J and Teresi D 2018 Pati-Salam explanations of the B-meson anomalies *J. High Energy Phys.* JHEP12(2018)103
[284] Balaji S, Foot R and Schmidt M A 2019 Chiral SU(4) explanation of the $b \to s$ anomalies *Phys. Rev.* D **99** 015029
[285] Fornal B, Gadam S A and Grinstein B 2019 Left-right SU(4) Vector leptoquark model for flavor anomalies *Phys. Rev.* D **99** 055025
[286] Balaji S and Schmidt M A 2020 Unified SU(4) theory for the $R_{D^{(*)}}$ and $R_{K^{(*)}}$ anomalies *Phys. Rev.* D **101** 015026
[287] Mohapatra R N and Marshak R 1980 Local B–L symmetry of electroweak interactions, majorana neutrinos and neutron oscillations *Phys. Rev. Lett.* **44** 1316
[288] Davidson A 1979 $B-L$ as the fourth color within an $SU(2)_L \times U(1)_R \times U(1)$ model *Phys. Rev.* D **20** 776
[289] Pati J C, Salam A and Sarkar U 1983 $\Delta B = -\Delta L$, neutron —> $e^-\pi^+$, e^-K^+ , $\mu^-\pi^+$ and μ^-K^+ decay modes in $SU(2)_L$ X $SU(2)_R$ X $SU(4)^{col}$ or SO(10) *Phys. Lett.* B **133** 330
[290] Pati J C 1984 Nucleon Decays Into Lepton + Lepton + Anti-lepton + Mesons Within SU(4) of Color *Phys. Rev.* D **29** 1549
[291] Rudaz S 1992 Chiral symmetry, broken scale invariance and the nuclear equation of state *Workshop on QCD Vacuum Structure* p 10
[292] O'Donnell P J and Sarkar U 1993 Three lepton decay mode of the proton *Phys. Lett.* B **316** 121
[293] Brahmachari B, O'Donnell P J and Sarkar U 1997 A Model for the three lepton decay mode of the proton *Z. Phys.*C **74** 171
[294] Weinberg S 1979 Baryon and lepton nonconserving processes *Phys. Rev. Lett.* **43** 1566

[295] Weinberg S 1980 Varieties of baryon and lepton nonconservation *Phys. Rev.* D **22** 1694
[296] Weldon H A and Zee A 1980 Operator analysis of new physics *Nucl. Phys.* B **173** 269
[297] Saad S 2019 Fermion masses and mixings, leptogenesis and baryon number violation in Pati–Salam model *Nucl. Phys.* B **943** 114630
[298] Super-Kamiokande collaboration 2014 Search for trilepton nucleon decay via $p \to e^+\nu\nu$ and $p \to \mu^+\nu\nu$ in the Super-Kamiokande experiment *Phys. Rev. Lett.* **113** 101801
[299] Chen M-C and Takhistov V 2014 Charged lepton spectrum approximation in a three body nucleon decay *Phys. Rev.* D **89** 095003
[300] Sakharov A D 1967 Violation of CP Invariance, C asymmetry, and baryon asymmetry of the universe *Pisma Zh. Eksp. Teor. Fiz.* **5** 32
[301] Kuzmin V 1970 Cp violation and baryon asymmetry of the universe *Pisma Zh. Eksp. Teor. Fiz.* **12** 335
[302] Nussinov S and Shrock R 2002 N—anti-N oscillations in models with large extra dimensions *Phys. Rev. Lett.* **88** 171601
[303] Chang L and Chang N 1980 *B–L* nonconservation and neutron oscillation *Phys. Lett.* B **92** 103
[304] Kuo T-K and Love S 1980 Neutron oscillations and the existence of massive neutral leptons *Phys. Rev. Lett.* **45** 93
[305] Cowsik R and Nussinov S 1981 Some constraints on $\Delta b = 2\text{n}-\text{n}$ oscillations *Phys. Lett.* B **101** 237
[306] Rao S and Shrock R 1982 $n \leftrightarrow \bar{n}$ Transition operators and their matrix elements in the MIT bag model *Phys. Lett.* B **116** 238
[307] Rao S and Shrock R E 1984 Six Fermion ($B-L$) violating operators of arbitrary generational structure *Nucl. Phys.* B **232** 143
[308] Phillips D G I 2016 Neutron-antineutron oscillations: theoretical status and experimental prospects *Phys. Rept.* **612** 1
[309] Addazi A *et al* 2021 New high-sensitivity searches for neutrons converting into antineutrons and/or sterile neutrons at the HIBEAM/NNBAR experiment at the european spallation source *J. Phys. G* **48** 070501
[310] Marshak R E and Mohapatra R N 1980 Quark—Lepton symmetry and B-L as the U(1) generator of the electroweak symmetry group *Phys. Lett.* B **91** 222
[311] Babu K S, Dev P S B and Mohapatra R N 2009 Neutrino mass hierarchy, neutron—anti-neutron oscillation from baryogenesis *Phys. Rev.* D **79** 015017
[312] Babu K S, Dev P S B, Fortes E C F S and Mohapatra R N 2013 Post-Sphaleron baryogenesis and an upper limit on the neutron-antineutron oscillation time *Phys. Rev.* **D87** 115019
[313] Babu K S, Mohapatra R N and Nasri S 2006 Post-sphaleron baryogenesis *Phys. Rev. Lett.* **97** 131301
[314] Mohapatra R N, Okada N and Yu H-B 2008 Diquark Higgs at LHC *Phys. Rev.* D **77** 011701
[315] Chen C-R, Klemm W, Rentala V and Wang K 2009 Color sextet scalars at the CERN large hadron collider *Phys. Rev.* D **79** 054002
[316] Berger E L, Cao Q-H, Chen C-R, Shaughnessy G and Zhang H 2010 Color sextet scalars in early LHC experiments *Phys. Rev. Lett.* **105** 181802
[317] Baldes I, Bell N F and Volkas R R 2011 Baryon number violating scalar diquarks at the LHC *Phys. Rev.* D **84** 115019
[318] Chivukula R S, Ittisamai P, Mohan K and Simmons E H 2015 Color discriminant variable and scalar diquarks at the LHC *Phys. Rev.* D **92** 075020
[319] CMS collaboration 2020 Search for high mass dijet resonances with a new background prediction method in proton-proton collisions at $\sqrt{s} = 13$ TeV *J. High Energy Phys.* JHEP05(2020)033
[320] Pascual-Dias B, Saha P and London D 2020 LHC constraints on scalar diquarks *J. High Energy Phys.* JHEP07(2020)144
[321] Dev P S B and Mohapatra R N 2015 TeV scale model for baryon and lepton number violation and resonant baryogenesis *Phys. Rev.* D **92** 016007
[322] Allahverdi R, Dev P S B and Dutta B 2018 A simple testable model of baryon number violation: baryogenesis, dark matter, neutron-antineutron oscillation and collider signals *Phys. Lett.* B **779** 262
[323] Grojean C, Shakya B, Wells J D and Zhang Z 2018 Implications of an improved neutron-antineutron oscillation search for baryogenesis: a minimal effective theory analysis *Phys. Rev. Lett.* **121** 171801

[324] Arkani-Hamed N and Schmaltz M 2000 Hierarchies without symmetries from extra dimensions *Phys. Rev.* D **61** 033005
[325] Girmohanta S and Shrock R 2020 Baryon-number-violating nucleon and dinucleon decays in a model with large extra dimensions *Phys. Rev.* D **101** 015017
[326] Girmohanta S and Shrock R 2020 Nucleon decay and n–$\bar{n}$ oscillations in a left-right symmetric model with large extra dimensions *Phys. Rev.* D **101** 095012
[327] Girmohanta S, Mohapatra R N and Shrock R 2021 Neutrino masses and mixing in models with large extra dimensions and localized fermions *Phys. Rev.* D **103** 015021
[328] Girmohanta S and Shrock R 2021 Extra-dimensional model of dark matter *Phys. Rev.* D **104** 115021
[329] Arnold J M, Fornal B and Wise M B 2013 Simplified models with baryon number violation but no proton decay *Phys. Rev.* D **87** 075004
[330] Baldo-Ceolin M *et al* 1994 A New experimental limit on neutron—anti-neutron oscillations *Z. Phys.*C **63** 409
[331] Super-Kamiokande collaboration 2015 The Search for $n - \bar{n}$ oscillation in Super-Kamiokande I *Phys. Rev.* D **91** 072006
[332] Super-Kamiokande collaboration 2021 Neutron-antineutron oscillation search using a 0.37 megaton-years exposure of Super-Kamiokande *Phys. Rev.* D **103** 012008
[333] Friedman E and Gal A 2008 Realistic calculations of nuclear disappearance lifetimes induced by n anti-n oscillations *Phys. Rev.* D **78** 016002
[334] Milstead D 2015 A new high sensitivity search for neutron-antineutron oscillations at the ESS *PoS* **EPS-HEP2015** 603
[335] NNbar collaboration 2017 The NNbar Experiment at the European Spallation Source *7th Meeting on CPT and Lorentz Symmetry* 265–7 arXiv:1607.07271
[336] Hewes J E T 2017 Searches for Bound Neutron-Antineutron Oscillation in Liquid Argon Time Projection Chambers *PhD Thesis* Manchester U. arXiv:10.2172/1426674
[337] Girmohanta S and Shrock R 2020 Improved upper limits on baryon-number violating dinucleon decays to dileptons *Phys. Lett.* B **803** 135296
[338] de Gouvea A, Herrero-Garcia J and Kobach A 2014 Neutrino masses, grand unification, and baryon number violation *Phys. Rev.* D **90** 016011
[339] Littenberg L S and Shrock R E 1992 Upper bounds on lepton number violating meson decays *Phys. Rev. Lett.* **68** 443
[340] Appel R *et al* 2000 Search for lepton flavor violation in K^+ decays *Phys. Rev. Lett.* **85** 2877
[341] Littenberg L S and Shrock R 2000 Implications of improved upper bounds on $|\Delta L| = 2$ processes *Phys. Lett.* B **491** 285
[342] NA62 collaboration 2019 Searches for lepton number violating K^+ decays *Phys. Lett.* B **797** 134794
[343] NA62 collaboration 2021 Search for lepton number and flavor violation in K^+ and π^0 Decays *Phys. Rev. Lett.* **127** 131802
[344] Littenberg L S and Shrock R E 1992 Upper bounds on $\Delta L = 2$ decays of baryons *Phys. Rev.* D **46** R892
[345] HyperCP collaboration 2005 Search for the lepton-number-violating decay $\Xi^- \to p\mu^-\mu^-$ *Phys. Rev. Lett.* **94** 181801
[346] Frejus collaboration 1991 Lifetime limits on (B–L) violating nucleon decay and dinucleon decay modes from the Frejus experiment *Phys. Lett.* B **269** 227
[347] Seidel S *et al* 1988 Search for multitrack nucleon decay *Phys. Rev. Lett.* **61** 2522
[348] McGrew C *et al* 1999 Search for nucleon decay using the IMB-3 detector *Phys. Rev.* D **59** 052004
[349] Jenkins E E, Manohar A V and Stoffer P 2018 Low-energy effective field theory below the electroweak scale: operators and matching *J. High Energy Phys.* JHEP03(2018)016
[350] Hambye T and Heeck J 2018 Proton decay into charged leptons *Phys. Rev. Lett.* **120** 171801
[351] Fonseca R M and Hirsch M 2018 $\Delta L \geqslant 4$ lepton number violating processes *Phys. Rev.* D **98** 015035
[352] Chakrabortty J, Prakash S, Rahaman S U and Spannowsky M 2021 Uncovering the root of LEFT in SMEFT *EPL* **136** 11002
[353] Abbott L F and Wise M B 1980 The effective hamiltonian for nucleon decay *Phys. Rev.* D **22** 2208

[354] Caswell W E, Milutinovic J and Senjanovic G 1983 Matter—antimatter transition operators: a manual for modeling *Phys. Lett.* B **122** 373
[355] Babu K S and Mohapatra R N 2012 *B–L* violating proton decay modes and new baryogenesis scenario in SO(10) *Phys. Rev. Lett.* **109** 091803
[356] Babu K S and Mohapatra R N 2012 *B–L* violating nucleon decay and GUT scale baryogenesis in SO(10) *Phys. Rev.* D **86** 035018
[357] Kobach A 2016 Baryon Number, Lepton Number, and Operator Dimension in the Standard Model *Phys. Lett.* B **758** 455
[358] Heeck J and Takhistov V 2020 Inclusive Nucleon Decay Searches as a Frontier of Baryon Number Violation *Phys. Rev.* D **101** 015005
[359] Nussinov S and Shrock R 2020 Using $\bar{p}p$ and e^+e^- annihilation data to refine bounds on the Baryon-number-violating dinucleon decays $nn \to e^+e^-$ and $nn \to \mu^+\mu^-$ *Phys. Rev.* D **102** 035003
[360] Hou W-S, Nagashima M and Soddu A 2005 Baryon number violation involving higher generations *Phys. Rev.* D **72** 095001
[361] Girmohanta S and Shrock R 2019 Improved lower bounds on partial lifetimes for nucleon decay modes *Phys. Rev.* D **100** 115025
[362] Dreiner H K, Luhn C and Thormeier M 2006 What is the discrete gauge symmetry of the MSSM? *Phys. Rev.* D **73** 075007
[363] Banks T and Seiberg N 2011 Symmetries and strings in field theory and gravity *Phys. Rev.* D **83** 084019
[364] Krauss L M and Wilczek F 1989 Discrete gauge symmetry in continuum theories *Phys. Rev. Lett.* **62** 1221
[365] Babu K S, Gogoladze I and Wang K 2003 Natural R parity, μ-term, and fermion mass hierarchy from discrete gauge symmetries *Nucl. Phys.* B **660** 322
[366] Lee H M *et al* 2011 A unique $\mathbb{Z}_4^R$ symmetry for the MSSM *Phys. Lett.* B **694** 491
[367] Chen M-C, Ratz M and Takhistov V 2015 *R* parity violation from discrete *R* symmetries *Nucl. Phys.* B **891** 322
[368] Hiçyı Y, Selbuz L, Solmaz L and Ün C S Model Characterization and Dark Matter in the Secluded $U(1)'$ Model arXiv:2111.11930
[369] Farrar G R and Fayet P 1978 Phenomenology of the production, decay, and detection of new hadronic states associated with supersymmetry *Phys. Lett.* B **76** 575
[370] Barbieri R and Masiero A 1986 Supersymmetric models with low-energy baryon number violation *Nucl. Phys.* B **267** 679
[371] Dimopoulos S and Hall L J 1987 Baryogenesis at the MeV era *Phys. Lett.* B **196** 135
[372] Brahmachari B and Roy P 1994 Constraints on baryon nonconserving Yukawa couplings in a supersymmetric theory *Phys. Rev.* D **50** R39
[373] Goity J L and Sher M 1995 Bounds on $\Delta B = 1$ couplings in the supersymmetric standard model *Phys. Lett.* B **346** 69
[374] Barbier R *et al* 2005 R-parity violating supersymmetry *Phys. Rept.* **420** 1
[375] Chemtob M 2005 Phenomenological constraints on broken R parity symmetry in supersymmetry models *Prog. Part. Nucl. Phys.* **54** 71
[376] Smirnov A Y and Vissani F 1996 Upper bound on all products of R-parity violating couplings lambda-prime and lambda-prime-prime from proton decay *Phys. Lett.* B **380** 317
[377] Super-Kamiokande collaboration 2014 Search for dinucleon decay into kaons in Super-Kamiokande *Phys. Rev. Lett.* **112** 131803
[378] Super-Kamiokande collaboration 2015 Search for dinucleon decay into pions at Super-Kamiokande *Phys. Rev.* D **91** 072009
[379] Schechter J and Valle J W F 1982 Neutrinoless double beta decay in SU(2) x U(1) theories *Phys. Rev.* D **25** 2951
[380] Dolinski M J, Poon A W P and Rodejohann W 2019 Neutrinoless double-beta decay: status and prospects *Ann. Rev. Nucl. Part. Sci.* **69** 219
[381] Babu K S and Mohapatra R N 2015 Determining majorana nature of neutrino from nucleon decays and $n - \bar{n}$ oscillations *Phys. Rev.* **D91** 013008
[382] Morrissey D E and Ramsey-Musolf M J 2012 Electroweak baryogenesis *New J. Phys.* **14** 125003
[383] Gu P-H and Sarkar U 2011 Baryogenesis and neutron-antineutron oscillation at TeV *Phys. Lett.* B **705** 170

[384] Buchmuller W, Di Bari P and Plumacher M 2005 Leptogenesis for pedestrians *Annals Phys.* **315** 305
[385] Nir Y 2007 Introduction to leptogenesis *6th Rencontres du Vietnam Challenges in Particle Astrophysics* vol 2, pp 1–7 arXiv:hep-ph/0702199
[386] Davidson S, Nardi E and Nir Y 2008 Leptogenesis *Phys. Rept.* **466** 105
[387] Pilaftsis A 2009 The Little Review on Leptogenesis *J. Phys. Conf. Ser.* **171** 012017
[388] Bari P Di 2012 An introduction to leptogenesis and neutrino properties *Contemp. Phys.* **53** 315
[389] Fong C S, Nardi E and Riotto A 2012 Leptogenesis in the Universe *Adv. High Energy Phys.* **2012** 158303
[390] Chun E J *et al* 2018 Probing Leptogenesis *Int. J. Mod. Phys.*A **33** 1842005
[391] Dev P S B, Di Bari P, Garbrecht B, Lavignac S, Millington P and Teresi D 2018 Flavor effects in leptogenesis *Int. J. Mod. Phys.*A **33** 1842001
[392] Bodeker D and Buchmuller W 2021 Baryogenesis from the weak scale to the grand unification scale *Rev. Mod. Phys.* **93** 035004
[393] Planck collaboration 2020 Planck 2018 results: I. Overview and the cosmological legacy of Planck *Astron. Astrophys.* **641** A1
[394] Fong C S, Meloni D, Meroni A and Nardi E 2015 Leptogenesis in SO(10) *J. High Energy Phys.* JHEP01(2015)111
[395] Di Bari P and Samanta R 2020 The SO(10)-inspired leptogenesis timely opportunity *J. High Energy Phys.* JHEP08(2020)124
[396] Mummidi V S and Patel K M 2021 Leptogenesis and fermion mass fit in a renormalizable SO(10) model *J. High Energy Phys.* JHEP12(2021)042
[397] Davidson S and Ibarra A 2002 A Lower bound on the right-handed neutrino mass from leptogenesis *Phys. Lett.* B **535** 25
[398] Covi L and Roulet E 1997 Baryogenesis from mixed particle decays *Phys. Lett.* B **399** 113
[399] Pilaftsis A 1997 CP violation and baryogenesis due to heavy Majorana neutrinos *Phys. Rev.* D **56** 5431
[400] Pilaftsis A and Underwood T E J 2004 Resonant leptogenesis *Nucl. Phys.* B **692** 303
[401] Akhmedov E K, Rubakov V A and Smirnov A Y 1998 Baryogenesis via neutrino oscillations *Phys. Rev. Lett.* **81** 1359
[402] Drewes M *et al* 2018 ARS Leptogenesis *Int. J. Mod. Phys.*A **33** 1842002
[403] Dev B, Garny M, Klaric J, Millington P and Teresi D 2018 Resonant enhancement in leptogenesis *Int. J. Mod. Phys.*A **33** 1842003
[404] Fong C S, Rahat M H and Saad S 2021 Low-scale resonant leptogenesis in SU(5) GUT with T13 family symmetry *Phys. Rev.* D **104** 095028
[405] Martin S P 1992 Some simple criteria for gauged R-parity *Phys. Rev.* D **46** R2769
[406] Kadastik M, Kannike K and Raidal M 2010 Matter parity as the origin of scalar dark matter *Phys. Rev.* D **81** 015002
[407] Kadastik M, Kannike K and Raidal M 2009 Dark matter as the signal of grand unification *Phys. Rev.* D **80** 085020
[408] Frigerio M and Hambye T 2010 Dark matter stability and unification without supersymmetry *Phys. Rev.* D **81** 075002
[409] Mambrini Y, Nagata N, Olive K A, Quevillon J and Zheng J 2015 Dark matter and gauge coupling unification in nonsupersymmetric SO(10) grand unified models *Phys. Rev.* D **91** 095010
[410] Mambrini Y, Olive K A, Quevillon J and Zaldivar B 2013 Gauge Coupling Unification and Nonequilibrium Thermal Dark Matter *Phys. Rev. Lett.* **110** 241306
[411] Nagata N, Olive K A and Zheng J 2015 Weakly-interacting massive particles in non-supersymmetric SO(10) grand unified models *J. High Energy Phys.* JHEP10(2015)193
[412] Boucenna S M, Krauss M B and Nardi E 2016 Dark matter from the vector of SO (10) *Phys. Lett.* B **755** 168
[413] Arbelaez C, Longas R, Restrepo D and Zapata O 2016 Fermion dark matter from SO(10) GUTs *Phys. Rev.* D **93** 013012
[414] Bandyopadhyay T and Raychaudhuri A 2017 Left–right model with TeV fermionic dark matter and unification *Phys. Lett.* B **771** 206
[415] Hall L J, Kostelecky V A and Raby S 1986 New flavor violations in supergravity models *Nucl. Phys.* B **267** 415

[416] Gabbiani F, Gabrielli E, Masiero A and Silvestrini L 1996 A Complete analysis of FCNC and CP constraints in general SUSY extensions of the standard model *Nucl. Phys.* B **477** 321
[417] Calibbi L, Faccia A, Masiero A and Vempati S K 2006 Lepton flavour violation from SUSY-GUTs: Where do we stand for MEG, PRISM/PRIME and a super flavour factory *Phys. Rev.* D **74** 116002
[418] Ciuchini M, Masiero A, Paradisi P, Silvestrini L, Vempati S K and Vives O 2007 Soft SUSY breaking grand unification: Leptons versus quarks on the flavor playground *Nucl. Phys.* B **783** 112
[419] MEG collaboration 2016 Search for the lepton flavour violating decay $\mu^+ \to e^+\gamma$ with the full dataset of the MEG experiment *Eur. Phys. J.* C **76** 434
[420] LIGO Scientific, Virgo collaboration 2016 Binary black hole mergers in the first advanced LIGO observing run *Phys. Rev. X* **6** 041015
[421] Kibble T W B 1976 Topology of cosmic domains and strings *J. Phys. A* **9** 1387
[422] Jeannerot R, Rocher J and Sakellariadou M 2003 How generic is cosmic string formation in SUSY GUTs *Phys. Rev.* D **68** 103514
[423] Kibble T W B 1985 Evolution of a system of cosmic strings *Nucl. Phys.* B **252** 227
[424] Bennett D P and Bouchet F R 1988 Evidence for a scaling solution in cosmic string evolution *Phys. Rev. Lett.* **60** 257
[425] Allen B and Shellard E P S 1990 Cosmic string evolution: a numerical simulation *Phys. Rev. Lett.* **64** 119
[426] Vilenkin A 1985 Cosmic strings and domain walls *Phys. Rept.* **121** 263
[427] Caldwell R R and Allen B 1992 Cosmological constraints on cosmic string gravitational radiation *Phys. Rev.* D **45** 3447
[428] Hindmarsh M B and Kibble T W B 1995 Cosmic strings *Rept. Prog. Phys.* **58** 477
[429] Cui Y, Lewicki M, Morrissey D E and Wells J D 2019 Probing the pre-BBN universe with gravitational waves from cosmic strings *J. High Energy Phys.* JHEP01(2019)081
[430] Auclair P *et al* 2020 Probing the gravitational wave background from cosmic strings with LISA *JCAP* **04** 034
[431] LIGO Scientific, Virgo collaboration 2019 Search for the isotropic stochastic background using data from advanced LIGO's second observing run *Phys. Rev.* D **100** 061101
[432] Janssen G *et al* 2015 Gravitational wave astronomy with the SKA *PoS* **AASKA14** 037
[433] LISA collaboration Laser interferometer space antenna arXiv:1702.00786
[434] Ruan W-H, Guo Z-K, Cai R-G and Zhang Y-Z 2020 Taiji program: gravitational-wave sources *Int. J. Mod. Phys.*A **35** 2050075
[435] TianQin collaboration 2016 TianQin: a space-borne gravitational wave detector *Class. Quant. Grav.* **33** 035010
[436] Corbin V and Cornish N J 2006 Detecting the cosmic gravitational wave background with the big bang observer *Class. Quant. Grav.* **23** 2435
[437] Seto N, Kawamura S and Nakamura T 2001 Possibility of direct measurement of the acceleration of the universe using 0.1 Hz band laser interferometer gravitational wave antenna in space *Phys. Rev. Lett.* **87** 221103
[438] Sathyaprakash B *et al* 2012 Scientific objectives of einstein telescope *Class. Quant. Grav.* **29** 124013
[439] LIGO Scientific collaboration 2017 Exploring the sensitivity of next generation gravitational wave detectors *Class. Quant. Grav.* **34** 044001
[440] MAGIS collaboration Mid-band gravitational wave detection with precision atomic sensors arXiv:1711.02225
[441] AEDGE collaboration 2020 AEDGE: atomic experiment for dark matter and gravity exploration in space *EPJ Quant. Technol.* **7** 6
[442] Badurina L *et al* 2020 AION: an atom interferometer observatory and network *J. Cosmol. Astropart. Phys.* JCAP05(2020)011
[443] Buchmüller W, Domcke V, Kamada K and Schmitz K 2013 The Gravitational Wave Spectrum from Cosmological $B-L$ Breaking *J. Cosmol. Astropart. Phys.* JCAP10(2013)003
[444] Buchmüller W, Domcke V, Murayama H and Schmitz K 2020 Probing the scale of grand unification with gravitational waves *Phys. Lett.* B **809** 135764
[445] King S F, Pascoli S, Turner J and Zhou Y-L 2021 Gravitational waves and proton decay: complementary windows into grand unified theories *Phys. Rev. Lett.* **126** 021802

[446] Super-Kamiokande collaboration 2017 Search for proton decay via $p \to e^+\pi^0$ and $p \to \mu^+\pi^0$ in 0.31 megaton·years exposure of the Super-Kamiokande water Cherenkov detector *Phys. Rev.* D **95** 012004
[447] King S F, Pascoli S, Turner J and Zhou Y-L 2021 Confronting SO(10) GUTs with proton decay and gravitational waves *J. High Energy Phys.* JHEP10(2021)225
[448] Dror J A, Hiramatsu T, Kohri K, Murayama H and White G 2020 Testing the seesaw mechanism and leptogenesis with gravitational waves *Phys. Rev. Lett.* **124** 041804
[449] Caprini C *et al* 2020 Detecting gravitational waves from cosmological phase transitions with LISA: an update *J. Cosmol. Astropart. Phys.* JCAP03(2020)024
[450] Caprini C *et al* 2016 Science with the space-based interferometer eLISA. II: Gravitational waves from cosmological phase transitions *J. Cosmol. Astropart. Phys.* JCAP04(2016)001
[451] Bian L, Cheng W, Guo H-K and Zhang Y 2021 Cosmological implications of a $B-L$ charged hidden scalar: leptogenesis and gravitational waves *Chin. Phys. C* **45** 113104
[452] Haba N and Yamada T 2020 Gravitational waves from phase transition in minimal SUSY $U(1)_{B-L}$ model *Phys. Rev.* D **101** 075027
[453] Hasegawa T, Okada N and Seto O 2019 Gravitational waves from the minimal gauged $U(1)_{B-L}$ model *Phys. Rev.* D **99** 095039
[454] Marzo C, Marzola L and Vaskonen V 2019 Phase transition and vacuum stability in the classically conformal *B–L* model *Eur. Phys. J.* C **79** 601
[455] Jinno R and Takimoto M 2017 Probing a classically conformal *B–L* model with gravitational waves *Phys. Rev.* D **95** 015020
[456] Di Bari P, Marfatia D and Zhou Y-L 2021 Gravitational waves from first-order phase transitions in Majoron models of neutrino mass *J. High Energy Phys.* JHEP10(2021)193
[457] Di Bari P, Marfatia D and Zhou Y-L 2020 Gravitational waves from neutrino mass and dark matter genesis *Phys. Rev.* D **102** 095017
[458] RBC, UKQCD collaboration 2016 Domain wall QCD with physical quark masses *Phys. Rev.* D **93** 074505
[459] Boyle P A *et al* 2016 Low energy constants of SU(2) partially quenched chiral perturbation theory from $N_f = 2+1$ domain wall QCD *Phys. Rev.* D **93** 054502
[460] Blum T *et al* 2020 Hadronic light-by-light scattering contribution to the muon anomalous magnetic moment from lattice QCD *Phys. Rev. Lett.* **124** 132002
[461] JLQCD collaboration 2000 Nucleon decay matrix elements from lattice QCD *Phys. Rev.* D **62** 014506
[462] Aoki Y, Dawson C, Noaki J and Soni A 2007 Proton decay matrix elements with domain-wall fermions *Phys. Rev.* D **75** 014507
[463] Aoki Y, Shintani E and Soni A 2014 Proton decay matrix elements on the lattice *Phys. Rev.* D **89** 014505
[464] Aoki Y, Izubuchi T, Shintani E and Soni A 2017 Improved lattice computation of proton decay matrix elements *Phys. Rev.* D **96** 014506
[465] Martin A and Stavenga G C 2012 Non-perturbative proton stability *Phys. Rev.* D **85** 095010
[466] Yoo J-S, Aoki Y, Boyle P, Izubuchi T, Soni A and Syritsyn S Proton decay matrix elements on the lattice at physical pion mass arXiv:2111.01608
[467] Claudson M, Wise M B and Hall L J 1982 Chiral lagrangian for deep mine physics *Nucl. Phys.* B **195** 297
[468] Hara Y, Itoh S, Iwasaki Y and Yoshie T 1986 Proton decay and lattice QCD *Phys. Rev.* D **34** 3399
[469] Bowler K C, Daniel D, Kieu T D, Richards D G and Scott C J 1988 Nucleon wave functions from lattice gauge theories: measurements of baryonic operators *Nucl. Phys.* B **296** 431
[470] CP-PACS, JLQCD collaboration 2004 Lattice QCD calculation of the proton decay matrix element in the continuum limit *Phys. Rev.* D **70** 111501
[471] RBC-UKQCD collaboration 2008 Proton lifetime bounds from chirally symmetric lattice QCD *Phys. Rev.* D **78** 054505
[472] Rinaldi E, Syritsyn S, Wagman M L, Buchoff M I, Schroeder C and Wasem J 2019 Neutron-antineutron oscillations from lattice QCD *Phys. Rev. Lett.* **122** 162001
[473] Rinaldi E, Syritsyn S, Wagman M L, Buchoff M I, Schroeder C and Wasem J 2019 Lattice QCD determination of neutron-antineutron matrix elements with physical quark masses *Phys. Rev.* D **99** 074510

[474] Buchoff M I and Wagman M 2016 Perturbative renormalization of neutron-antineutron operators *Phys. Rev.* D **93** 016005
[475] USQCD collaboration 2019 Hadrons and nuclei *Eur. Phys. J.*A **55** 193
[476] USQCD collaboration 2019 The role of lattice qcd in searches for violations of fundamental symmetries and signals for new physics *Eur. Phys. J.*A **55** 197
[477] Super-Kamiokande collaboration 2022 First gadolinium loading to Super-Kamiokande *Nucl. Instrum. Meth.*A **1027** 166248
[478] Super-Kamiokande collaboration 2014 Search for proton decay via $p \to \nu K^+$ using 260 kiloton·year data of Super-Kamiokande *Phys. Rev.* D **90** 072005
[479] Baldo-Ceolin M *et al* 1990 A new experimental limit on neutron antineutron transitions *Phys. Lett.* **B236** 95
[480] Super-Kamiokande collaboration 2012 Search for proton decay via $p - > \mu^+ K^0$ in Super-Kamiokande I, II, and III *Phys. Rev.* D **86** 012006
[481] Super-Kamiokande collaboration 2020 Search for proton decay into three charged leptons in 0.37 megaton-years exposure of the Super-Kamiokande *Phys. Rev.* D **101** 052011
[482] Super-Kamiokande collaboration 2015 Search for nucleon and dinucleon decays with an invisible particle and a charged lepton in the final state at the super-kamiokande experiment *Phys. Rev. Lett.* **115** 121803
[483] CORSIKA collaboration 2021 CORSIKA 8—contributions to the 37th International Cosmic Ray Conference in Berlin Germany (ICRC 2021) *37th Int. Cosmic Ray Conf.* vol 12arXiv:2112.11761
[484] MicroBooNE, Dune collaboration 2021 Neutron-antineutron oscillation search with MicroBooNE and DUNE *PoS* **ICHEP2020** 148
[485] Abratenko P *et al* (MicroBooNE Collaboration) 2022 A first search for argon-bound neutron-antineutron oscillation using the MicroBooNE LArTPC *MICROBOONE-NOTE-10XX-PUB*
[486] Rolke W A and López A M 2001 Confidence intervals and upper bounds for small signals in the presence of background noise *Nucl. Instrum. Meth.*A **458** 745–58
[487] DUNE collaboration 2020 Deep underground neutrino experiment (DUNE), Far detector technical design report, volume I introduction to DUNE *JINST* **15** T08008
[488] DUNE collaboration 2020 Deep underground neutrino experiment (DUNE), Far detector technical design report, volume IV: Far detector single-phase technology *JINST* **15** T08010
[489] DUNE collaboration Snowmass neutrino frontier: DUNE physics summary arXiv:2203.06100
[490] MicroBooNE collaboration 2020 First measurement of differential charged current quasielastic-like ν_μ-argon scattering cross sections with the MicroBooNE Detector *Phys. Rev. Lett.* **125** 201803
[491] DUNE collaboration 2020 First results on ProtoDUNE-SP liquid argon time projection chamber performance from a beam test at the CERN Neutrino Platform *JINST* **15** P12004
[492] DUNE collaboration 2020 First calorimetric energy reconstruction of beam events with arapuca light detector in protodune-sp *JINST* **15** C03033
[493] ArgoNeuT collaboration 2019 Demonstration of mev-scale physics in liquid argon time projection chambers using argoneut *Phys. Rev.* D **99** 012002
[494] ArgoNeuT collaboration 2020 First measurement of electron neutrino scattering cross section on argon *Phys. Rev.* D **102** 011101
[495] Barrow J L, Golubeva E S, Paryev E and Richard J-M 2020 Progress and simulations for intranuclear neutron-antineutron transformations in $^{40}_{18}Ar$ *Phys. Rev.* D **101** 036008
[496] JUNO collaboration 2022 JUNO physics and detector *Prog. Part. Nucl. Phys.* **123** 103927
[497] Zou J H *et al* 2015 SNiPER: an offline software framework for non-collider physics experiments *J. Phys. Conf. Ser.* **664** 072053
[498] Andreopoulos C *et al* 2015 The GENIE neutrino monte carlo generator: physics and user manual arXiv:1510.05494
[499] KamLAND collaboration 2015 Search for the proton decay mode $p \to \overline{\nu} K^+$ with KamLAND *Phys. Rev.* D **92** 052006
[500] Undagoitia T M *et al* 2005 Search for the proton decay p —> K+ anti-nu in the large liquid scintillator low energy neutrino astronomy detector LENA *Phys. Rev.* D **72** 075014
[501] Feldman G J and Cousins R D 1998 A Unified approach to the classical statistical analysis of small signals *Phys. Rev.* D **57** 3873
[502] Theia collaboration 2020 THEIA: an advanced optical neutrino detector *Eur. Phys. J.* C **80** 416

[503] KamLAND collaboration 2006 Search for the invisible decay of neutrons with KamLAND *Phys. Rev. Lett.* **96** 101802
[504] SNO+ collaboration 2019 Search for invisible modes of nucleon decay in water with the SNO+ detector *Phys. Rev.* **D99** 032008
[505] Djurcic Z *et al* 2020 Searches for proton-decay with additional signatures from nuclear deexcitations and with precise timing from photon detectors in large lartpcs
[506] Dune module of opportunity workshop, 2019.
[507] Q-Pix collaboration 2022 Enhanced low energy supernova burst detection in large liquid argon time projection chambers enabled by Q-Pix, to be published
[508] MicroBooNE collaboration 2020 Selection of charged-current neutrino-induced K+ production interactions in MicroBooNE, MICROBOONE-NOTE-1071-PUB
[509] Andreopoulos C *et al* 2010 The GENIE neutrino Monte Carlo generator *Nucl. Instrum. Meth.* **A614** 87
[510] Snider E and Petrillo G 2017 LArSoft: Toolkit for simulation, reconstruction and analysis of liquid argon TPC neutrino detectors *J. Phys. Conf. Ser.* **898** 042057
[511] Barrow J L 2021 Towards Neutron Transformation Searches *PhD thesis* U. Tennessee, Knoxville
[512] Golubeva E S, Barrow J L and Ladd C G 2019 Model of $\bar{n}$ annihilation in experimental searches for $\bar{n}$ transformations *Phys. Rev.* **D99** 035002
[513] Mohapatra R N and Perez-Lorenzana A 2003 Neutrino mass, proton decay and dark matter in TeV scale universal extra dimension models *Phys. Rev.* D **67** 075015